STUDY ON PARAMETERS AFFECTING SPRINGBACK OF FORMING OF ADVANCED HIGH STRENGTH STEEL SHEETS (AHSS)

WATCHARAPONG SIRIGOOL

A THESIS SUBMITTED IN PARTIAL FULFILLMENT

OF THE REQUIREMENT FOR THE DEGREE OF

MASTER OF ENGINEERING IN AUTOMOTIVE ENGINEERING

(INTERNATIONAL PROGRAM)

INTERNATIONAL COLLEGE

KING MONGKUT'S INSTITUTE OF TECHNOLOGY LADKRABANG

2010

KMITL-2010-IC-M-004-006

Thesis Title	Study on Parameters Affecting Springback of Forming of Advanced High Strength Steel Sheets (AHSS)
Student	Watcharapong Sirigool
Student ID.	50061923
Degree	Master of Engineering
Program	Automotive Engineering (International Program)
Year	2010
Thesis Advisor	Dr. Nattawoot Depaiwa
	Dr. Suwat Jirathearanat
	Prof. Dr. Tadaharu Adachi

ABSTRACT

Recently, advanced high strength steels (AHSS) are becoming widely used in many applications in place of mild steels, especially in automotive part manufacturing, due to its low weight, high strength and fairly good formability. However, the unavoidable obstacle of AHSS sheet metal forming is springback, which is a result of elastic recovery and residual stress. The aim of this study is to determine proper process parameters enabling reduction of springback defects in AHSS forming process. This work was divided into two parts, regarding to the effects of numerical parameters and process parameters on forming AHSS. In this paper, a U-shape and a Butt-shape forming were used to examine springback behaviors, which are springback angle, sidewall curl, and twist, through FEM and experiment. Simulation numerical parameters affecting springback prediction, which are element size, number of integration points through thickness, adaptive meshing, and mass scaling increase were investigated to identify suitable simulation numerical settings for accurate springback prediction. Then, the simulation model was applied to study effects of blank holder force on springback behaviors and formability of the U-shape and Butt shape forming in an attempt to find proper blank holder force profiles for springback-reduction-emphasized die design guidelines.

ACKNOWLEDGMENTS

This thesis could not be completed without the assistance of many persons to whom I would like to express my sincere appreciation.

First, I would like to sincerely thank my advisor, Dr. Suwat Jirathearanat, who has given me many helpful suggestions, useful advice and fruitful discussions during the undertaken research.

I would also like to sincerely thank Dr. Nattawoot Depaiwa for kind advising and helping, and Prof. Dr. Tadaharu Adachi for the suggestion of pure bending simulation.

Moreover, I would like to acknowledge Iron & Steel Institute of Thailand, for supplying the Advanced High Strength Steel Sheets, which was very useful for this research work. I would like to show gratitude to National Metal and Materials Technology Center (MTEC), especially the sheet metal forming laboratory for providing the laboratory equipments and instruments as well as financial support.

I am grateful to National Science and Technology Development Agency (NSTDA), which provided the full scholarship for studying in the master program.

Special thanks go to MTEC the sheet metal forming laboratory's members and room's M329 for helping me during the experiment

Finally, I am very grateful to my family for all love, caring, understanding and motivation throughout my life.

Watcharapong Sirigool

CONTENTS

CONTENTS (CONT.)

CONTENTS (CONT.)

CONTENTS (CONT.)

LIST OF TABLES

LIST OF FIGURES

LIST OF FIGURES (CONT.)

LIST OF FIGURES (CONT.)

CONTENTS (CONT.)

CONTENTS (CONT.)

Figures

CHAPTER 1

INTRODUCTION

1.1 Significance and background

Recently, the new steel grades has been developed by the steel industry which is responded to rivalry improve alternative materials for lightweight and performance enhancements as the optimal automotive material. The advanced high strength steels (AHSS) such as dual-phase steels are becoming widely used in many applications in place of mild steels, especially in automotive parts manufacturing, owning to its lightweight, high strength and good formability. AHSS is widely used as sheet steels of choice for structural components such as rails, pillars, cross members and load beams.

However, the unavoidable obstacle of AHSS sheet metal forming is springback, which is refer to as the geometry changes of a part after tool removal. In metal forming process, springback is mainly cause by residual stress distributions after elastic recovery both in plane and through thickness of product. The severity of that residual stress depends on sheet metal mechanical properties (E, YS and n-value), material thickness, die geometry (die & punch radii, tool clearance), as well as forming process parameters (blankholder force and part-die lubricity) used during forming. With severe springback defects, AHSS part assemblies are difficult if not possible at all due to each individual part geometric deviations. Consequently, inevitably die geometry and process parameters need to adjust in the expense of time and money. Now, the sheet metal forming simulation is usually used to evaluate a forming process, and reduce cost and time compensation in design process. Force, fracture and thinning can be obtained using simulation. However, some simulation process, such as springback simulation, is still an on-going research to improve an accuracy of springback simulation through well-adjusted numerical parameters.

1.2 Objectives

1.2.1 To study the numerical parameters effect to improve springback prediction accuracy of process FEM.

1.2.2 To study the process parameters affecting springback behavior via both FEM and experiment process using a U-shape tooling.

1.2.3 To obtain the optimum process parameters and die design guideline for reduction of springback systematically.

1.3 Scopes

1.3.1 The first study was an investigation of springback behavior using U & Butt-shape, simplified part on FEM.

1.3.2 The second study was an investigation of the effect of process parameters on springback by using both FEM and U & Butt-shape experiment.

1.4 Expected results

1.4.1 Understanding of springback behavior.

1.4.2 Understanding the effect of the numerical parameters affecting on springback simulation accurately.

1.4.3 Die design guideline on how to use the suitable process parameters to reduce springback behavior systematically.

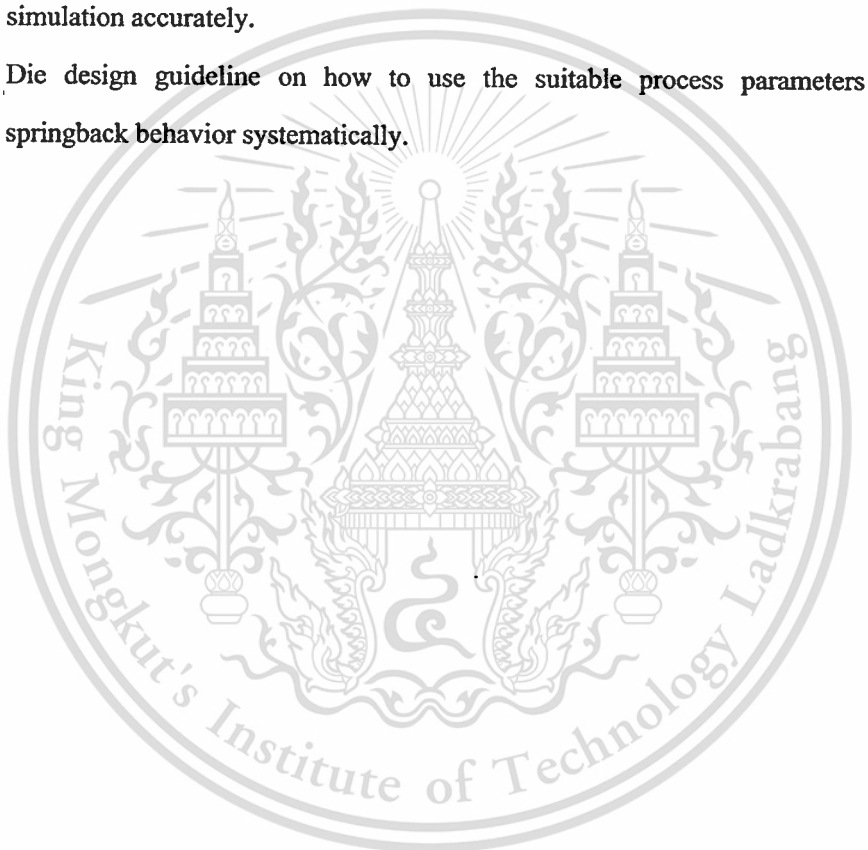

CHAPTER 2

THEORY AND LITERATURE REVIEWS

2.1 Characteristic of advance high strength steel

The ULSAB (Ultralight Steel Auto Body) classified a new groups of steels, steels with tensile strength 500 – 1000 MPa., called Advance High Strength Steels (AHSS), and Ultra High Strength Steel with tensile strength higher than 900 MPa. In Figure 2.1 show ranges of tensile strength for AHSS. The group of steels can be classified type by tensile strength as below.

Conventional Steels

- BH: Bake Hardenable (180–300 MPa tensile strength)
- HSLA: High Strength Low Alloy (270-550 MPa tensile strength)

Advanced High Strength Steels

- DP: Dual Phase (~ 500-1000 MPa tensile strength)
- CP: Complex Phase (~ 500-1000 MPa tensile strength)
- TRIP: Transformation Induced Plasticity (~500-1000 MPa tensile strength)

Ultra High Strength Steels

- MS: Martensitic (900-1500 MPa tensile strength)

The principal difference between AHSS and conventional steel is microstructure. The convention steel has single-phase, ferrite. AHSS's are multi-phase which include ferrite, pearlite, martensite, bainite, and/or retained austenite in quantities sufficient to produce unique mechanical properties. The combination of high strength and good formability of AHSS comes from high strain hardening capacity (World Auto Steel. 2009).

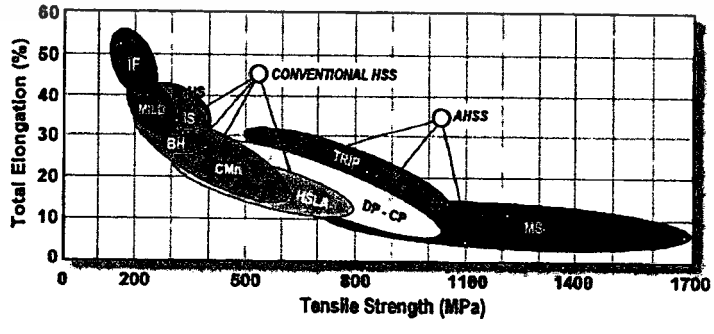

Figure 2.1 Advanced High Strength Steels range of tensile strength is between 270 – 700 MPa. (World Auto Steel. 2009).

2.2 Material property

The most important considerations to select a material are related to the relationship functions of a part and qualities such as strength, formability and stiffness. For the sheet material, the ability to transform shaped, called "formability", should also be considered. We can know behavior of the sheet from mechanical tests. In sheet metal forming, we are interested in two principles that are elastic and plastic deformation.

2.2.1 Stress

Stress is define as force, F, at a point

$$\sigma = \frac{F}{A} \tag{2.1}$$

Where A is the area at force action

In Figure 2.2 as show the components of stress. The normal stress is the force acting normal to the plane. It may be tensile or compressive. The shear stress component is the force acts parallel to the plan (Hosford and Caddell, 2007).

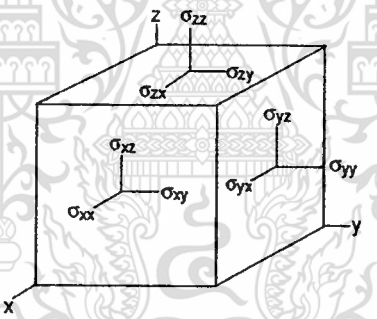

Figure 2.2 Components of stress on element (Hosford and Caddell, 2007).

2.2.2 Strain

Strain is total deformation in body, when the points in body are displaced by deformation, which can be divided into 2 types that are elastic strain and plastic strain. The elastic strain means when the deformed shape has no force acting, element in body will move back to origin shape. But the plastic strain when unloading, the shape has permanent deformation. We identify the plastic deformation by equation (2.2)

$$\varepsilon = \frac{\Delta l}{l_0} \tag{2.2}$$

Where Δl = Length Deviation

l_0 = Gage Length

2.2.3 Tensile Test

There is a number of standard tests. A tensile test specimen is shown in Figure 2.3. The initial thickness is t_0 and the length of tensile test specimen that is four times longer than the width, w_0. The load on the specimen, F, is measured by a load cell in the testing machine. The gauge length l_0 is monitored by an extensometer in the middle of the specimen and the change in width is measured by a transverse extensometer. During the test, load and extension will be recorded in a data acquisition system. (Marciniak et al., 2002).

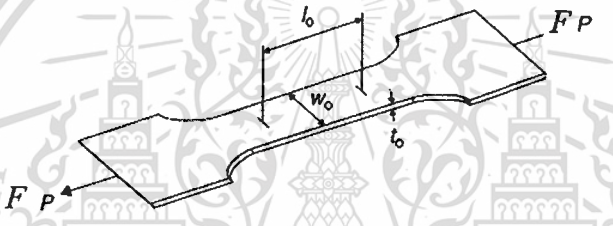

Figure 2.3 Typical tensile specimen (Marciniak et al., 2002).

2.2.4 The Engineering Stress-Strain Curve

Figure 2.4 shows load-extension diagram for a tensile test. The elastic extension is so small that it can not be seen. The initial yield load, F_y, where is plastic deformation commences. During this part of the test, the cross-sectional area of specimen decreases while the length increases; the load maximum, F_{max}, is a point reached when the strain-hardening effect balanced the rate of decrease in area.

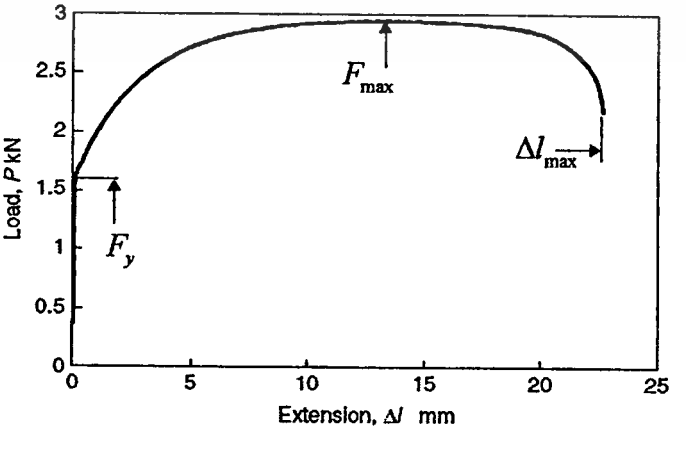

Figure 2.4 Load-extension diagram for tensile test (Marciniak et al., 2002).

The engineering stress-strain curve obtained by the initial cross-sectional area, $A_0 = w_0 \cdot t_0$, and the extension by l_0. The engineering stress–strain curve is still widely used and a number of properties are derived from it. Figure 2.5 shows the engineering stress strain curve calculated from the load, extension diagram

Engineering stress can be calculated by this equation

$$\sigma_{eng} = \frac{F}{A_0} \tag{2.3}$$

And engineering strain as

$$e_{eng} = \frac{\Delta l}{l_0} \times 100\% \tag{2.4}$$

In Figure 2.5, the initial yield stress is

$$(\sigma_f)_0 = \frac{F_y}{A_0} \tag{2.5}$$

The maximum of engineering stress is called tensile strength and calculated as

$$TS = \frac{P_{max}}{A_0} \tag{2.6}$$

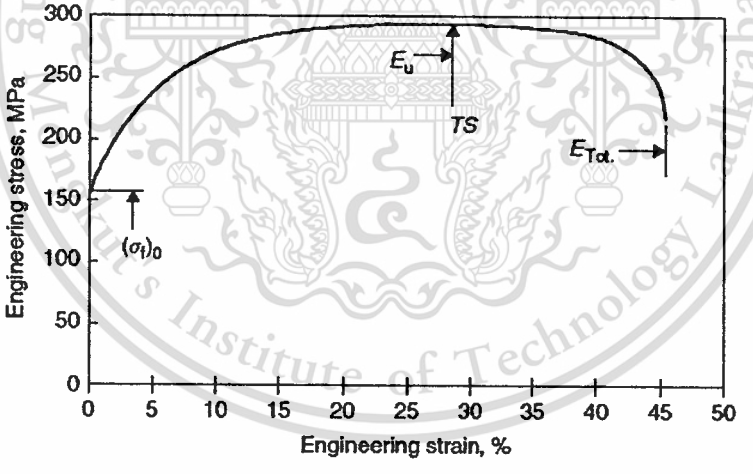

Figure 2.5 Engineer stress-strain curve (Marciniak, Z.et al. 2002).

The maximum uniform elongation, E_u, is the elongation at maximum load at maximum load as the cross-sectional area is no longer A_0.

If the strain scale near the origin is greatly increased, the elastic part of the curve would be seen, as shown in Figure 2.6 . The strain at initial yield, e_y, is very small, typically about 0.1%. The slope of the elastic part of the curve is the elastic modulus, also called Young's modulus:

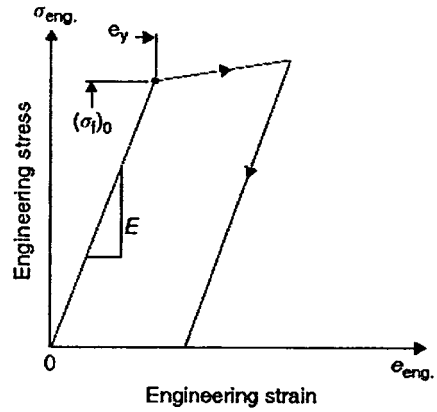

Figure 2.6 The elastic behavior of typical tensile test (Marciniak, Z.et al. 2002).

In some materials, the transition from elastic to plastic deformation is not sharp and it is difficult to establish an accurate yield stress. This is the stress to produce a specified small plastic strain 0.2%, i.e. the elastic strain at yield. Proof stress is determined by drawing a line parallel to the elastic loading line which is offset by the specified amount, as shown in Figure 2.7.

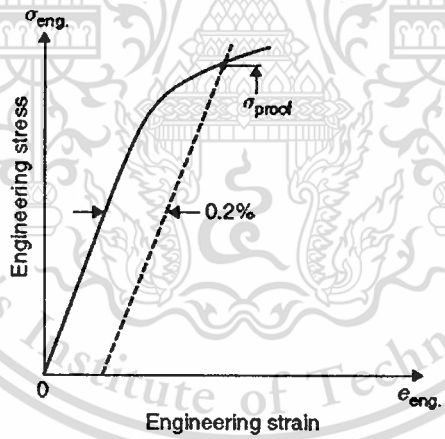

Figure 2.7 Diagram used to determine the proof stress in a material (Marciniak, Z.et al. 2002).

2.2.5 Anisotropy

In the principle of Anisotropy properties, the material properties are not equal in all directions. Therefore the values of r necessary to average in each direction (0°, 45°, 90°) as shown in Figure 2.8 and the r value in each direction will an average to use.

$$\overline{R} = \frac{R_0 + 2R_{45} + R_{90}}{4} \tag{2.3}$$

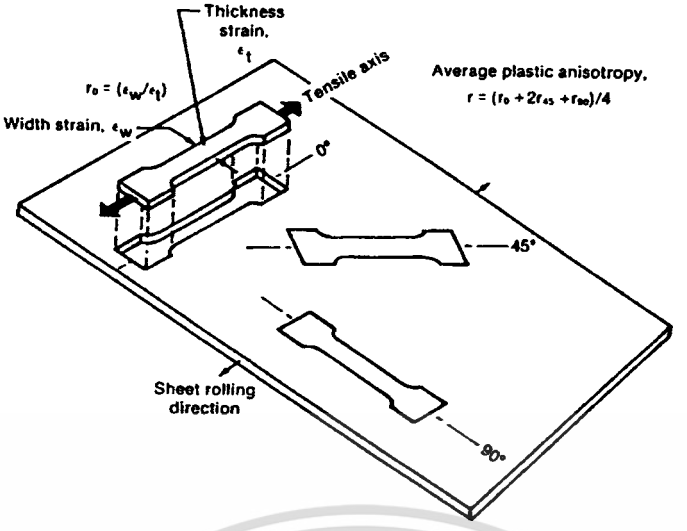

Figure 2.8 Measurement of r value by tensile specimen from three directions (ASTM, 1998).

2.3 Analytical solutions for springback in forming process

Simple analytical solutions for springback which are plane-strain pure bending and plane-strain pure bending with superimposed tension were derived long time ago. The elastic-perfectly plastic material behavior was assumed to investigate solutions (Caeden W.D. et al. 2002). Then, the analytical mathematic for springback of simple case forming which are flanging (Livatyali H et al. 2001), U-bending (Chou I.N. et al. 1999 ; Zhang D. et al. 2007) and V-bending (Asnafi N. 2000; Leu D.-K. 1997; Zhang L.C. et al. 1997). Apart from the complicated case, these is another case that are draw bending and stretch bending.

The author presented to predict springback and curvature of sidewall using draw bending. The curvature and through-thickness stresses obtained from the finite-element analysis which caused by bending and unbending of the sheet, and calculated analytically thickness strains. For different materials, the developed theory was capable of predicting practically observed differences in springback and sidewall curl (Pourboghrat F. and Chu E 1995).

All sheet-forming operations involve bending. Regularly a feature of springback occurs after the bending forces are removed and the material contains residual stresses (Hosford, W.F. and Caddell, R.M. 2007). If the bend radius is too small, the failure by splitting during a bending process is usually limited to high-strength (Marciniak, Z.et al. 2002).

2.3.1 Sheet Bending

The pure bending moment caused by the bending of a non–strain-hardening material a Figure 2.9 shows the coordinate system. Where z is the distance of an element from the mid-plane

and r is the radius of curvature measured at the mid-plane. The engineering strain at z can be derived by considering the arc length, L. The arc length at the mid-plane, L_0, does not change during bending and the arc length is $L_0 = r\theta$, where θ is the bend angle. At z, the arc length is $L = (r+z)\theta$. So the engineering strain, *e*, is. (Marciniak, Z.et al. 2002).

$$e = (\frac{l - l_0}{l_0}) = \frac{z\theta}{r\theta} = \frac{z}{r} \tag{2.4}$$

The true strain is

$$\varepsilon_x = \ln(1 + \frac{z}{r}) \tag{2.5}$$

When the strains is enough we can approximate true strain.

$$\varepsilon_x = \frac{z}{r} \tag{2.6}$$

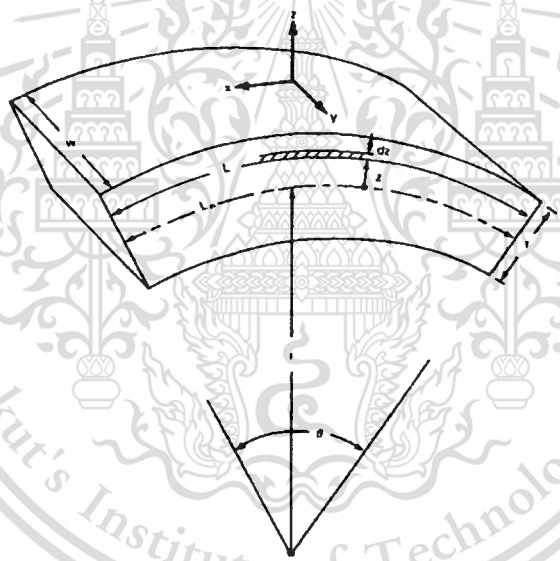

Figure 2.9 Coordinate system for sheet bending (Hosford, W.F. and Caddell, R.M. 2007).

When the width of the sheet metal is greater than the thickness, the width strain, ε_y is negligible. Therefore, the bending sheet can considered to be plan strain condition, $\varepsilon_z = -\varepsilon_x$. In Figure 2.10 shows the value of e_x varying from $-t/(2r)$ on the inside ($z = -t/2$) to zero at the mid-plane and $+t/(2r)$ on the outside surface for small strain $\varepsilon_x = e_x$. Assume that the material is elastic-ideally plastic (no strain hardening). The internal stress distribution is found by the strain distribution and the stress–strain curve.

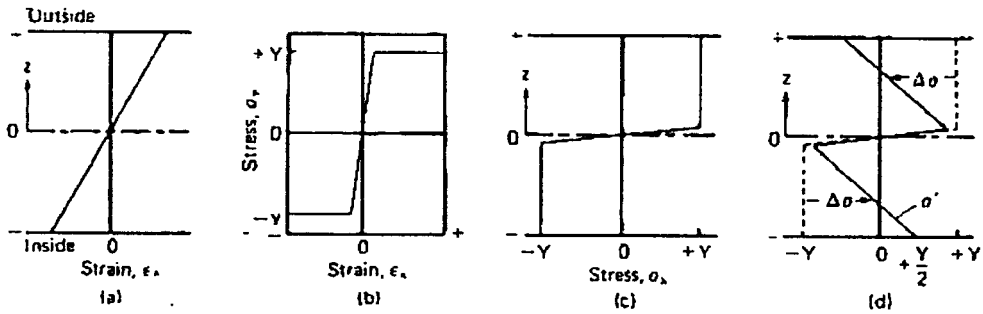

Figure 2.10 Stress and strain distribution across a sheet thickness. During bending the strain varies linearly across section (a). With a non–strain-hardening material (b) the bending causes the stress distribution in (c). Elastic unloading results in the residual

2.3.2 Moment bending

In Figure 2.10 shows the strain and stress distribution. The entire cross section at a stress σ_x= Y or –Y except for an elastic core near the mid-plane, so the flow stress in plain strain is $\sigma_0 = \sqrt{4/3}Y$. For most bending operations this elastic core can be neglected.

The bending moment can be calculated by assuming that there is no external force, F_x. However, there are internal forces, $dF_x = \sigma_x w dz$ acting on incremental elements of the cross section. The contribution of stress on every element to the bending moment is product the incremental force and its lever arm.

$$dM = z\sigma_x w dz \tag{2.7}$$

The total moment can be found in equation (2.7).

$$M = \int_{-t/2}^{+t/2} w\sigma_x z dz = 2\int_0^{t/2} w\sigma_x z dz \tag{2.8}$$

For an ideally plastic material, It is simpler to take twice the integral between 0 and *t*/2 because the sign of σ_x changes at the mid-plane.

$$M = 2wY\int_0^{t/2} z dz = wYt^2/4 \tag{2.9}$$

During unloading, it is clear that the external bending moment applied by the tools and the internal moment resisting bending must be equal. When the tools are removed, the external moment becomes zero and therefore the internal moment must also vanish. During springback the material unbends elastically and the magnitude of internal stresses will decrease. The final stress distribution results in zero bending moment. The change of internal stresses due to elastic unloading:

$$\Delta\sigma_x = E'\Delta\varepsilon_x \tag{2.10}$$

Where $E' = E/(1+v^2)$ and change of strain become, ε_x

$$\Delta\varepsilon_x = \frac{z}{r} - \frac{z}{r'} \tag{2.11}$$

Where r' is the value of radius of springback, the internal stress changes because of the bending moment is changing, ΔM

$$\Delta M = 2w\int_0^{t/2} \Delta\sigma_x z dz = 2w\int_0^{t/2} E'(1/r - 1/r')z^2 dz \tag{2.12}$$

Integrate,

$$\Delta M = (\frac{wE't^3}{12})(\frac{1}{r} - \frac{1}{r'}) \tag{2.13}$$

If the bending moment is $wYt^2/4$ Therefore, after springback the bending moment must be zero, $M - \Delta M = 0$.

$$wYt^2/4 = (\frac{wE't^3}{12})(\frac{1}{r} - \frac{1}{r'}) \tag{2.14}$$

$$(\frac{1}{r} - \frac{1}{r'}) = 3Y/(tE') \tag{2.15}$$

For work hardening material, $\sigma_x = K'\varepsilon_x^n$, the moment is then.

$$M = \left(\frac{2}{2+n}\right)(wK'/r^n)(t/2)^{n+2} \tag{2.16}$$

Substituting M from (2.9) and ΔM from (2.13) to $M - \Delta M = 0$.

$$\left(\frac{1}{r} - \frac{1}{r'}\right) = \left(\frac{6}{2+n}\right)\left(\frac{K'}{E'}\right)\left(\frac{t}{2r}\right)^n\left(\frac{1}{t}\right) \tag{2.17}$$

2.3.3 Air Bending

Wang, J. et al. studied practical incremental bending methodology to control punch displacement to achieve more accurate final bend angles by using air bending. When the punch is removed at the end deformation, it can be observed bend angle changing show in Figure 2.11.

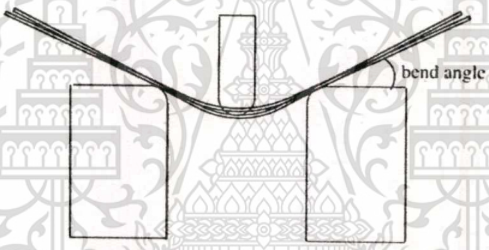

Figure 2.11 Springback after air bending (Wang, J. et al.2008).

In the air bending process, the bending moment is linearly distributed from the maximum value at the punch tip to zero at the die contact. This results in regions in sheet metal with fully elastic and elastic–plastic deformation modes. To simplify the geometry for practical implementation, the non-constant bend radius is approximated by a single bend radius such that simple but reasonably accurate models can be used. In equation (2.15), Hosford and Caddell presented springback models that can be used for an elastic-ideally plastic material. For work hardening material model can be used equation (2.17) to calculate bending moment (Wang, J. et al.2008).

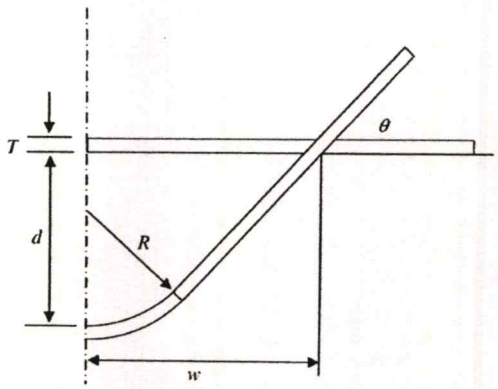

Figure 2.12 Approximation of bend geometry (Wang, J. et al.2008).

The springback can be predicted by mathematical model. Assuming the single curvature bend radius is tangent to two straight sections, the initial (loaded) bend radius R can be approximated from the tooling geometry, the material thickness, and the measured bend angle as shown in Figure 2.12 by this equation.

$$R = \frac{w \tan\theta_1 + \frac{T}{2} - d}{\sec\theta_1 - 1} \tag{2.18}$$

Where w is the approximate half die width, θ_1 is the loaded bend angle, and d is the punch travel depth with thickness offset.

2.4 Springback behavior

The value of high strength steel with higher stress than mild steel will have more elastic recovery at equal levels of strain, and consequently that makes higher springback tendency. Generally, amount of springback in AHSS parts is greater than amount of springback in mild steels. The springback is a function of flow stress show in Figure 2.13. The three type of springback found in channel and rail component parts are springback angle, curl and twisting.

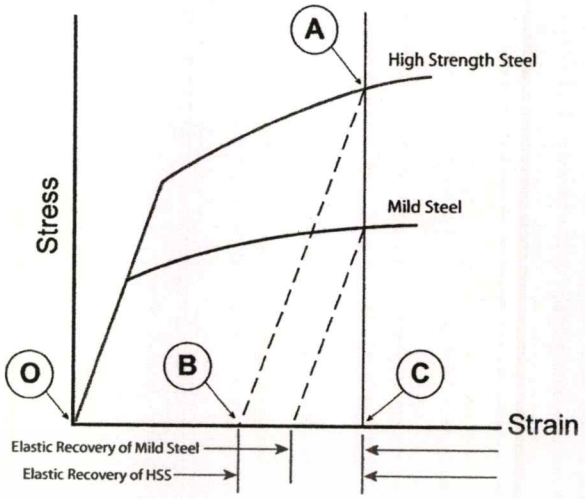

Figure 2.13 Diagram showing amount of springback is proportional to stress (World Auto Steel. 2009).

2.4.1 Springback angle

When an AHSS steel sheet is deformed (loading) and removed from die (unloading), the shape of the part always deviates from the shape of punch and die as shown in Figure 2.14. This shape deviation is loosely called springback.

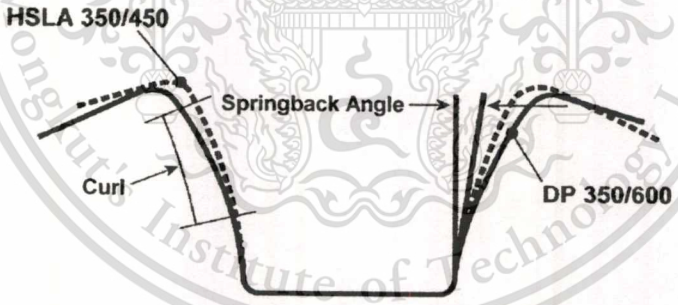

Figure 2.14 Springback behavior is angular change and sidewall curl (World Auto Steel. 2009).

2.4.2 Curvature of sidewall curl

AHSS is known to exhibit sidewall curl deflect. The cause is uneven stress distribution in sheet metal from bending and unbending over die radius. The elastic recovery difference in side A and side B is main cause of deviation in sidewall curl. The higher strength of sheet metal is the great magnitude and difference in elastic recovery between side A and B and increase sidewall curl in Figure 2.15.

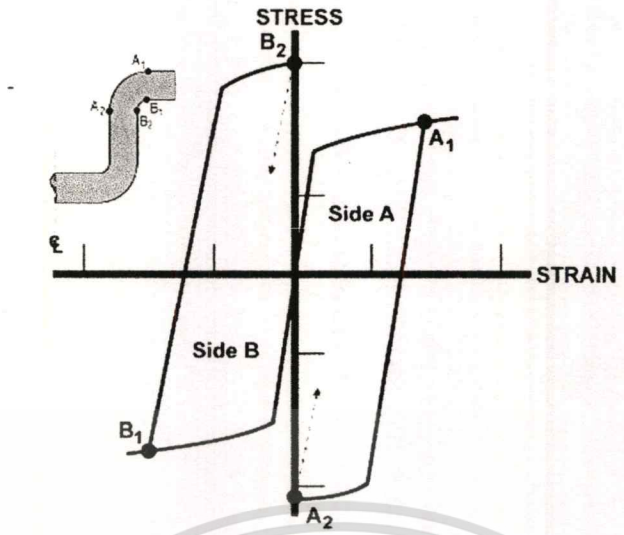

Figure 2.15 Bauschinger effect (World Auto Steel. 2009).

2.4.3 Twisting angle

Twist is defined as cross section rotating differently along axis. Twist is caused by torsion moment in cross section. The twist is generated by unbalance springback and residual stresses in part. The torsion moment can come from in plane residual stress in flange, sidewall or both as shown in Figure 2.16.

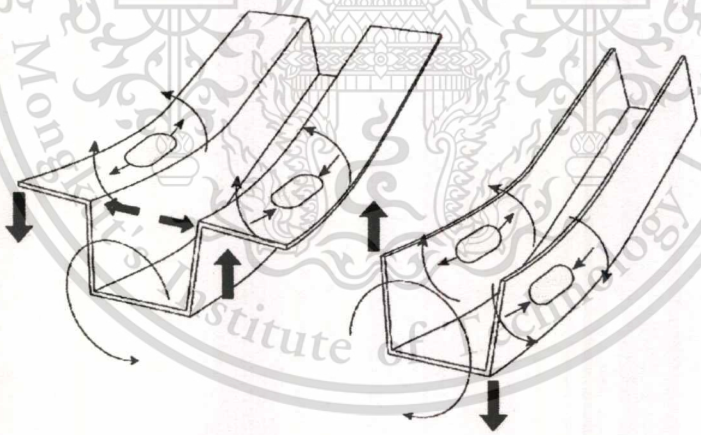

Figure 2.16 Twisting behavior of channel component (World Auto Steel. 2009).

The tendency for part to twist can be overcome by reducing imbalance in residual stresses. Unbalanced forces are likely to happen in unsymmetrical parts and in parts with changing cross section areas. Though in geometrically symmetrical parts, unbalanced force can be generated by strain in parts are. Some common causes of non-symmetrical strains in symmetrical parts are uneven blankholder force, lubrication or blank placement.

2.5 Springback prediction using FEM

2.5.1 Adaptive Remeshing

In adaptive remeshing, the size of elements in the blank is changed during the forming analysis in order to place elements are needed most in the right place. Figure 2.17 4-noded shell elements can be subdivided into 4 smaller 4-noded shells

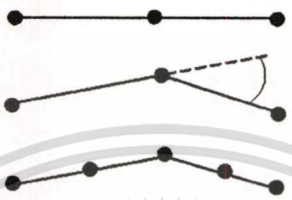

Figure 2.17 Adaptive remeshing(Galbraith, P.C. 2004).

After the forming simulations were completed, it was clear that the adaptive and non-adaptive models provided different results. Figure 2.18, the effective plastic strain is plotted on the deformed geometries from the two simulations. As Figure 2.18 shows, the general pattern of strain is very similar, but the peak values were different between models. The non-adaptive mesh, with small elements throughout the analysis, showed a greater tendency to wrinkle, and slightly higher plastic strains as a result.

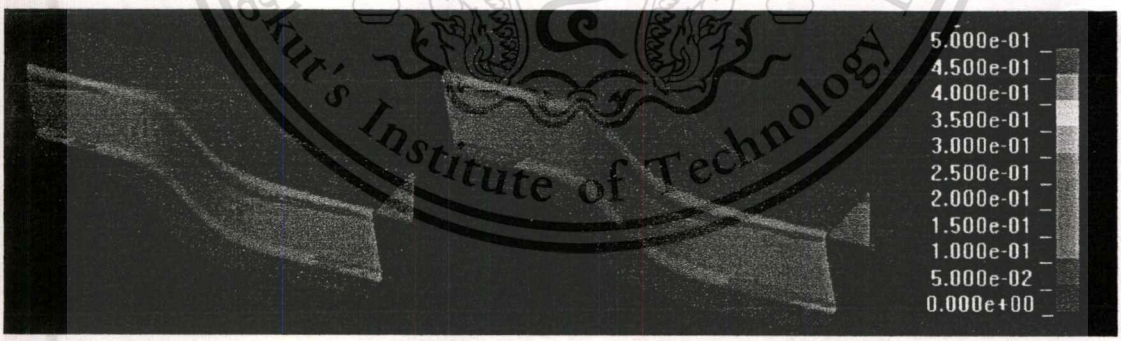

Figure 2.18 Contours of effective plastic strain are plotted on the forming models. Left Adaptive mesh and Right Non-adaptive mesh. (Galbraith, P.C. 2004).

2.5.2 Number of Integration Point

The sensitivity of springback prediction to the number of integration points through the shell thickness was even more dramatic and contrary to typical forming simulation practice. As shown in Figure 2.19, many integration points are required to obtain springback results within 1% of

the limiting case (with sufficient integration points that springback angle no longer changes with additional points).Although Figure 2.19 shows that for two cases the minimum number of integration points is 21 or 35, depending on back force, 51 integration points were required to ensure springback numerical accuracy within 1% of the large-number limit for all of the springback cases simulated (Wagoner, R.H. and Li, M. 2007).

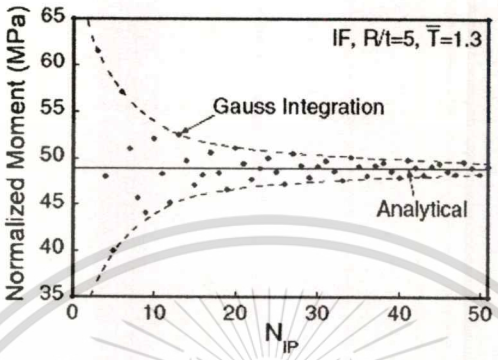

Figure 2.19 Variation of normalized moments with number of through-thickness integration points (NIP) (Wagoner, R.H. and Li, M. 2007).

The U-bending process in NUMISHEET'93, the author found effect of number of integration point is too many or too few a number of integration point has disadvantage for the explicit solution in springback simulation. Usually seven integration points is rather optimum value (Xu et. al. 2004).

2.5.3 Element size

The element size has a direct influence on the stress field after forming. Especially, the size of elements of the contacting the radius of the tooling will represent. The effects of the bending affect the springback. Therefore, the number of element on radius of tooling was significant to determine the optimum of number of element on radius of tooling. In experiment of author, the number of element on radius of tooling was investigated that are 3,5 and 7 element on radius. The element size is sensitive in springback simulation. (Xu et. al. 2004)

2.5.4 Constrains

All static simulations, including implicit springback analysis, require that rigid body motions be eliminated by defining constraints. These constraints are required since dynamic inertia effects are not included in a static analysis. Without constraints, a tiny applied load would cause the entire work piece to move rigidly (Maker, N.B. and Zhu, X. 2001).

Enough constraints must be defined to eliminate six rigid body motions in the model – three translations and three rotations. In theory, this could be accomplished by constraining all six

degrees of freedom at a single shell element node point. In practice, numerical truncation error is introduced when rotational degrees of freedom are used to eliminate rigid body motion. The recommended method is therefore to constrain selected translational degrees of freedom at three nodes.

The three constraint nodes should be chosen well separated from each other, and away from edges and flexible areas in the part. The first node "A" receives constraints to all three translational degrees of freedom, and defines the reference point in the model where springback displacements are zero. The second node "B" is located away from node "A" along the global X-direction. Constraints are applied at node "B" to eliminate global Y- and Z-translation. The third node "C" is located away from node "A" along the global Y-direction. Only the global Z-translation is constrained at node "C". Figure 2.20 shows a diagram of the location of these nodes on the model.

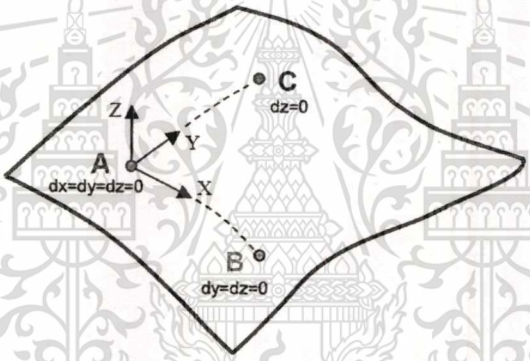

Figure 2.20 Diagram showing location of constraint nodes on a typical springback model (Maker, N.B. and Zhu, X. 2001).

Some stamping models are symmetrical shape, such as a hood or deck lid. In these cases, symmetry constraints are applied along one edge of the mesh. To eliminate rigid body motion during springback for these parts, constraints need only be added to two nodes chosen on the symmetry plane: completely constraining all translations for the first node, and eliminating one additional in-plane motion for the second node. Over-constraining a symmetric model by choosing three nodes according to Figure 2.20 can lead to incorrect results. Figure 2.21 shows an example for the case of symmetry in the X-Z plane.

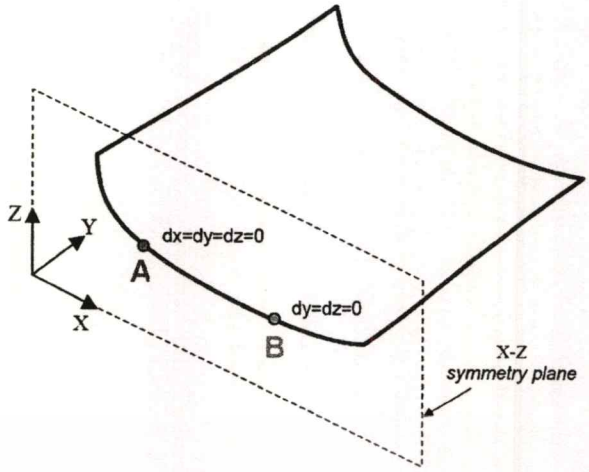

Figure 2.21 Diagram showing location of constraint nodes for a symmetric part (Maker, N.B. and Zhu, X. 2001).

2.5.5 Time Step size

In dynamic explicit codes, the time step depends on the material density and minimum mesh size. It is necessary to use mass scaling together with adaptive mesh refinement to avoid too small of a time step and high computational cost. Generally, a non-mass scaling model should have more accurate results, because it has no additional inertial force incurred by the added mass. In springback prediction, the time step size is crucial parameters affecting accuracy of springback simulation. The time step size was investigated effect of mass scaling. The mass scaling was various form no mass scaling to 12 time of mass scaling, the optimum of time step was 3.0 e^{-7} which used baseline model to compare springback accuracy with another case (Yao. Et al. 2002)

2.6 Springback Reduction

2.6.1 Die design

Figure 2.22 show die design for advance high strength steel parts with more complex geometry, a die process using upper and lower pads may be required. A lower pad delayed return system must be employed with this two-pad process in order to avoid upstroke deformation of the part. Post radii should be small to reduce spring back on walls. Flange radii may need to be slightly larger

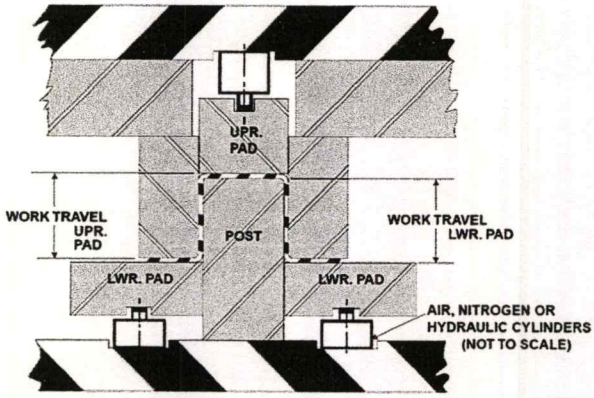

Figure 2.22 Form Die Draw Action (Auto/Steel Partnership. 2000).

The form die draw action uses a lower pad with a lock step and high pressure to stretch the part over the die post before the die bottoms. The lower pad has only minimal travel, enough to stretch the part sidewalls at least 2%; this process can be very effective in reducing springback and sidewall curl of AHSS stampings that do not have severe compression flanges shown in Figure 2.23

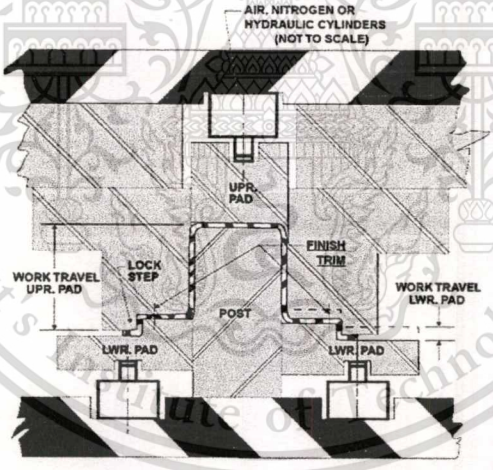

Figure 2.23 Post-Stretch Form Die (Auto/Steel Partnership. 2000).

In Figure 2.24 shows feature of drawbead for AHSS, the draw beads should not extend around corners of the draw die. This will result in locking out the metal flow and cause splitting in corners of stamping. Draw beads should "run out" at the tangent of the corner radius to minimize metal compression in corners

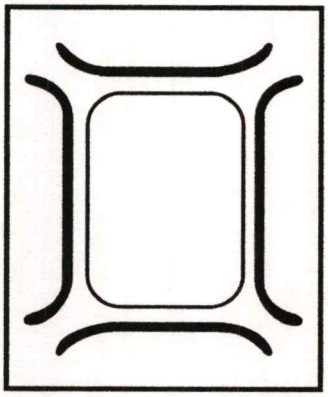

Figure 2.24 Run out drawbead for AHSS (Auto/Steel Partnership. 2000).

2.6.2 Blank holder force

Blankholder force control. The method is based on increasing or decreasing the binder force during forming in the sheet metal. Various studies were performed to investigate the proper profile of the blankholder force during forming. These authors, which are Chirita and Pourboghrat, investigated the impact of these parameters on the springback appearing in a 2D U-draw bending using constant blankholder forces as shown in Figure 2.25. The springback was decrease by increasing tension in the material.

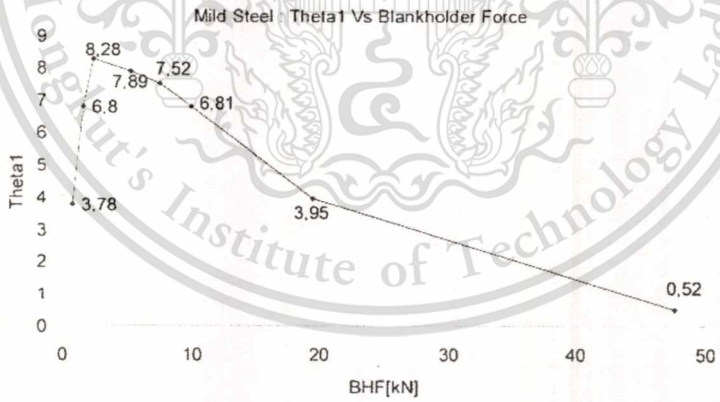

Figure 2.25 The springback angle VS. constant blankholder force (Papeleux, L. and Ponthot, J.P 2002)

However, the constant blankholder force has a limitation which affects that quality of part thickness. While the tension in the material increases the thickness of part is reduced. The forming quality of parts using variable blankholder force was better than constant blankholder force for both in avoid fracture and reduce a springback angle (Liu et. al. 2002 and Du C. et. al. 2004)

2.6.3 Multiple step forming

Forming of a product is performed by means of several tool sets or by means of one tool set with some additional mechanisms. Typical examples of this type of operations are redrawing, or "bottoming" (Chou, I.N. and Hung, C. 1999). The process of "bottoming" is shown in Figure 2.26. The major idea behind the method is to use the springback caused by making the bottom curved to compensate the amount of springback in the wall.

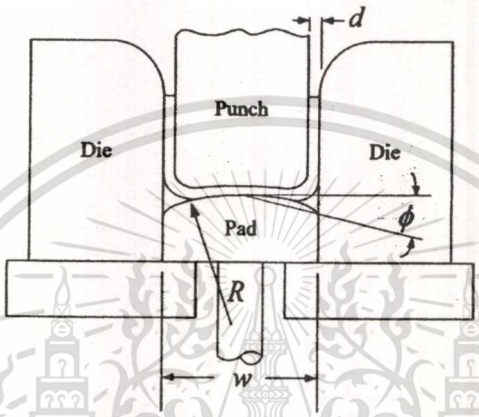

Figure 2.26 Arc bottoming (Chou, I.N. and Hung, C. 1999)

The spanking, it uses effect double bend technique to reduce springback. After the first operation of the U-channel bending process using a punch with radius *R*1, the part was re-strike with a second punch radius *R*2 that is used in the following operation in Figure 2.27.

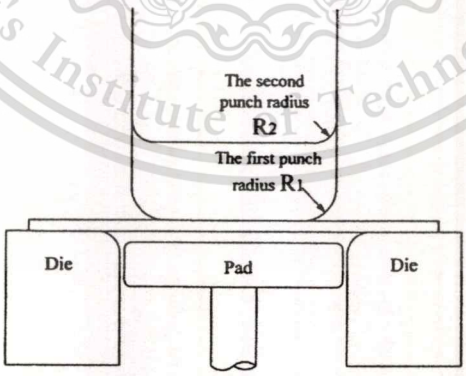

Figure 2.27 Spanking (Chou, I.N. and Hung, C. 1999)

The basic concept of the pinching die method is that a bead will be placed on the punch to locally compress the material which can compensate the springback as shown in Figure 2.28.

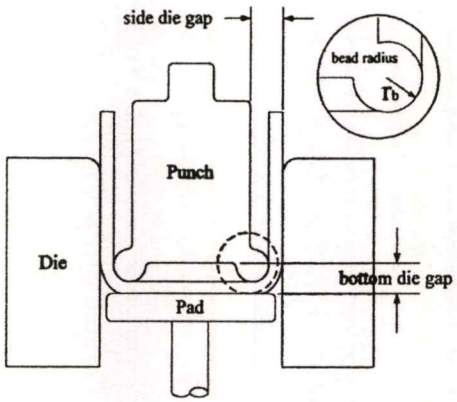

Figure 2.28 The pinching die (Chou, I.N. and Hung, C. 1999)

2.6.4 Springback compensation

The compensation methodology can reduce deflection of the formed product by carry out the suitable modifications of the tools. The modification of the tool geometry is based on the results of simulations or the measurements of the part after forming. They are several methods available for springback compensation.

Spring forward. According to this method, the forces affect the tools at the end of forming stage. These forces are applied to the target geometry, and a finite element simulation is carried out. The shape obtained from the result of simulation is considered to be the desired shape of the tool geometry, which can compensate springback (Karafillis A.P. and Boyce M.C. 1996; Wagoner R.H. and Gan W. 2004). It can occur that the desired shape. In this case, the procedure is repeated with the new forces, obtained from a new simulation with the tools' geometry obtain after first iteration. The algorithm continues until there are no deviations from the desired shape of the part

Displacement adjustment. According to this method, the difference between the desired and obtained shapes is calculated first. The obtained displacement is multiplied with a specific compensation factor. The geometry of the tools is compensated by a result. The compensation factor depends on the geometry of the desire product and material. Based on the results of the first iteration another it can be started to reach the desired shape of the product (Lingbeek R. 2005; Wagoner R.H. and Gan W. 2004).

Surface controlled overbending. According to this method, this method is also based on the displacement adjustment method. The coefficient of surface geometry can be input for a displacement adjustment process, producing compensation geometry. Bezier and B-spline surfaces were used to compensate geometry, because they are capable of modeling complex shapes while remaining stable (Lingbeek R. et. al. 2005).

The advanced high strength steels (AHSS) such as dual-phase steels are becoming widely used in many applications in place of mild steels, especially in automotive parts manufacturing, owning to its lightweight, high strength and good formability. However, the obstacle of AHSS sheet metal forming is springback, which is referred to as the geometry changes of a part after tool removal. This behavior can be the major cause of assembly problems.

The quality of part depends on proper process parameters such as material, blankholder force and other process parameters. In order to understand springback behavior, experimental try-outs & error or simulations are used. Now, the sheet metal forming simulation is usually used to evaluate a forming process, and reduce cost and time compensation in the design process. Force, fracture and thinning can be obtained using simulation.

Presently, the numerical analysis is not accurate to predict the springback of forming part. The reason for inaccurate springback prediction is that this behavior is inaccurately represented in finite element formulations. Inaccuracy material property introduces the modeling error. In addition, the accuracy of the springback prediction is affected numerical parameters of the forming simulation. Chosen element size, adaptive tolerance, number of integration point and time step size can be other reasons for significant deviation of the springback prediction.

Currently, the researchers make an effort to improve springback reduction. The springback depends on material property, material thickness and process parameters such as die geometry, forming process (blankholder force and part lubricity). In order to reduce springback systematically, process parameters are used to investigate effect springback reduction, which can be a powerful device for reduce a springback problem in the industry. The objective of literature is to understand a springback to study numerical parameters for accurately predict a springback and to study process parameter effects for development of die design for springback reduction.

CHAPTER 3

RESEARCH METHODOLOGY

This research is an investigation on parameters affecting springback after forming process of advanced high strength steel sheets (AHSS). First, were determined effects of numerical parameters on springback prediction accuracy by using FEM. The parameters studied are element size, adaptive tolerance degree, number of integration point and time step. Second, experiments were conducted to study process parameters affecting springback, which are variable process parameters such as punch radius, die radius, tool gap and blankholder force. Simplified parts were used to investigate the numerical parameters and the process parameters by using both U-shape and Butt-shape models. The materials was used in the experiment that is advance high strength steel sheets (sphc590) to achieve the objectives and scope of this research. The procedure of research is as follows.

1. Study tools and equipment used in research.
2. Study materials properties used in the experiments.
3. Study the forming process.
4. Learn how to use Dynaform.
5. Conduct tensile test on SPHC 590.
6. Run springback simulations for numerical parameter investigation.
7. Conduct of experiment, collect and analyze the data
8. Summarize die design guidelines.

3.1 Numerical Investigation

3.1.1 U-shape and Butt-shape Die Design

The U-shape and Butt-shape simulation setup consist of die, punch, binder, pad and blank specimen. In Figure 3.1, the numerical parameters were conducted to investigate affecting accuracy of springback prediction by using simulation set up. In this study, simplified part geometries, which are U-shape and Butt-shape, were used for forming and springback simulations. The geometry of U-shape resembling to rail components and pillar-like Butt-shape were chosen to examine part springback angle, curvature of sidewall curl, and twisting. The

punch and die radii of the U-shape and Butt shape are 12 mm. which is 10 times of its thickness. Figure 3.2 shows the geometry of U-shape and Butt-shape.

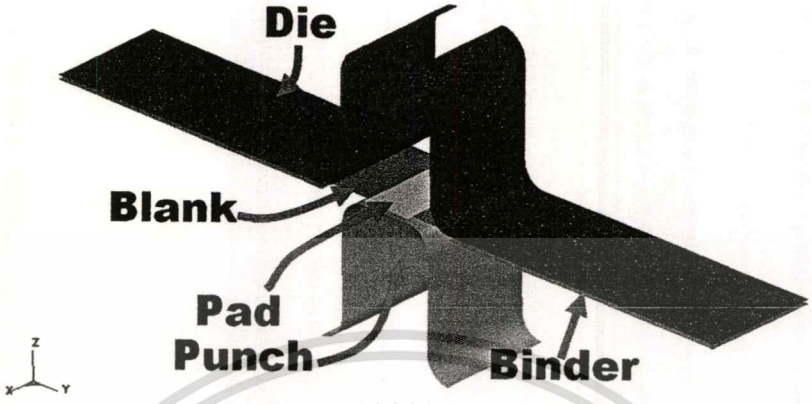

Figure 3.1 The U & Butt-shape simulation set up

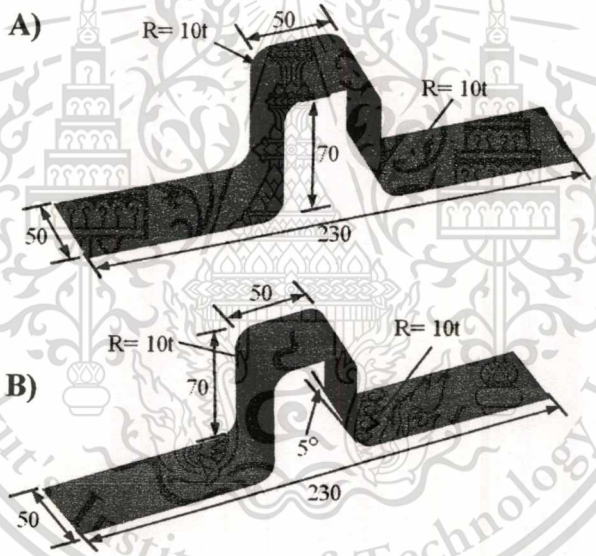

Figure 3.2 Simplified models for numerical investigation A). U-shape model B). Butt-shape model

3.1.2 Numerical Parameters Investigation

An array of U-shape forming and springback simulations was conducted to investigate numerical parameters affecting accuracy of springback prediction. The procedure of numerical parameter investigation followed was to study one parameter at a time, shown in Figure 3.3, in such an order that interactions between these parameters are made minimum. First, effect of element size is investigated, and then a proper element size is chosen to analyze effect of adaptive angle tolerances. The proper element size and adaptive angle tolerances are chosen to

further analyze effect of number of integration point. Then, effect of time-step size (mass scaling) is studied with a proper set of previously determined parameters. The detail of numerical parameters condition used to investigate effect of accuracy of springback prediction is shown in Table 3.1.

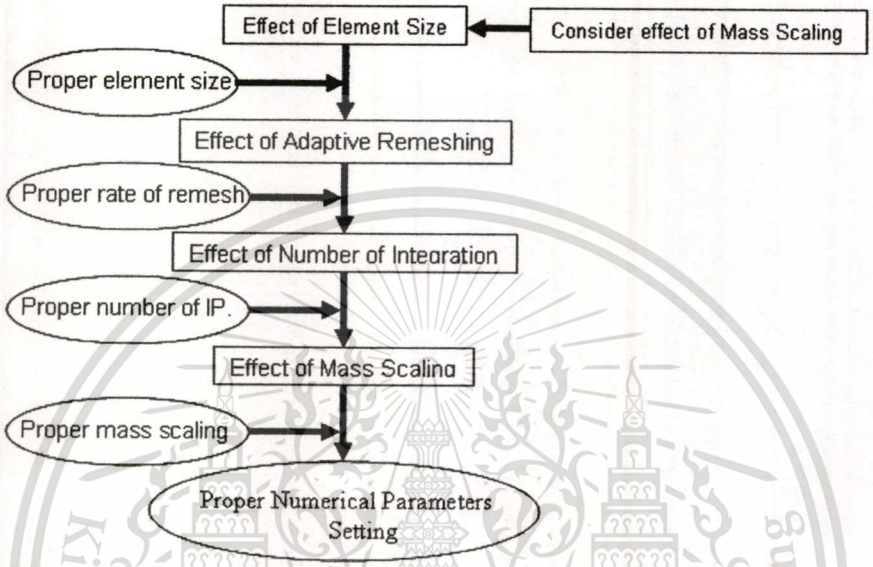

Figure 3.3 Procedure of numerical investigation for springbcak simulation

Table 3.1 Numerical parameters condition

Numerical parameters	Condition
Element size	3, 4, 5, 7, 9 deg : the turning angle per element over die radius
Adaptive angle tolerance	1, 2, 3, 4, 5 deg
Number of integration point through thickness	5,9,25,41,57,73,89,105,121,137,153,169,185,201,217,233
Time step size	0, 3e-7, 6.37e-7, 1.145e-6, 1.165e-6, 2.16e-6

3.1.3 Process Parameters Investigation

In this investigation on springback simulation, a proper set of previously determined numerical parameters were used to conduct springback simulation to investigate effect of blankholder force. Simplified part geometries, which are U-shape and Butt-shape, were used for investigation effect of BHF. All the trial BHF profiles can be grouped in two; first BHF is kept constant throughout the forming stroke – "constant BHF profiles", and second BHF is kept constant up to certain forming strokes then increased linearly up to the end stroke – "variable

BHF profiles" as shown in Figure 3.4. For each part geometry all constant BHF profiles are bounded by the lowest BHF, which is 10 tons as it is the lowest BHF available in our hydraulic press, and the highest BHF, by which the part can be form without necking. It was found that the highest BHF is 20 tons for U-shape and Butt shape. Most of the trial variable BHF profiles run between these lowest and highest values of BHF applied in the cases of constant BHF. However, two variable profiles exceeding the highest BHF value were applied without any part fracture.

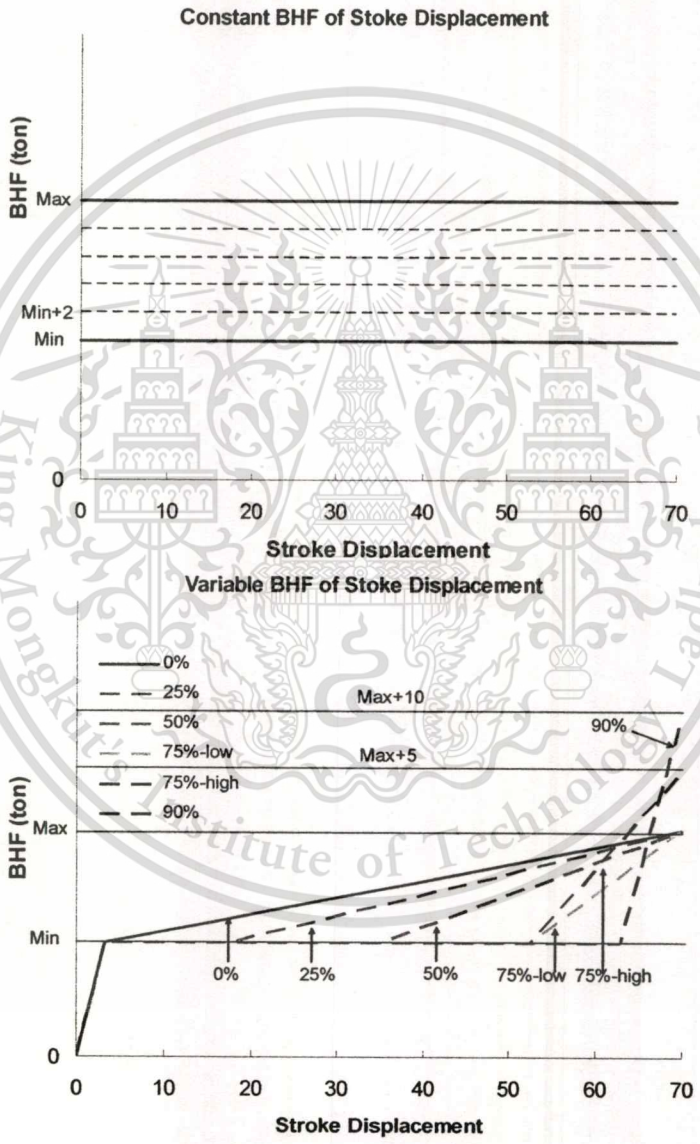

Figure 3.4 The schematic of blankholder force profile

3.1.4 Springback Measurement

The geometry of U-shape resembling to rail components was chosen to examine part springback angle, curvature of sidewall curl. Butt-shape was chosen to examine part springback angle, curvature of sidewall curl due to unsymmetrical of the model are occurred twisting angle. θ_1 is an angle that a straight line passing through point A, C makes to the referenced vertical axis. ρ is a curvature of the sidewall curl constructed by point A, B and C. θ_2 is a twisting angle that the part flange line makes to the referenced horizontal axis. All springback measurements are shown in Figure 3.5.

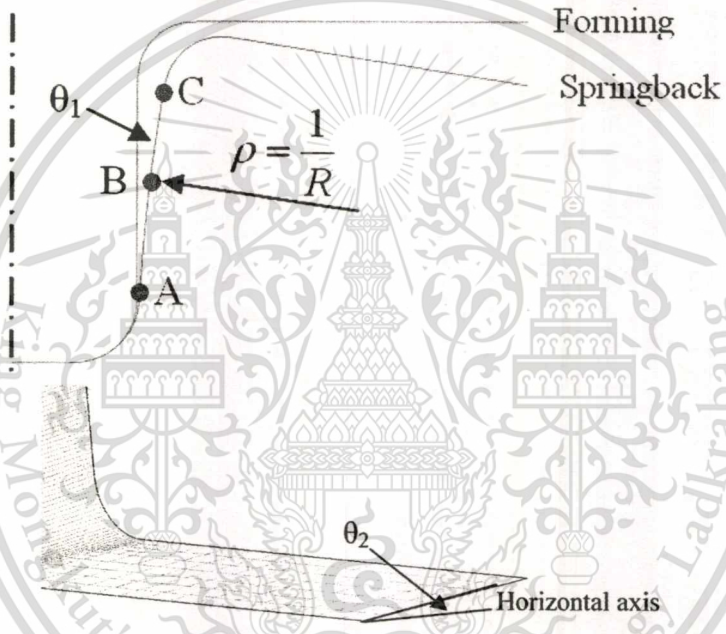

Figure 3.5 Springback measurement of U-shape & Butt-shape model

3.1.5 Air Bending Validation

In this research, Air bending simulation was selected to validate ability of simulation to predict the occurrence of springback against analytical solution and experiment. To prove the accuracy of simulation for study the effect of numerical parameters that affect accuracy in the prediction of the springback of U-shape & Butt-shape. Five final punch positions were used in the experiments that consist of 4.06, 6.60, 7.78, 8.38 and 10.41 mm., In Figure 3.6.

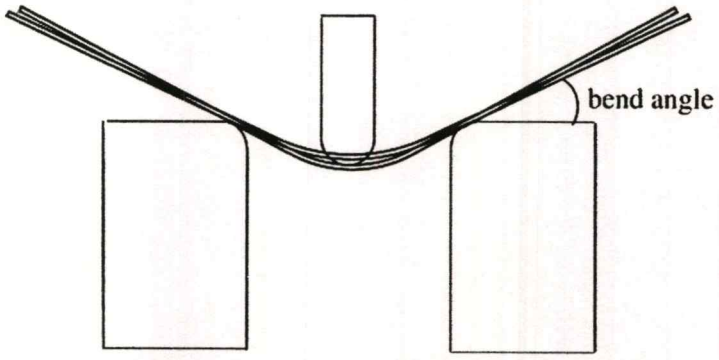

Figure 3.6 Springback air bending

In Figure 3.7, the measurements of interest are curvature (R) and springback angle (θ). The springback angle was measured to compare result from Wang. J, et. al., and the curvature of air bend simulation was measured to compare result with equation below.

$$R = \frac{w\tan\theta_1 + \frac{t}{2} - d}{\sec\theta_1 - 1}$$

Where w is approximated to be half of die width, θ_1, is the loaded bend angle, and d is the punch travel depth with thickness offset.

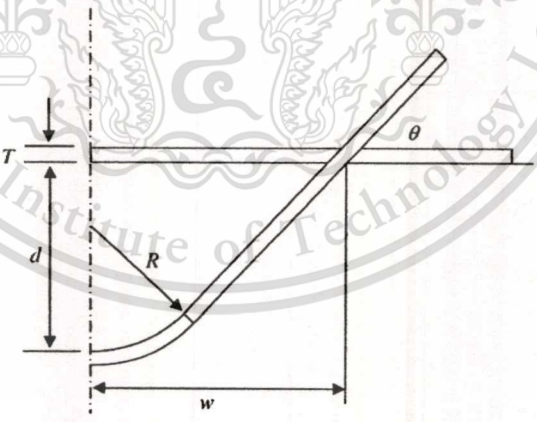

Figure 3.7 Aprroximate of bend geometry

3.2 Experimental Investigation

3.2.1 Experimental Die Set

A die set with interchangeable die component was designed and built to accommodate both U-shape die inserts and Butt-shape die inserts (i.e. die, binder and punch), as

shown in Figure 3.8. This die set was used to conduct forming experiments of U-shape parts and Butt-shape parts to investigate effect of process parameters. The upper die was consisting of die insert and pad as shown in Figure 3.9.

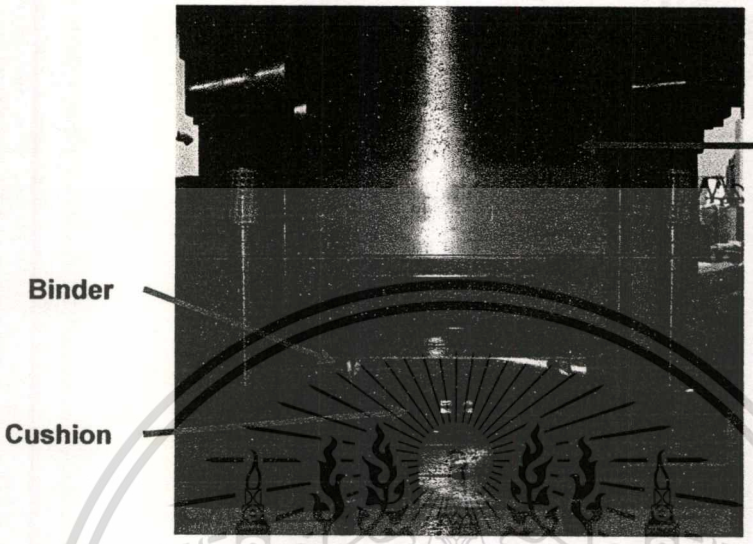

Figure 3.8 U-shape & Butt-shape die

Figure 3.9 Die insert and pad on upper die

The die set and punch insert set used in this research consist of 12 die inserts and 4 punch inserts, as shown in Figure 3.10 and Figure 3.11. Details of testing conditions were tested in different conditions as follows. The die set was used to conduct to determine process parameters which consist of die radius, punch radius and tool gap as shown in Table 3.2

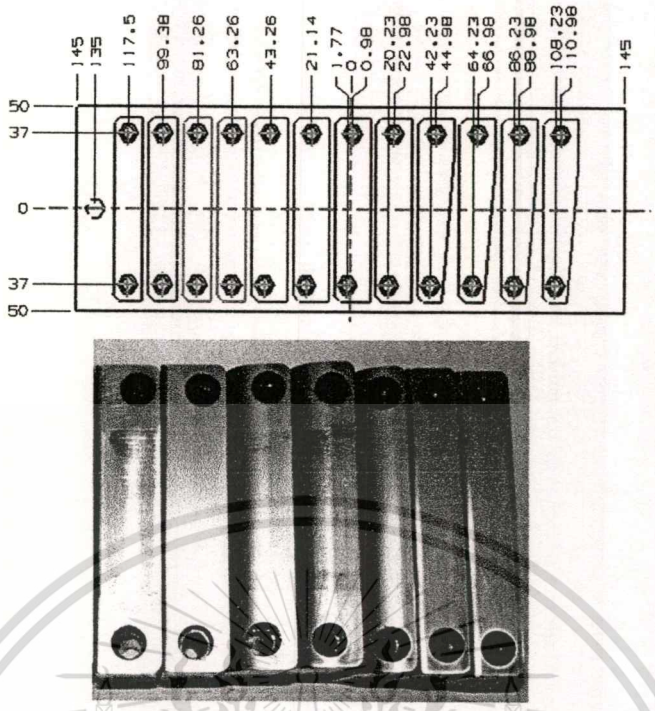

Figure 3.10 Die inserts used in springback experiment

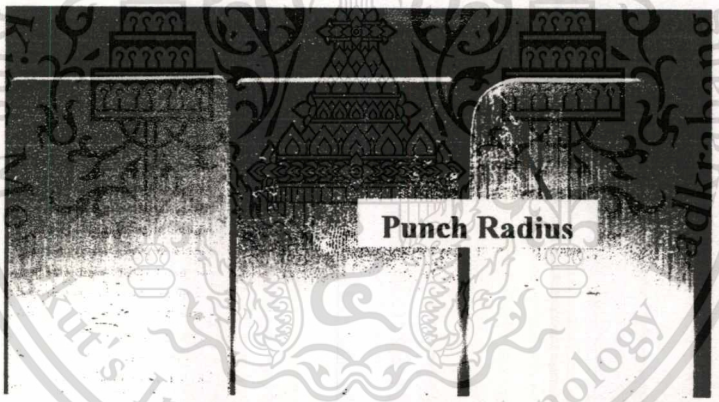

Figure 3.11 Punch inserts used in springback experiment

3.2.2 Experiment Plan

In this investigation on springback experiment, the springback experiments were conducted to determine the effect of process parameters which consist of punch radius, die radius, tool gap and BHF profile as shown in Table 3.2. First, the size of the punch radius used to study the effect of springback. The two sizes of punch radius are 2.4 mm. and 12 mm. (which are 2 times and 10 times the sheet thickness, respectively.) for use in investigation influence of these parameters. Second, the size of the die radius was used to study the effect of springback behavior which is 2.4 mm. and 12 mm. (which are 2 times and 10 times the sheet thickness, respectively.). Next, tool gap is variable parameters that were used to study the effect of springback which

includes gap size 1.2 mm and 1.32 mm. Finally, a variable parameters was used to study the process parameters that is divided the BHF has two profile, which are constant BHF and variable BHF as shown in Figure 3.4.

Table 3.2 Process parameters investigation

Process parameters	Condition
Punch insert	2.4 mm. (2 times thickness) / 12mm. (10 times thickness)
Die insert	2.4 mm. (2 times thickness) / 12mm. (10 times thickness)
Tool gap	1.2 mm. (1 times thickness) / 1.32mm. (1.1 times thickness)
Blankholder Force	Constant BHF (10 ton & 20 ton) / Variable BHF

3.2.3 Hydraulic Press

A 200 ton hydraulic press was used in all the springback experiments. The press is controlled by a CNC controller to achieve the Ram forming speed of 1 mm/s, which was used in all experiments as shown in Figure 3.12. The cushion force curve given to the controller can vary to follow any cushion force-stroke.

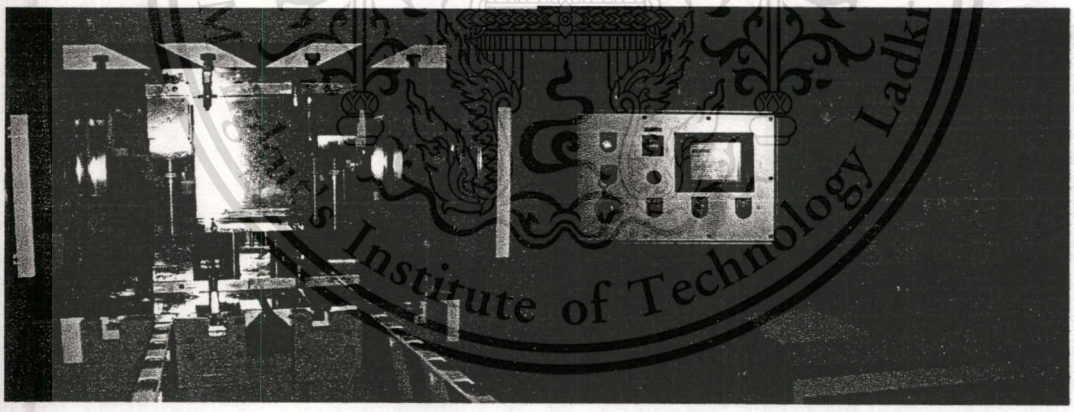

Figure 3.12 Hydraulic press

3.2.4 Tensile test machine

In Figure 3.13, the universal test machine dynamic type was used to test mechanical property of SPHC 590.These mechanical properties are very important parameters for prediction of springback simulation. Twenty-five pieces of sheet specimens, including three different direction (0°, 45°, 90°), were prepared to test their tensile properties including strain hardening

exponent(n), strength coefficient (k), ultimate tensile strength, anisotropy and elongation according to the ASTM standard (E8M) for determination of tensile properties.

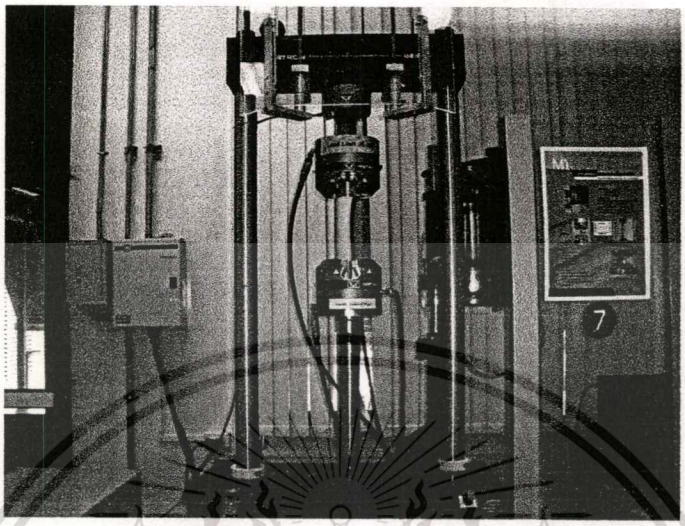

Figure 3.13 Universal test machine Dynamic type INSTRON 8801

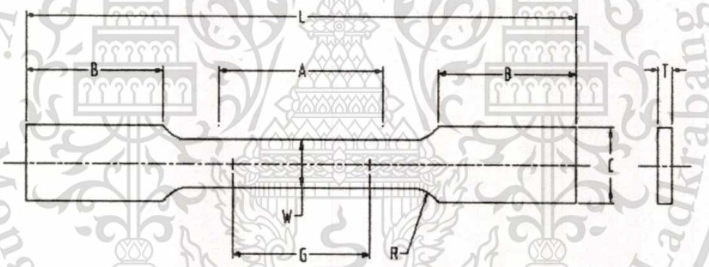

Nominal width	ASTM E8M Standard
	Dimension (mm.)
G – Gage length	50±0.1
W - Width	12.5±0.2
T - Thickness	Thickness of material
R – Radius of fillet, min	12
L – Overall length	200
A – Length of reduce section, min	75
B – Length of grip section, min	50
C – Width of grip section, approximate	20

Figure 3.14 Dimension of tensile specimen form ASTM standard

3.2.5 3D Scanner Optical Measurement

In Figure 3.15, a 3D scanner was used to scan all the formed specimens (i.e. U-shape and Butt-shape) to obtain accurate springback dimensions. Solidwork a CAD software, was used to measure these springback dimensions from the scanned part geometry.

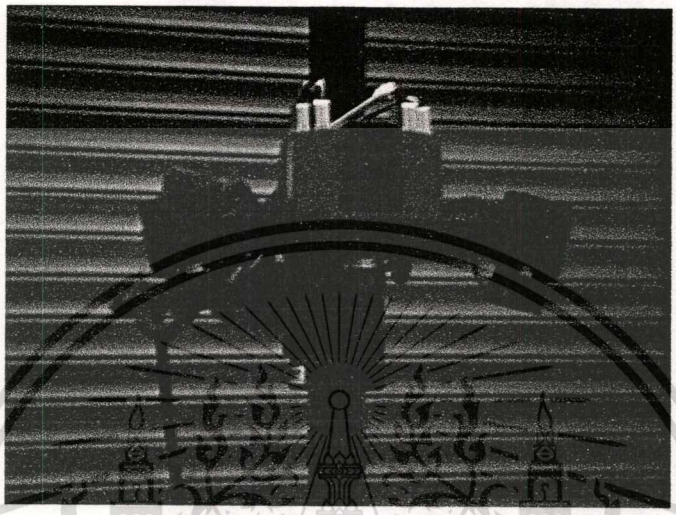

Figure 3.15 3D Optical scanner

3.2.6 Springback Test Specimens

Dimensions of springback test specimens are shown in Figure 3.16. These SPHC 590 specimens were formed in both U-shape and Butt-shape experiments. In all the experiments, the specimen was brushed on both sides with a "Renoform" lubricant. A measured amount of 1cc. of lubricant was applied on each side of the specimen before forming

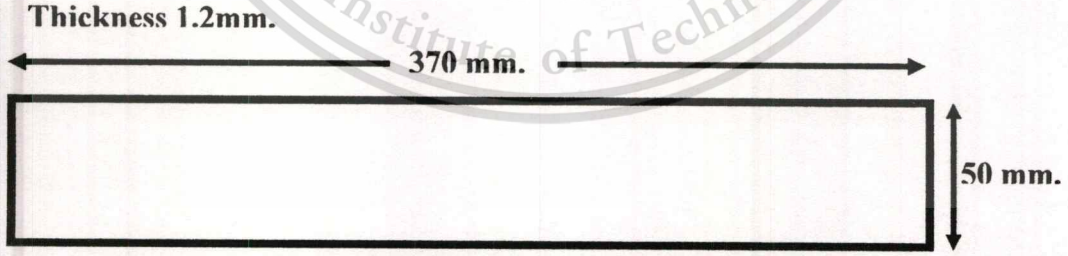

Figure 3.16 Dimensions of springback sepcimen

3.2.7 Thickness of Specimens Measurement

After forming process the experimental specimen thickness is measured thickness that is quality of work. To investigate the process parameters are occurred that reduce springback and remain the quality of work. The thickness measurement of specimen was measured on the side of

model at three points that are on, middle and lower by using the ultrasonic device as shown in Figure 3.17 .

Figure 3.17 Thickness measurement using Ultrasonic device

CHAPTER 4

NUMERICAL INVESTIGATION RESULTS OF EFFECT OF NUMERICAL PARAMETERS ON SPRINGBACK BEHAVIOR

This chapter discusses the results from the numerical investigation. First, numerical parameters used in FEA of U-shape and Butt-shape forming and springback were studied to understand their effects on the springback prediction. Second, FEA simulations were used to conduct an effect study of the process parameters, i.e. blankholder force.

4.1 Material Property

Tensile testing was conducted to obtain mechanical properties of SPHC 590 advanced high strength steel sheets, as shown in the table and figure. Figure 4.1, the results were used as input in the FE model to study numerical parameters that affect the accuracy of springback simulation on forming AHSS, and effects of blankholder force.

Table 4.1 Material properties SPHC 590

Yield strength 0.2% (YS)	365.13 MPa
Tensile strength (UTS)	661.02 MPa
Elongation (e_t)	25.8
Strain hardening exponent (n)	0.164
Strength coefficient (k)	1075.46 MPa
Young modulus (E)	207.22 MPa

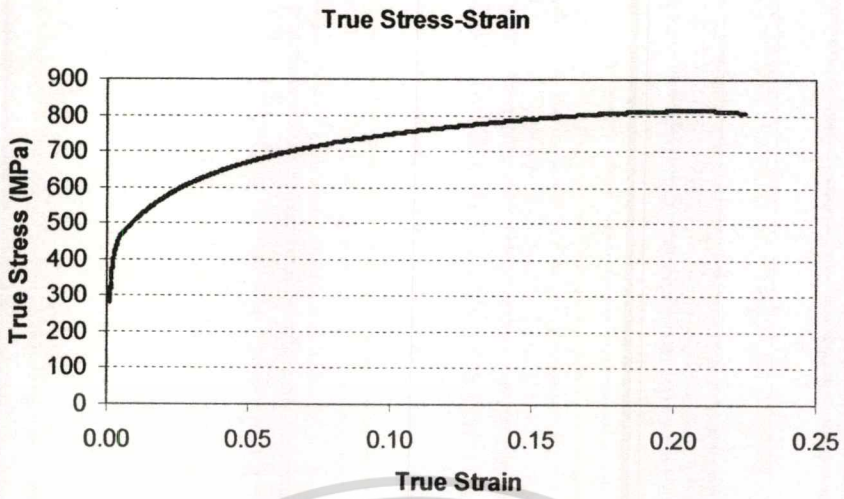

Figure 4.1 Flow curve of SPHC 590

4.2 The Effect of Numerical Parameters on Springback Simulation on U-shape

The U-shape part and Butt-shape with R_d = 10t and R_p = 10t was used in conducting the numerical parameters investigation. In Figure 4.2, the procedure of numerical parameter investigation followed was to study one parameter at a time. First, the effect of element size was investigated, and the proper element size was selected further investigate the effect of adaptive angle tolerance then proper element size and adaptive angle tolerance were chosen to investigate the effect of number integration point, and then the effect of time step size was investigated with the proper numerical parameters obtained previously.

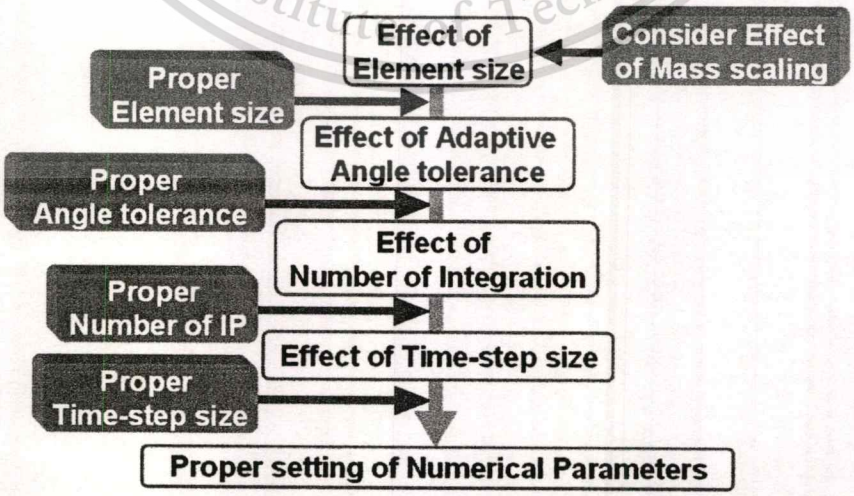

Figure 4.2 Flow chart of numerical parameter investigation

Figure 4.3, the springback measurement consists of 3 springback behaviors, which are θ_1 is an angle that a straight line passing through point A, C makes to the referenced vertical axis. ρ is a curvature of the sidewall curl constructed by point A, B and C using U- shape model. The butt-shape model was chosen to examine part springback angle, curvature of sidewall curl, and twisting angle θ_2 due to unsymmetrical of the model. The twisting angle is measured by the angle that the part flange line makes to the referenced horizontal axis. These measurements were used to investigate the effects of the numerical parameters affecting accuracy of springback prediction.

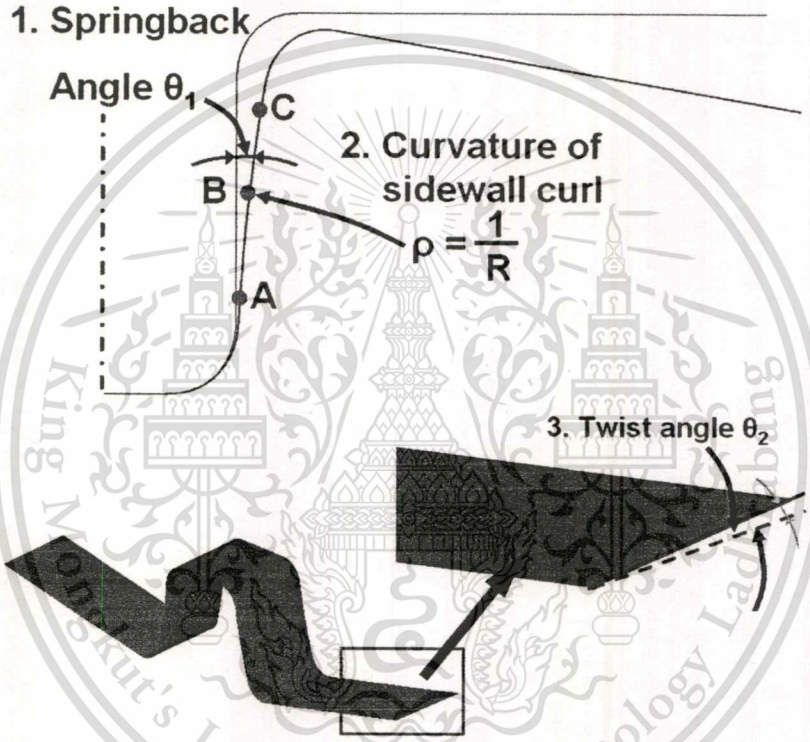

Figure 4.3 The springback measurement

4.2.1 Element Size

In this section, the investigated numerical parameter was an element size on turning angle over die radius. The die radius and punch radius were used to investigate the effect of the numerical parameters that is 12 mm. for study affecting accuracy of springback prediction. The element size was each 4 degrees on turning angle over die radius that has 1 element on there. The example of element size was show in Figure 4.4.

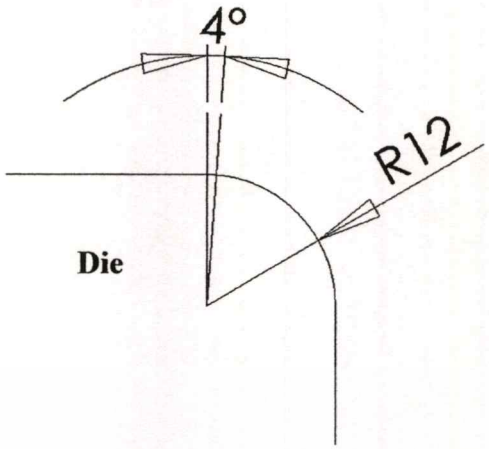

Figure 4.4 Schematic element size on turning angle over die radius

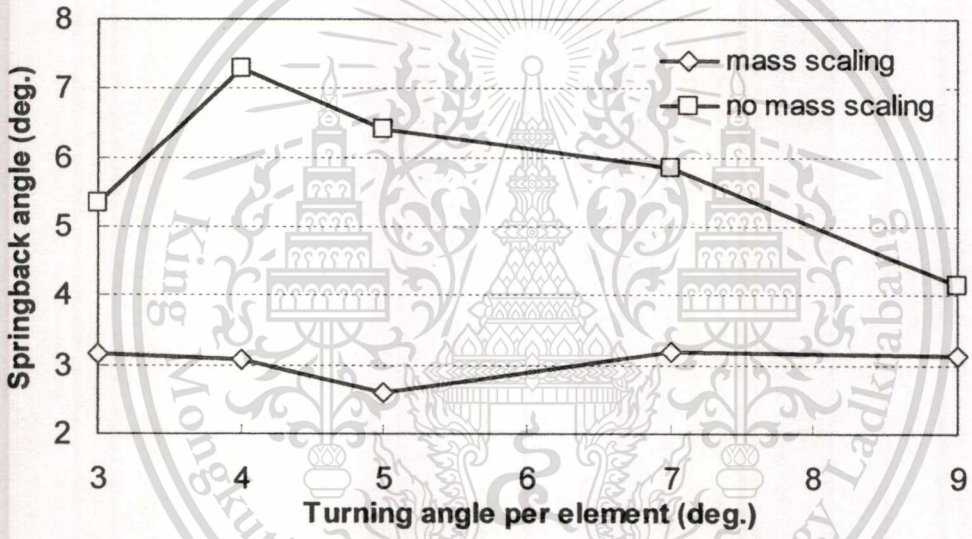

Figure 4.5 Effect of element size on springback angle

Figure 4.5 shows effects of element size and use of mass scaling on calculation of springback opening angle. The effect of mass scaling was consistent; simulations without mass scaling predicted more springback than with mass scaling for all the element sizes considered. Generally, a no mass scaling model should give more accurate results, because it has no additional inertial force incurred by the added mass. The element size per turning degrees of tool radii is known to greatly affect accuracy of springback prediction as it can better represent part geometry when it becomes smaller but at the expense of increased computation time, Figure 4.5. From the figure, springback seem to increase as the element size becomes smaller except at element size of 3 degrees. With the absence of experimental data, the size of element per 4 degree

seems to be a proper choice considering it giving maximum springback at reasonable computational time (about one third of the simulation with element size of 3 degrees).

Figure 4.6 shows effects of element size and use of mass scaling on calculation of curvature of sidewall curl. The element size per turning degrees of tool radii is known to greatly affect accuracy of springback prediction as it can better represent part geometry when it becomes smaller but at the expense of increased computation time as shown in Figure 4.7. Figure 4.6 from the figure, with the absence of experimental data, the size of element per 4 degree seems to be a proper choice considering it giving maximum curvature of sidewall curl at reasonable computational time

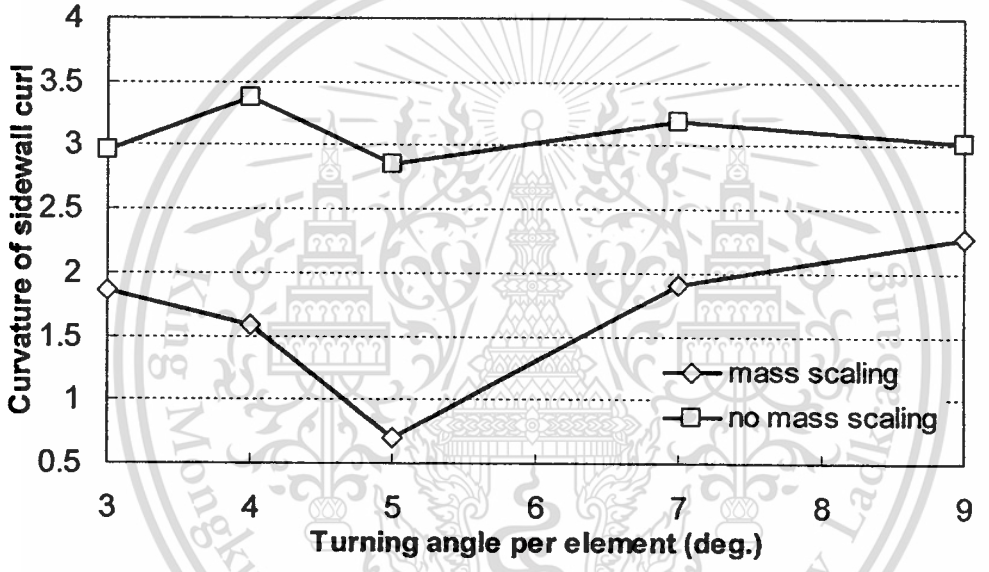

Figure 4.6 Effect of element size on curvature of sidewall curl

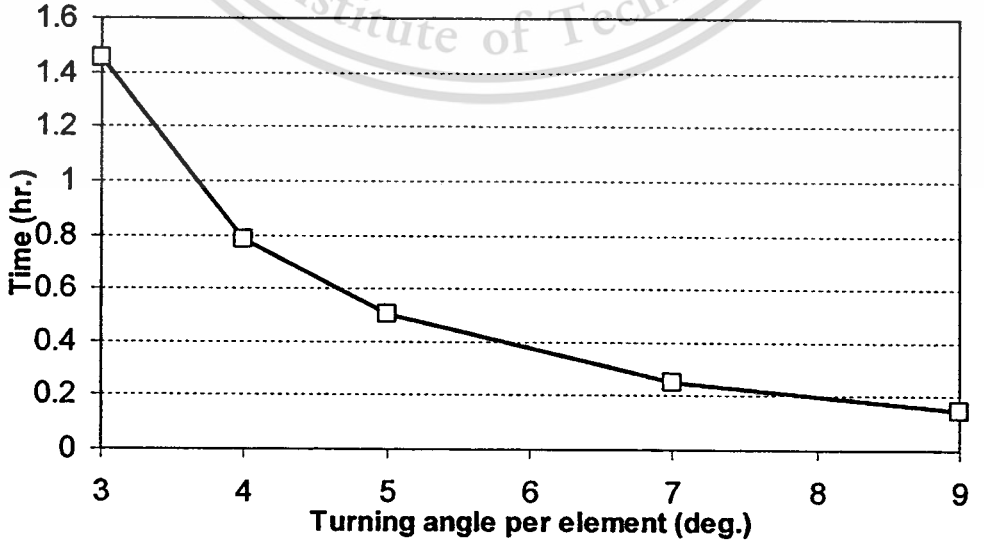

Figure 4.7 Computational time of springback simulation

4.2.2 Adaptive Angle Tolerance

The adaptive angle tolerance degree was rate of subdivision element size with significant area. When, the angle between elements exceeds tolerance value. The both element was separated 2 elements into 4 elements as shown in Figure 4.8.

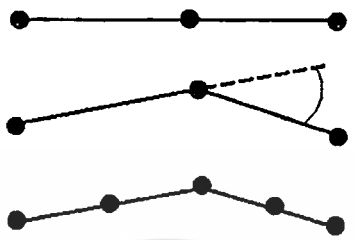

Figure 4.8 Schematic adaptive angle tolerance

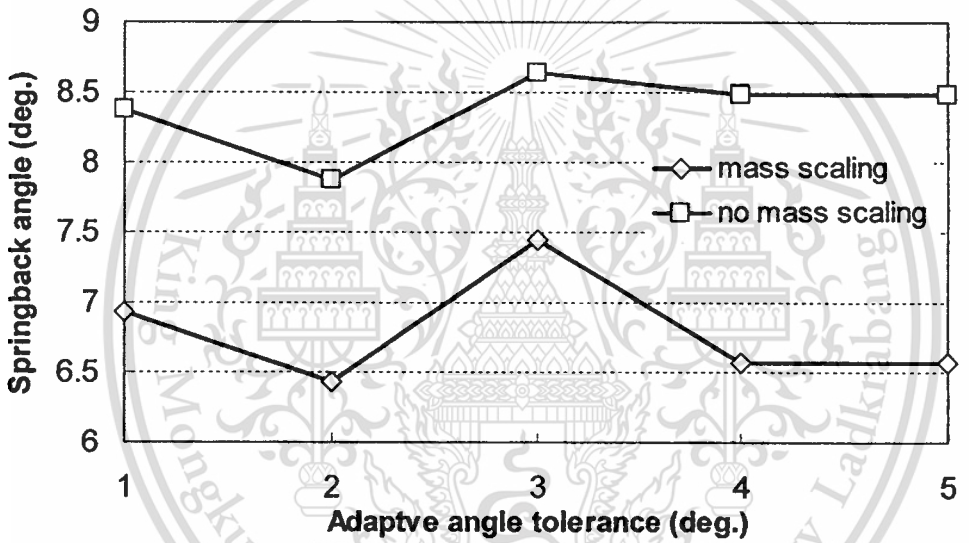

Figure 4.9 Effect of adaptive angle tolerance on springback angle

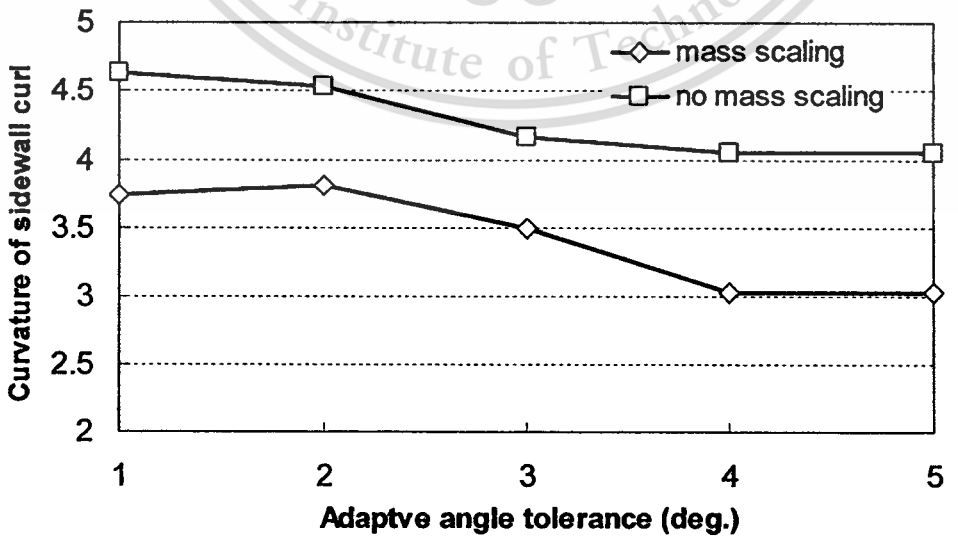

Figure 4.10 Effect of adaptive angle tolerance on curvature of sidewall curl

Figure 4.9 shows effect of adaptive angle tolerance, by which the part mesh is refined when the angle between any adjacent elemental normal vectors exceed. In the case without mass scaling simulation, the springback were again larger than the case with mass scaling for all the adaptive angle tolerance. The springback predictions are stagnant at first but later become larger as the adaptive angle tolerance is much smaller; elements become smaller at a faster rate. The small adaptive angle tolerance of 1 degree is much more sensitive to part geometry based mesh refinement than 5 degree tolerance. Therefore, 1 degree tolerance is chosen as a proper adaptive angle tolerance.

Figure 4.10 show the curvature of sidewall curl were larger than the case with mass scaling for all the adaptive angle tolerance. The springback predictions are stagnant at first but later become larger as the adaptive angle tolerance is much smaller; elements become smaller at a faster rate. The small adaptive angle tolerance of 1 degree is much more sensitive to part geometry based mesh refinement than 5 degree tolerance. Therefore, 1 degree tolerance is chosen as a proper adaptive angle tolerance.

4.2.3 Number of Integration Points

The springback behavior depends on bending moment. The number of integration point was used to observe stress distribution in though thickness direction that is number integration point is uneven numbers always as shown in Figure 4.11. The circles represent integration point on thickness of specimen.

Figure 4.11 Number of integration point though thickness direction

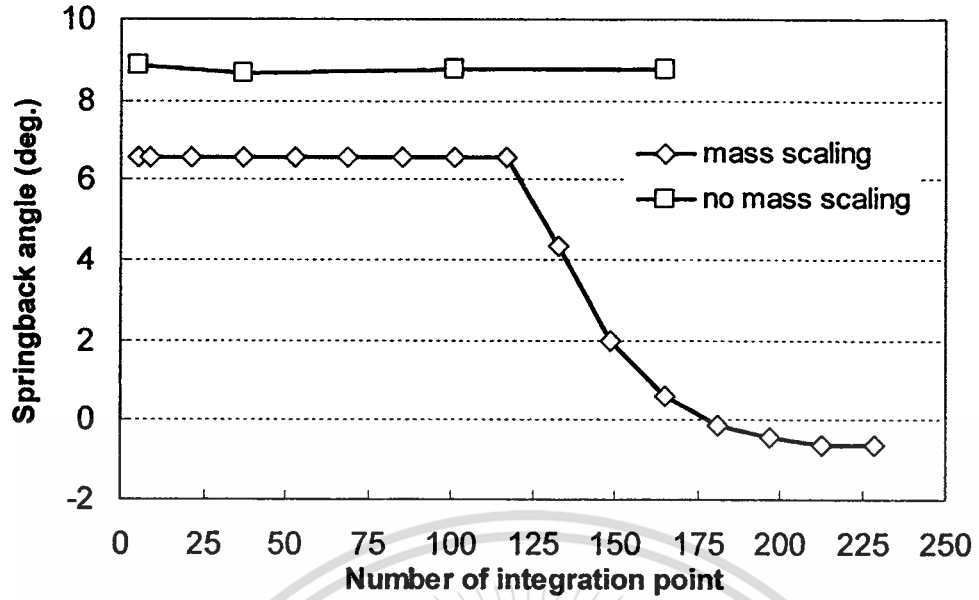

Figure 4.12 Effect of number of integration point on springback angle

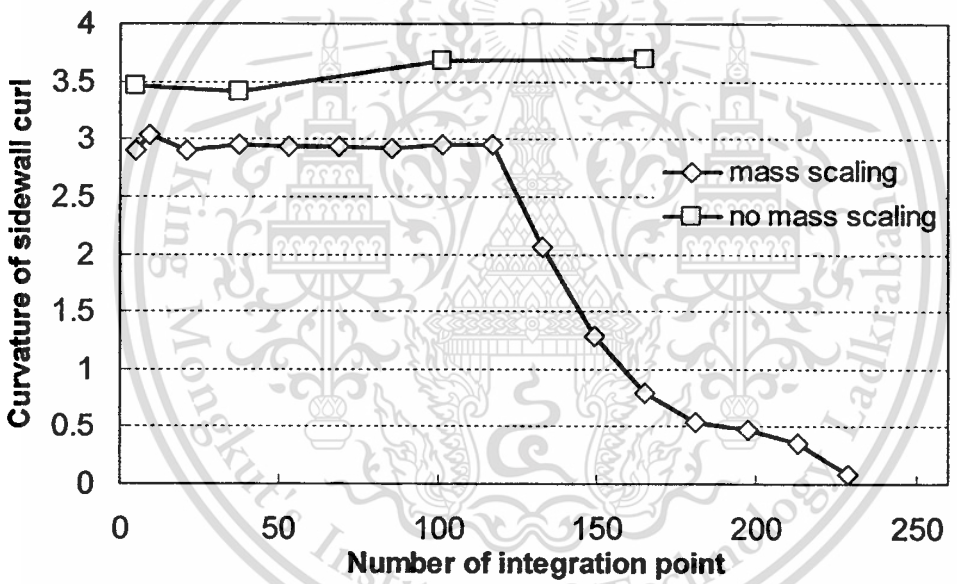

Figure 4.13 Effect of number of integration point on Curvature of sidewall curl

Effects of number of integration point through thickness were shown in Figure 4.12 and Figure 4.13. With no mass scaling applied, springback angle prediction seemed somewhat constant while the curvature of sidewall curl increased slightly as the number of integration points increased. Interestingly, it can be found from the figure that the proper number of integration point is low for springback angle calculation compared to that of curvature of sidewall curl calculation. Considering computational time spent, in this case, the number of integration point of 9 was chosen to be proper. The simulations employing mass scaling clearly

underpredicted the springback, especially when the number of integration point was larger than 125.

4.2.4 Time Step

In dynamic explicit code, the time step size depends on material density and minimum element size. The necessary time step size decreases as the mass scaling decreases requiring more computational time. Generally, non-mass scaling should have more accuracy results

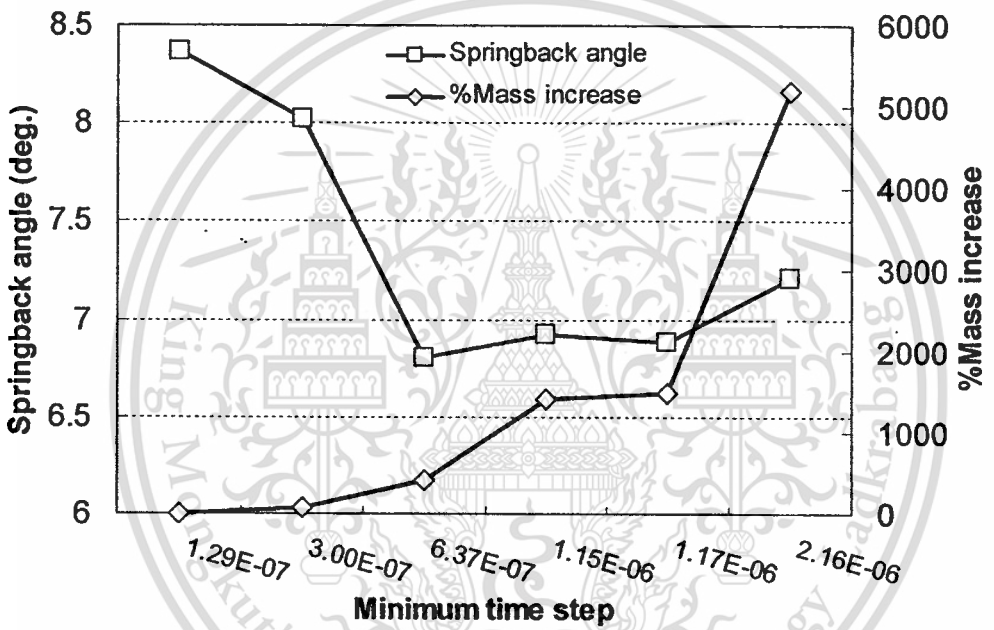

Figure 4.14 Effect of time step size on springback angle

Based on the simulation results up to this point, it is evident that simulations with mass scaling technique give erroneous springback prediction. However, it is usually more time-efficient to allow a careful application of mass scaling when adaptive mesh refinement is used to avoid too small of time step size leading up to extremely long computational time. Figure 4.14 shows relationship of mass scaling increase and time step size, and their effect on springback angle prediction. The necessary time step size decreases as the mass scaling decreases requiring more computational time

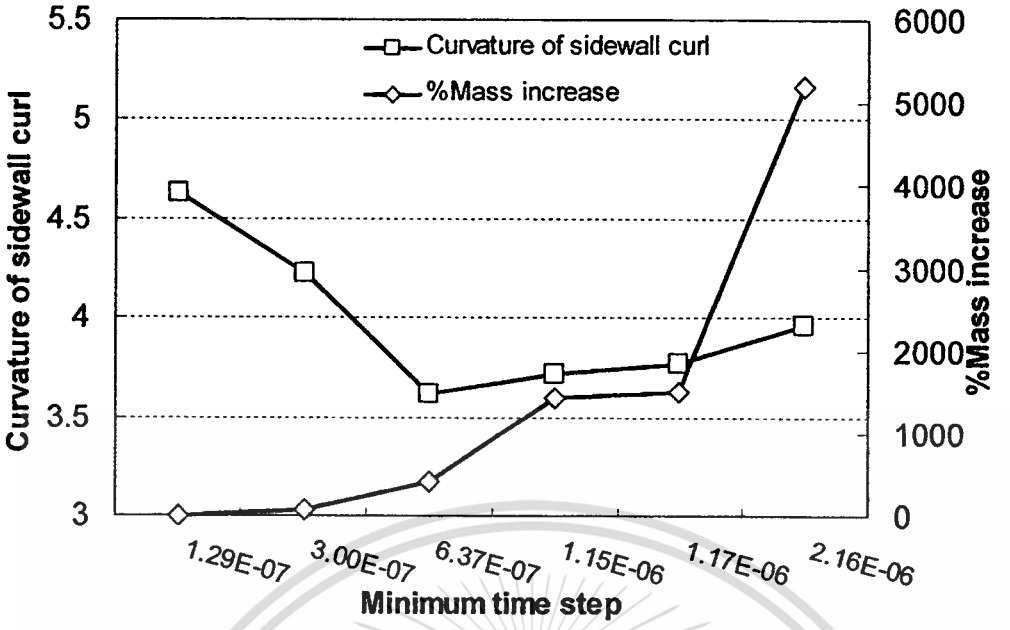

Figure 4.15 Effect of time step size on curvature of sidewall curl

Figure 4.15 shows relationship of mass scaling increase and time step size, and their result of curvature of sidewall curl on springback prediction. The necessary time step size decreases as the mass scaling decreases requiring more computational time. Springback is predicted larger as minimum time step decreases. In this case, the minimum time step is 1.29E-07 sec when no-mass scaling is used. However, if only a small amount of mass scaling is applied (i.e. 70% mass increase) the necessary minimum time step is increased to 3.0E-07 sec resulting in 50% computational time reduction but with similar springback prediction. Thus, minimum mass increase (i.e. less than 100%) or equivalent to necessary minimum time step of 3.0E-07 sec seems to be a proper numerical setting for the proceeding process simulations.

4.3 Air Bending Simulation

The proper numerical parameters setting was used to simulate air bending simulation for determine springback accuracy. First, curvature of specimen after bending was conducted to investigate accuracy of simulation compared with analytical mathematic and FEM. Second, the springback angle was conducted to study accuracy of springback compared with experiment and FEM. The data of springback angle and final punch displacement was obtained from Wang's experiment to investigate effect of springback. (Wang, J. et al., 2008)

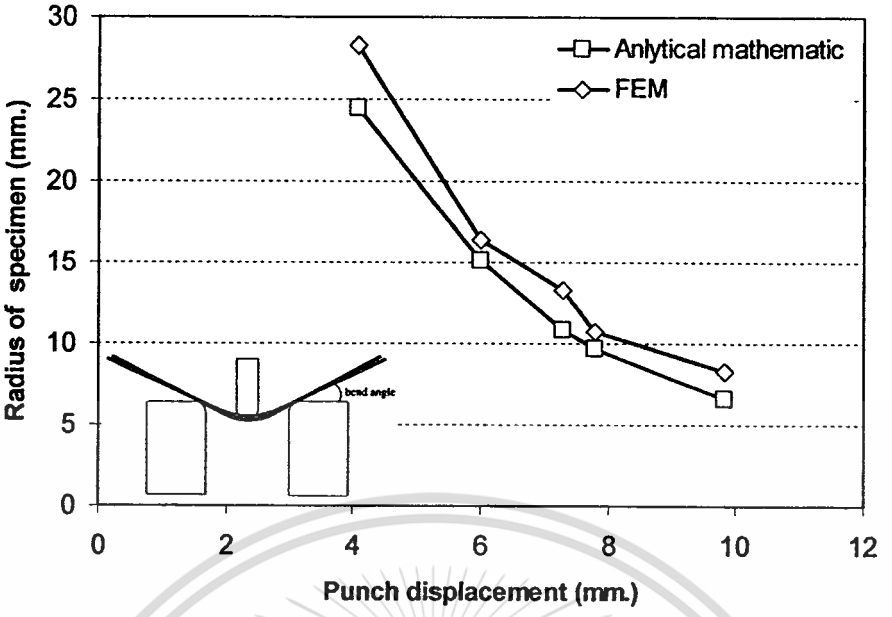

Figure 4.16 Curvature of specimen compare with mathematic and FEM

The radius of specimen was bent in various final punch displacements comparing with analytical mathematic method and FEM is shown in Figure 4.16. The FEM result was consistent; air bending simulations predicted more radius than with analytical mathematic. Nevertheless, the bent specimens with all final punch displacements showed a decrease in radius relative to their analytical calculation.

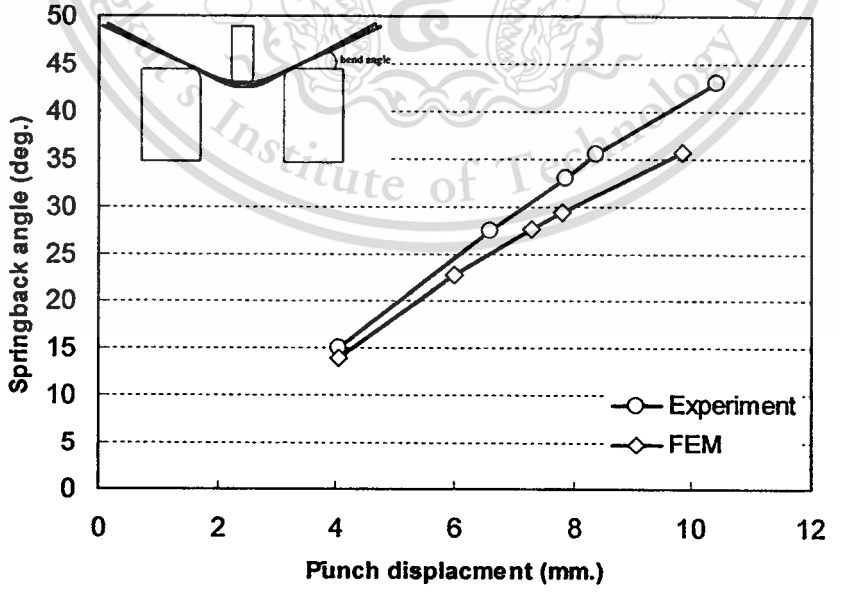

Figure 4.17 Springback angle comparison between FEM and experiment

The springback angle of specimen was bent in various final punch displacements comparing with experiment and FEM is shown in Figure 4.17. The results of air bending experiment were more springback angle than with FEM. However, the effect of springback angle was similar to the experimental results that FEM

4.4 The Effect of Blankholder Force on U-shape

4.4.1 Constant BHF on U-shape

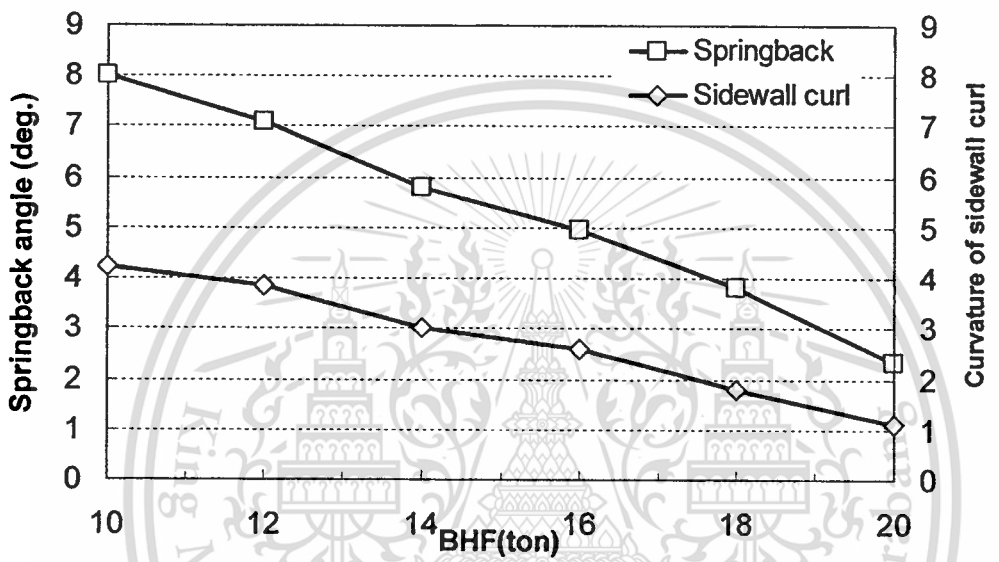

Figure 4.18 Effect of constant BHF

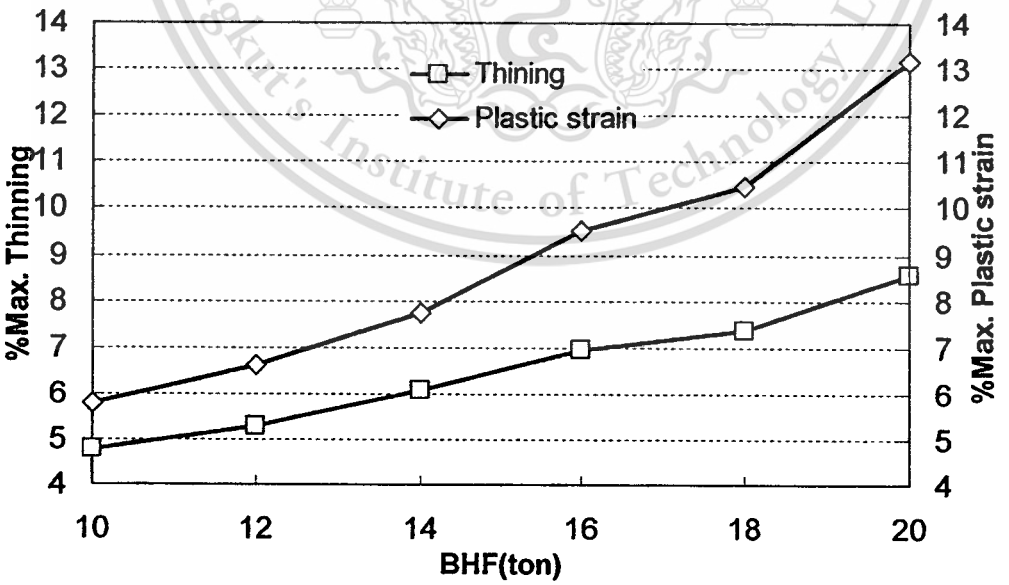

Figure 4.19 Effect of constant BHF on thinning and plastic strain

Figure 4.18 shows effect of constant BHF profiles and corresponding part formability; maximum thinning and effective strain. It was found that both springback angle and curvature of sidewall curl decreased as the level of constant BHF profile increased. In Figure 4.19, the defects were lowered by 75% while part thinning and effective strain increased over 100% at the highest constant BHF of 20 tons.

4.4.2 Variable BHF on U-shape

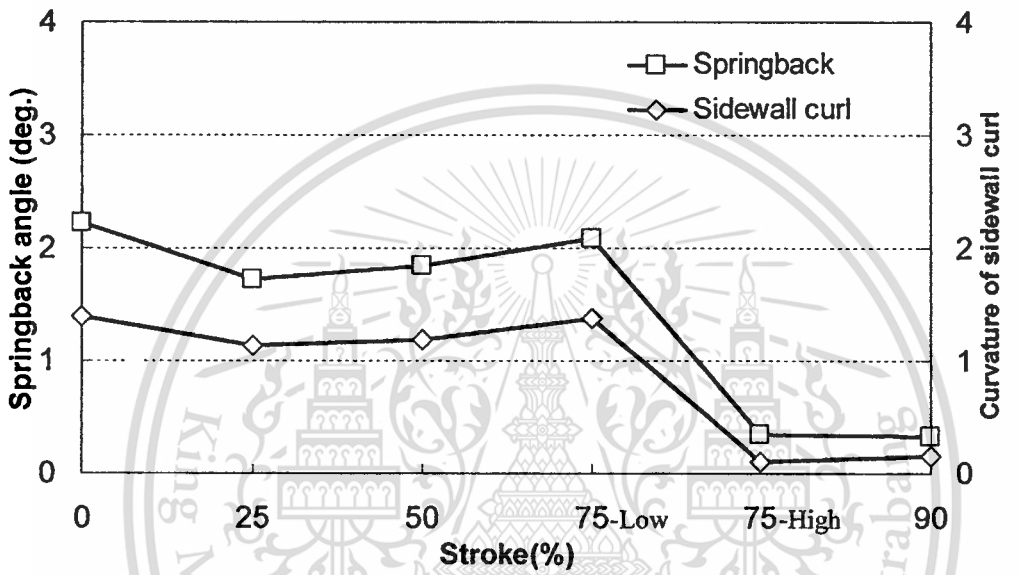

Figure 4.20 Effect of variable BHF

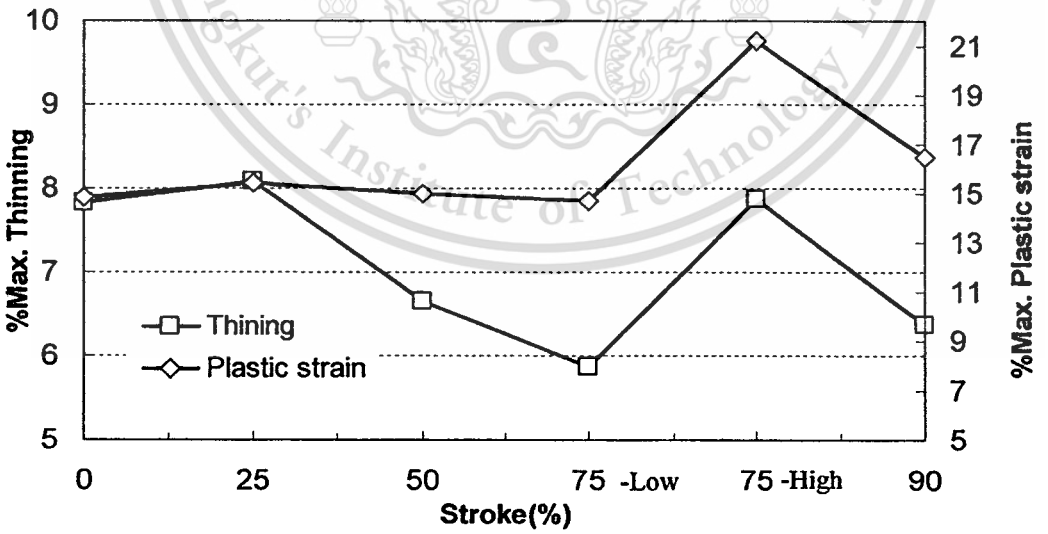

Figure 4.21 Effect of variable BHF on thinning and plastic strain

Clearly, larger constant BHF profiles resulted in reduced springback and sidewall curl. It was also found that these part deviations could be further reduced when applying appropriate variable BHF profiles, Figure 4.20. Both springback angle and curvature of sidewall curl almost disappeared when applying the 90% stroke BHF profile. The U-shape was formed with the lowest BHF of 10 tons up until the last 10% forming stroke allowing drawing type of metal flow. Then, a short intense stretching (by rapidly increasing the BHF of 30 tons) was applied during the last 10% forming stroke. The part thinning is similar to that formed by the maximum constant BHF profile, compare, Figure 4.20 and Figure 4.18. It should be pointed out that if the intense stretching was applied a little too early (e.g. 75%-high BHF profile) the part thinning could suffer.

4.5 The Effect of Blankholder Force on Butt-shape

4.5.1 Constant BHF on Butt-shape

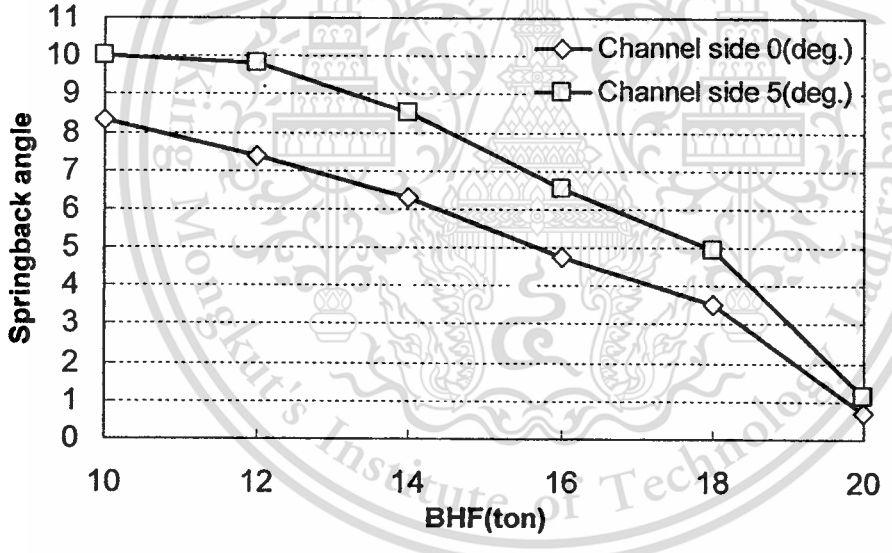

Figure 4.22 Effect of constant BHF on springback angle

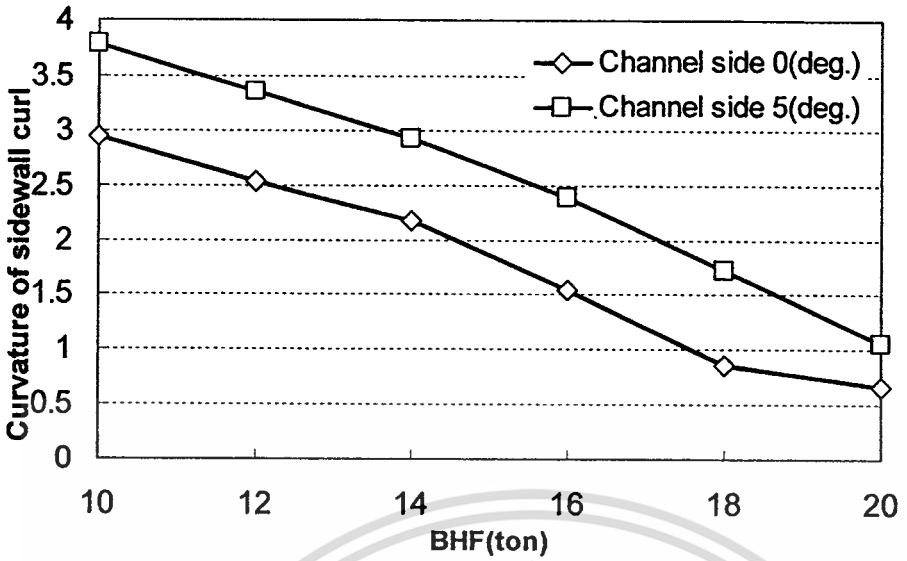

Figure 4.23 Effect of constant BHF on curvature of sidewall curl

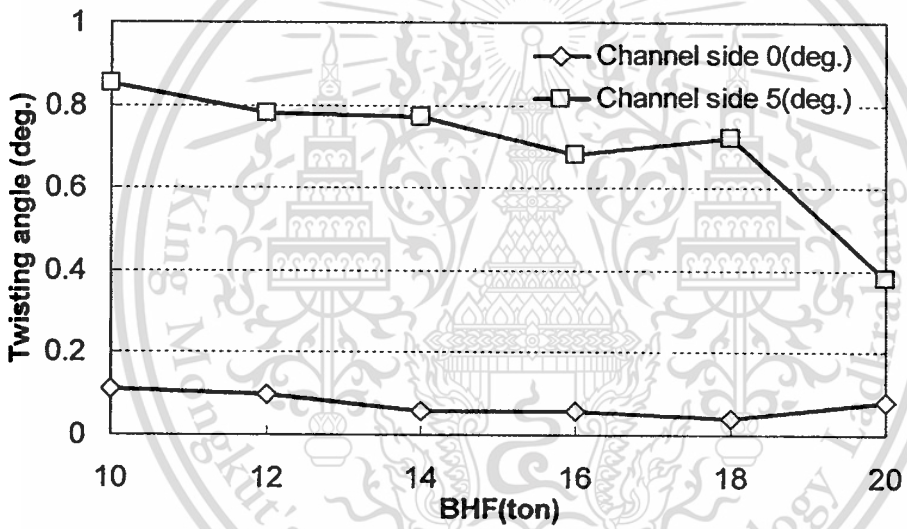

Figure 4.24 Effect of constant BHF on twisting angle

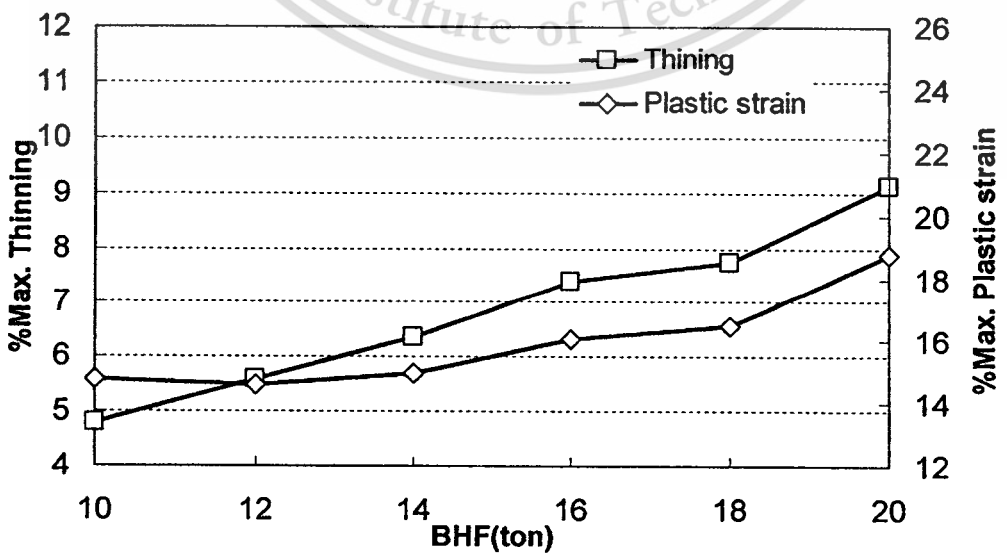

Figure 4.25 Effect of variable BHF on thinnimg and plastic strain

Similar constant and variable BHF profiles were applied to the Butt shape part. This part has an added part geometry deviation so called "twisting" caused by the unsymmetrical wall making a 5 degree angle to the channel axis, Figure 3.12. All the simulation results using constant BHF profiles are shown in Figure 4.22 – Figure 4.24. It can be seen from Figure 4.22 – Figure 4.24 that springback angle, curvature of sidewall curl, twisting angle reduce as the level of constant BHF profile is increased, and all the geometry deviations are worse on the slanted wall (channel side 5 degrees) than those of the parallel wall (channel side 0 degree). Twisting most occurs in the slanted wall. It is interesting that for this unsymmetrical part, Butt shape, the best BHF is the highest constant BHF profile as it is the case for the U-shape

4.5.2 Variable BHF on Butt-shape

All, the Butt shape simulation results using variable BHF profiles are shown in Figure 4.26 – Figure 4.29 below. It can be seen from the figure that the 75%-high and 90% variable BHF profiles form the part with the least geometry deviations at lowest part thinning. When compared with all cases using constant BHF profiles, almost all of the variable BHF profiles give much better part.

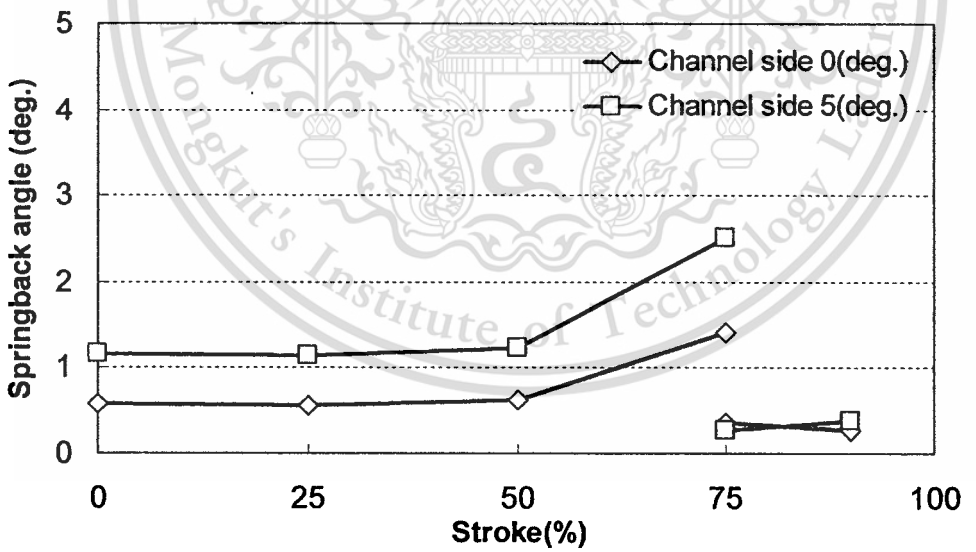

Figure 4.26 Effect of variable BHF on springback angle

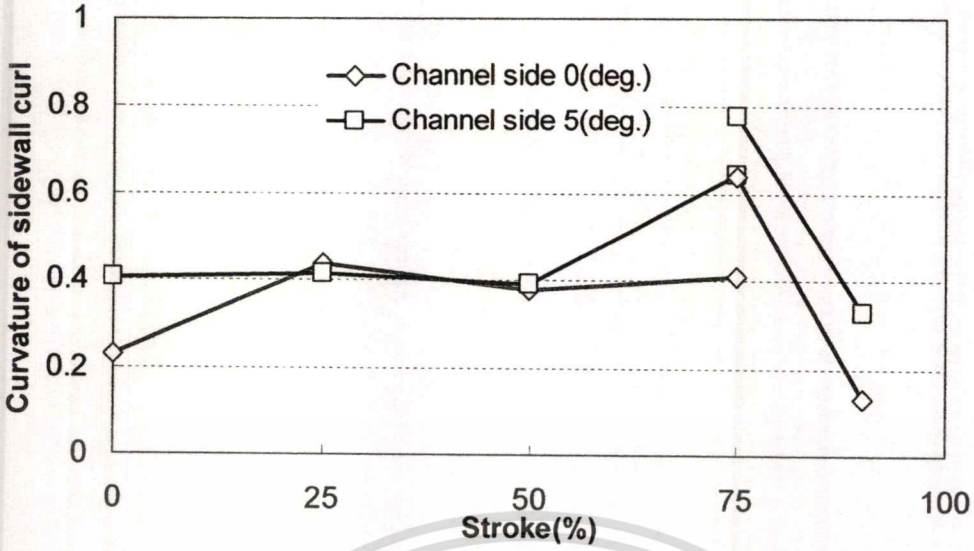

Figure 4.27 Effect of variable BHF on curvature of sidewall curl

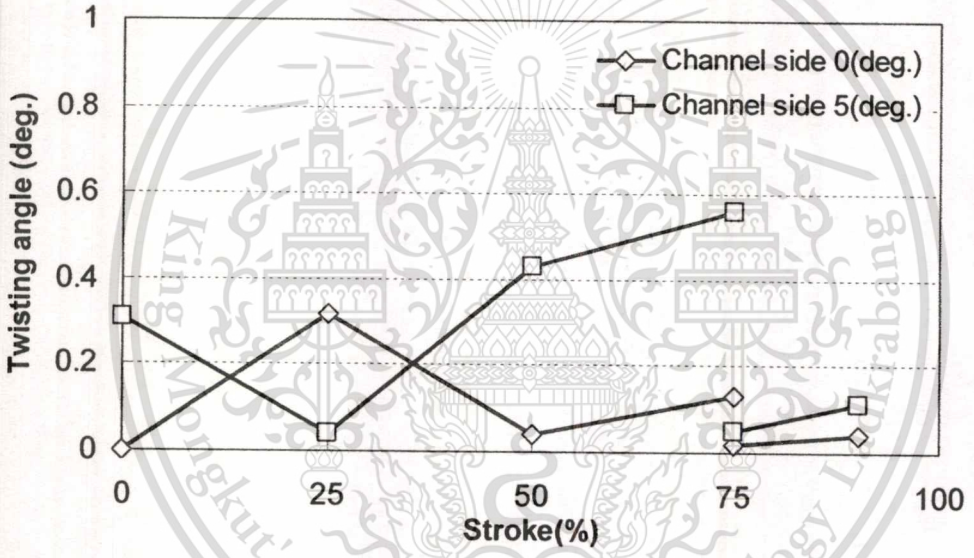

Figure 4.28 Effect of variable BHF on twisting angle

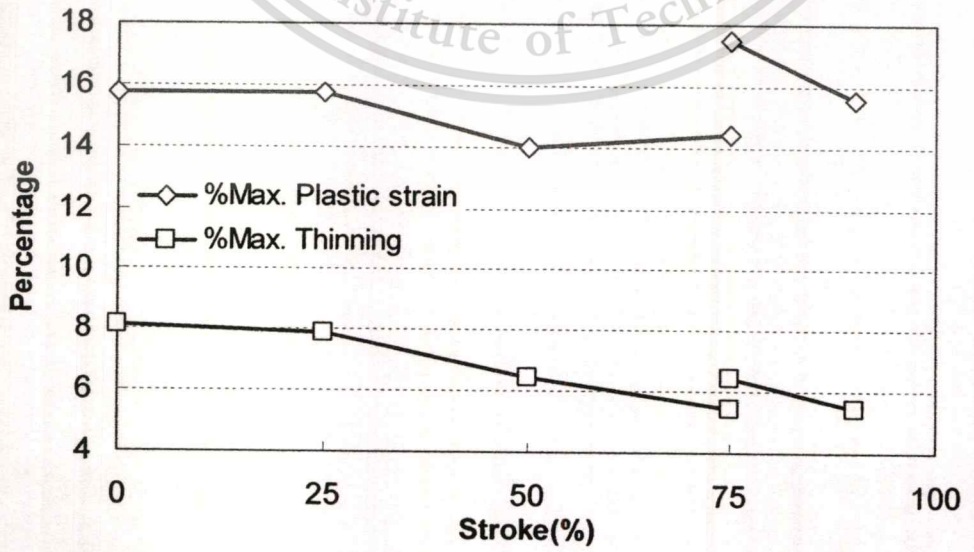

Figure 4.29 Effect of variable BHF on thinning and plastic strain

The numerical parameters used in finite element analysis of U and Butt-shape forming and springback were studied to understand their effects on the springback prediction. In order to improve accuracy of springback simulation, the numerical parameters consist of element size, adaptive angle tolerance, integration point and time step size were used to investigate on U-shape model. Then, the proper numerical parameters were used to investigate an effect of blankholder force profile on U-shape and Butt-shape simulation.

The bending and unbending occur around die or punch radius that is caused of springback. The element size over die radius was used to study numerical parameters affecting springback prediction. The author found the size of an element per 4 degrees seems to be a proper choice considering it giving maximum springback and approaching experimental data when a simulation predicted without mass scaling. After that, a proper element size is chosen to analyze an effect of adaptive angle tolerances. The small adaptive angle tolerance of 1 degree was much more sensitive to observe a significant area of part geometry. The springback behavior depends on bending moment through thickness direction. The integration point used to observe stress distribution in thickness. In this case, the number of integration point of 9 was chosen to be proper when considering a time computational. However, a no mass scaling should give more accurate results but a small mass scaling is useful to reduce computational time spend. The necessary minimum time step is increased to 3.0E-07 sec resulting in 50% computational time reduction but with similar springback prediction with no mass scaling.

The proper numerical parameters setting was used to study of the process parameters, i.e. blankholder force profile, on U and Butt-shape model in order to study blankholder force profile affecting springback reduction. The BHF profiles consist of constant and variable BHF profiles. The tendency of a springback angle and a curvature of a sidewall curl decreases when as the level of constant BHF profile increased on both U-shape and Butt-shape. However, the thickness of part decreases due to stretching of material in order to improve part of quality and reduce springback, so that the variable BHF profiles was used to apply. It can reduce deviations of a specimen, i.e. (springback angle and curvature of a sidewall curl) and kept part of quality when applying the 90% stroke BHF profile. In case of Butt-shape model, this part has an added part geometry deviation so called "twisting" caused by the unsymmetrical wall making a 5 degree angle to the channel axis. It was found that the 75%-high and 90% variable BHF profiles formed the part with the least geometry deviations at the lowest part thinning. Almost, all the variable blankholder force profiles providing a good quality of part.

CHAPTER 5

EXPERIMENTAL INVESTIGATION RESULTS OF EFFECTS OF PROCESS PARAMETERS ON SPRINGBACK BEHAVIOR

This chapter discusses the results from the process parameter investigation. It was studied to understand their effects on springback of U-shape and Butt-shape models. The experimental results were observed to obtain proper process parameters and die design guideline for springback reduction systematically.

5.1 Effects of Process Parameters on U-shape

Springback measurements obtained from the springback experiments with various process parameters are shown in Table 5.1. The results of process parameters can be arranged as follows.

Table 5.1 Result of springback experiment on U-shape

Result of springback experiment						
BHF	Tool gap	Radius of punch	Radius of die	Avg. Springback angle(Deg)	Avg. Curvature of sidewall (mm^{-1})	Avg. Thickness (mm)
Low (10 ton)	1t	R=2t	R=2t	1.570	3.238	0.942
			R=10t	3.175	4.651	1.071
		R=10t	R=2t	3.829	3.426	0.947
			R=10t	6.050	5.137	1.113
	1.1t	R=2t	R=2t	1.907	3.376	0.938
			R=10t	3.169	4.769	1.071
		R=10t	R=2t	4.891	3.866	0.969
			R=10t	5.863	5.386	1.122
High (20 ton)	1t	R=2t	R=2t	1.105	2.005	0.859
			R=10t	1.779	3.142	1.050
		R=10t	R=2t	1.762	2.971	0.858
			R=10t	2.825	3.233	1.087
	1.1t	R=2t	R=2t	0.706	1.100	0.878
			R=10t	1.886	3.331	1.041
		R=10t	R=2t	1.545	2.751	0.889
			R=10t	2.962	3.061	1.094
none BHF	1t	R=10t	R=10t	12.943	8.517	1.14
50%-25	1t	R=10t	R=10t	1.558	0.793	1.028
90%-25	1t	R=10t	R=10t	2.427	0.323	1.09
90%-28	1t	R=10t	R=10t	1.146	0.891	1.04

The specimen dimensions are 370 x 50 x 1.2 mm. SPHC 590 was chosen to investigate springback behaviors with various process parameters i.e., punch radius, die radius, tool gap and blankholder force. Each of process parameters was investigated using two levels that are low and high levels. All the BHF profiles can be grouped into two; first is constant BHF profiles and second is variable BHF profiles. Below are discussions of the effect found from each process parameter investigated.

5.1.1 Punch radius

Figure 5.1 compares springback angle between two levels of punch radii. It clearly shows that the springback angle was decreased from the case of Rp_{10} (punch radius equals to 10 times of thickness) when the Rp_2 (punch radius equals to 2 times of thickness) was applied to form U-shape. The effect of each punch radius on the springback angle is obtained from an average of all the eight cases. In comparison, the difference of springback only represents effect of change of the punch radius while the die radius, tool gap and blankholder force remain the same relatively. The small punch radius can reduce springback angle by an average of 54% in all cases.

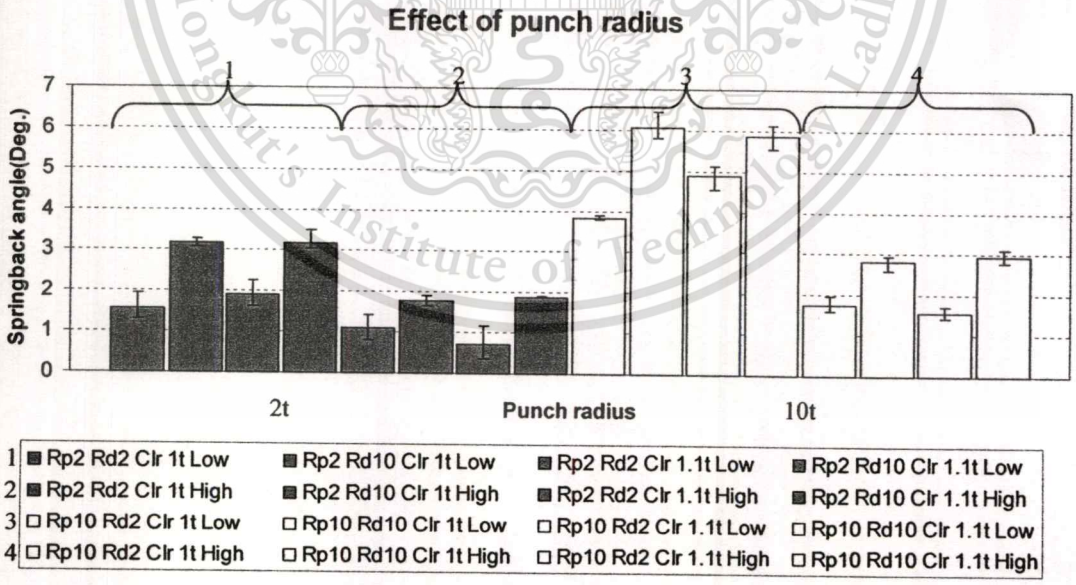

Figure 5.1 Effect of punch radius on springback angle

Figure 5.2 compares curvature of sidewall curl between two levels of punch radii. It clearly shows that the curvature of sidewall curl was a few decrease from the case of Rp_{10}

(punch radius equals to 10 times of thickness) when the Rp_2 (punch radius equals to 2 times of thickness) was applied. The effect of each punch radius on the curvature of sidewall curl is obtained from an average of all the eight cases. In comparison, the difference of springback only represents effect of change of the punch radius while the die radius, tool gap and blankholder force remain the same relatively. The small punch radius can reduce springback angle by an average of 23% in all cases.

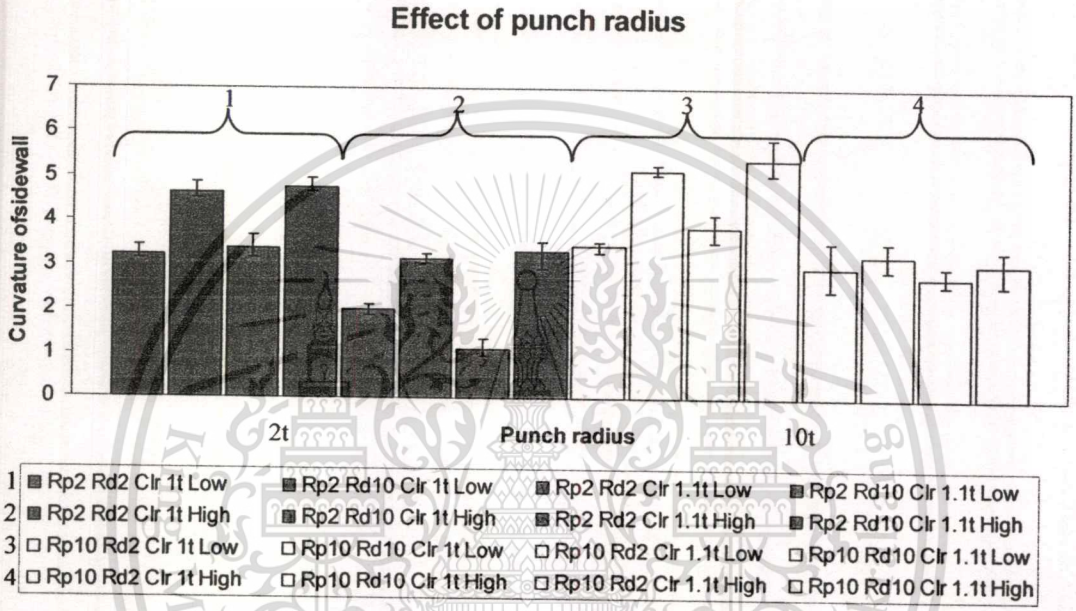

Figure 5.2 Effect of punch radius on curvature of sidewall curl

5.1.2 Die radius

Figure 5.3 compares springback angle between two levels of die radii. It clearly shows that the springback angle was decreased from the case of Rd_{10} (die radius equals to 10 times of thickness) when the Rd_2 (die radius equals to 2 times of thickness) was applied to form U-shape. The effect of each die radius on the springback angle is obtained from an average of all the eight cases. In comparison, the difference of springback only represents effect of change of the die radius while the punch radius, tool gap and blankholder force remain the same relatively. The small die radius can reduce springback angle by an average of 39% in all cases.

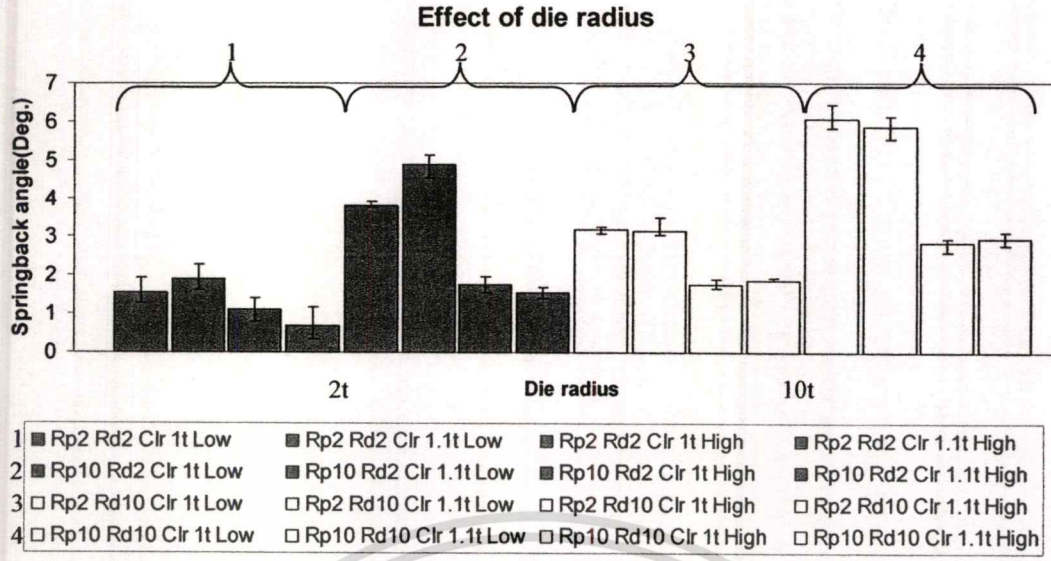

Figure 5.3 Effect of die radius on springback angle

Figure 5.4 compares curvature of sidewall curl between two levels of die radii. It clearly shows that the curvature of sidewall curl was decreased from the case of Rd_{10} (die radius equals to 10 times of thickness) when the Rd_2 (die radius equals to 2 times of thickness) was applied to form U-shape. The largest reduction curvature of sidewall curl was found in the case when using the smaller die radius (i.e., Rp_2Rd_{10}Clr1.1t BHF_H to Rp_2Rd_2Clr1.1t BHF_H). The smaller die radius tends to stretch the sidewall to a greater extent than does the larger die radius.

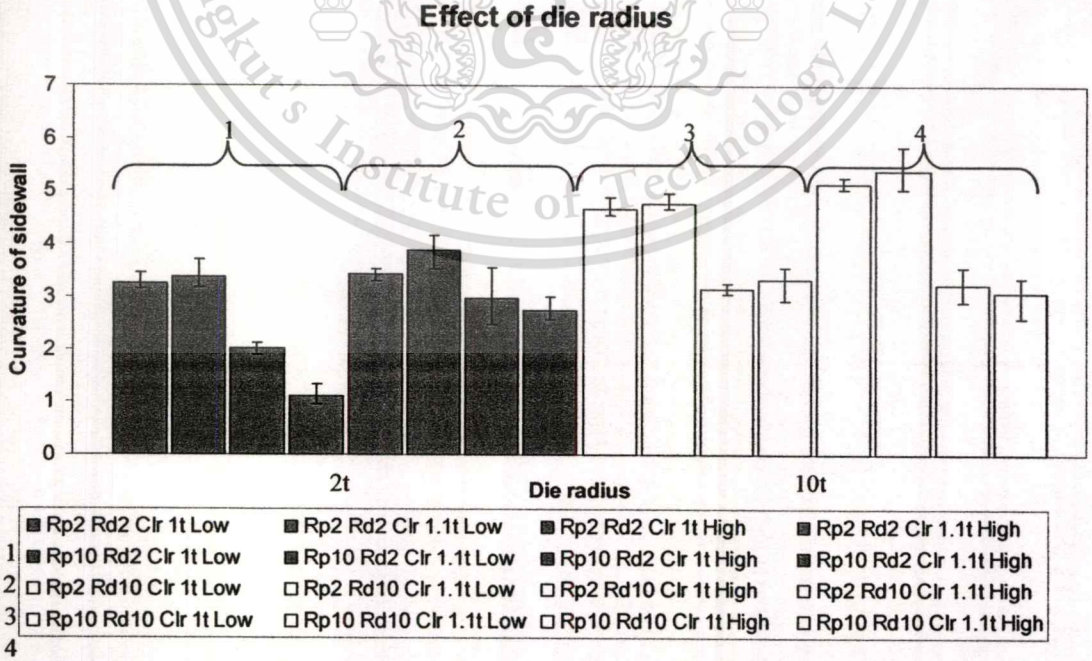

Figure 5.4 Effect of die radius on curvatue of side wall curl

5.1.3 Tool gap

Figure 5.5 compares springback angle between two levels of tool gap. It seems that tool gap does not affect the springback angle at all. Nevertheless, the largest springback angle reduced is found when replacing small tool gap with the bigger tool gap while using high BHF. There seems to be an interaction between tool gap and BHF. In comparison, the difference of springback only represents effect of change of the tool gap while the punch radius, die radius and blankholder force remain the same relatively. The small tool gap can reduce springback angle by an average of 3% in all cases.

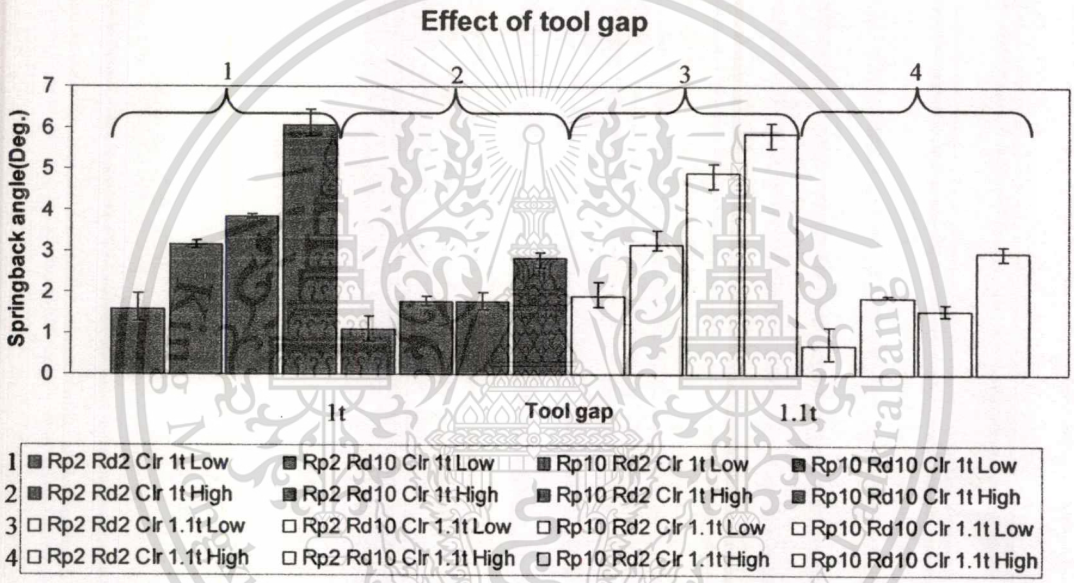

Figure 5.5 Effect of tool gap on springback angle

Figure 5.6 compares curvature of sidewall curl between two levels of tool gap. In comparison, the difference of curvature of sidewall only represents effect of change of the tool gap while the punch radius, die radius and blankholder force remain the same relatively. The small tool gap can reduce curvature of sidewall curl by an average of 1% in all cases. It seems that tool gap does not affect the curvature of sidewall curl at all.

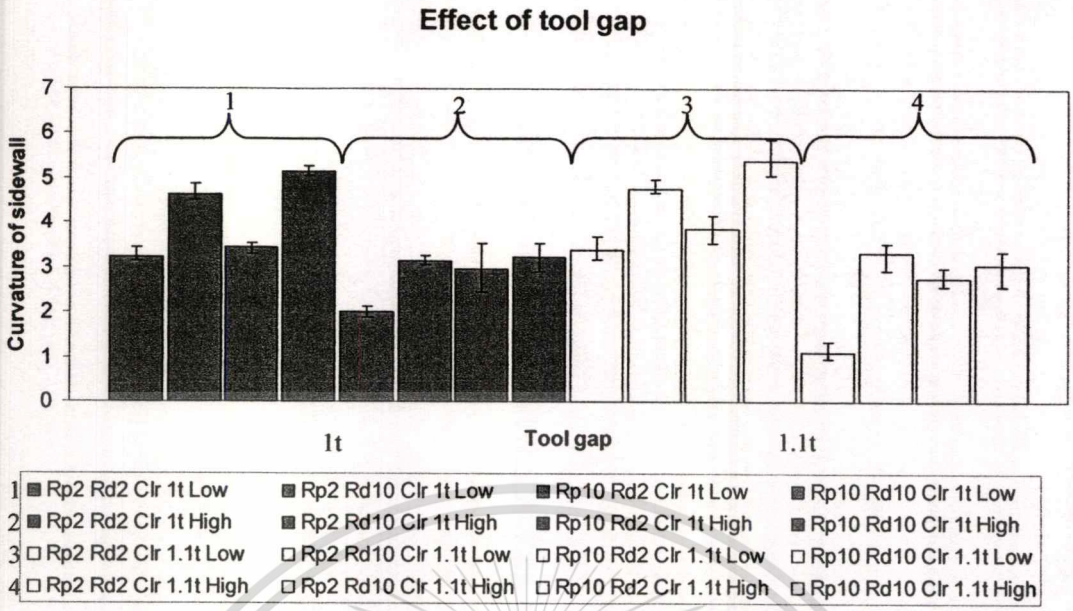

Figure 5.6 Effect of tool gap on curvatue of side wall curl

5.1.4 Constant blankholder force

Figure 5.7 and Figure 5.8 shows effect of constant BHF on springback angle and sidewall curvature relative. It was found that both springback angle and curvature of sidewall curl decreased as the level of constant BHF profile increased. In Figure 5.8, the average curvature of sidewall curl were lowered by 59% in all case while an average springback angle decreased by 66% at the highest constant BHF of 20 tons as shown in Figure 5.7.

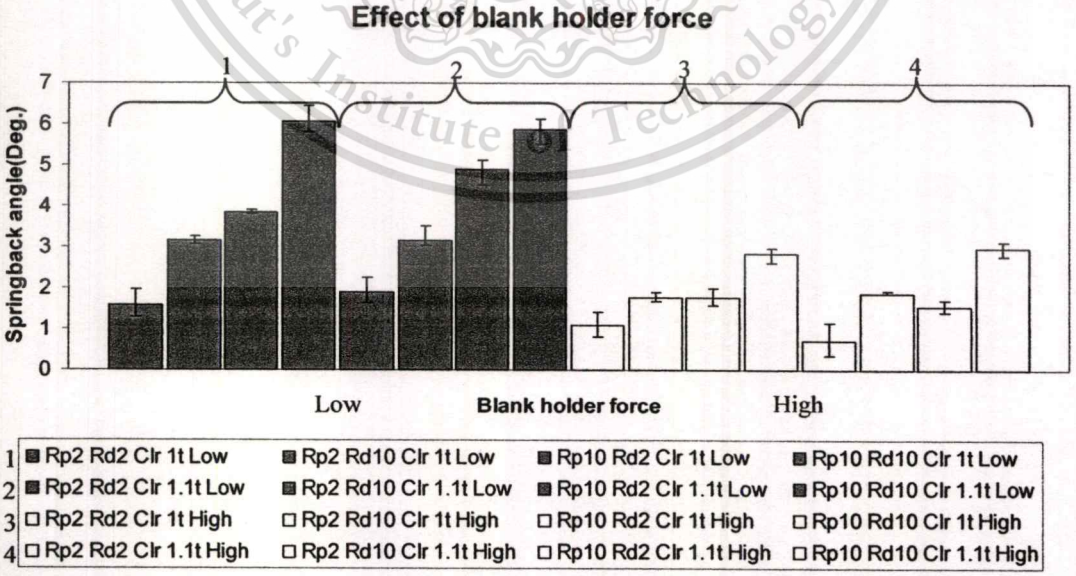

Figure 5.7 Effect of blankholder force on springback angle

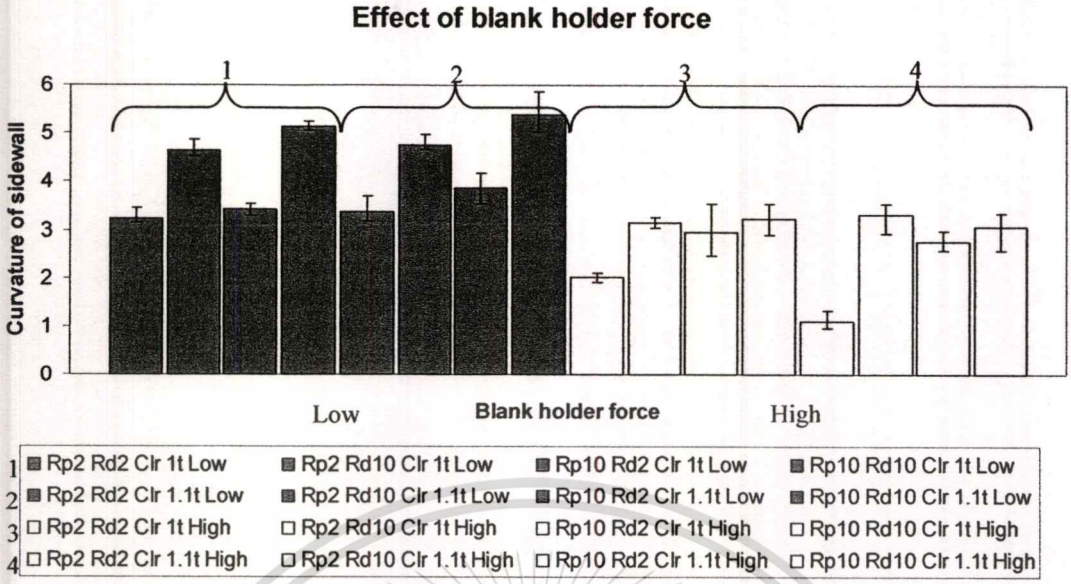

Figure 5.8 Effect of blankholder force on curvatue of side wall curl

5.1.5 Variable blankholder force

It has been found that, higher constant BHF resulted in reduced springback and sidewall curl. It was also found that these part deviations could be further reduced when applying appropriate variable BHF profiles. Figure 5.9 , both springback angle and curvature of sidewall curl almost disappeared when applying the variable BHF profile compare with high constant BHF. The U-shape was formed with the lowest BHF of 10 tons up until the last 10% forming stroke allowing drawing type of metal flow. Then, a short intense stretching (by rapidly increasing the BHF of 28 tons) was applied during the last 10% forming stroke. Figure 5.10 shows effect of various BHF profiles on the final part thickness.

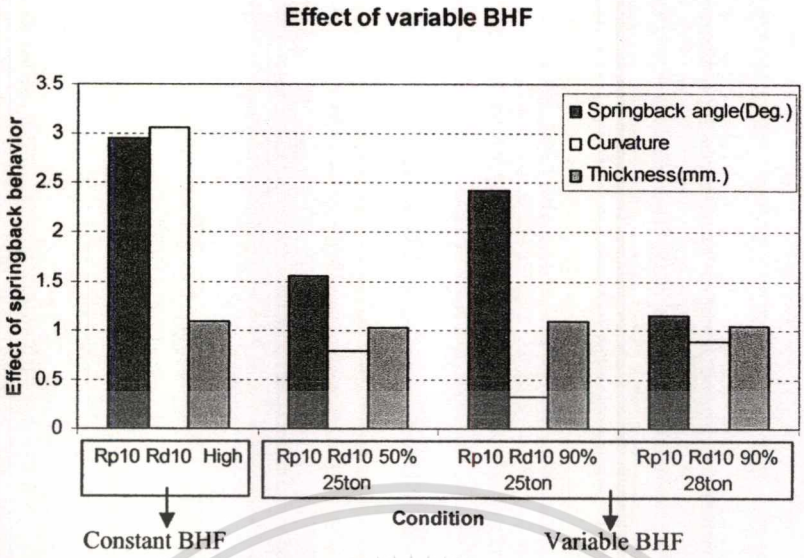

Figure 5.9 Effect of variable blankholder force on springback

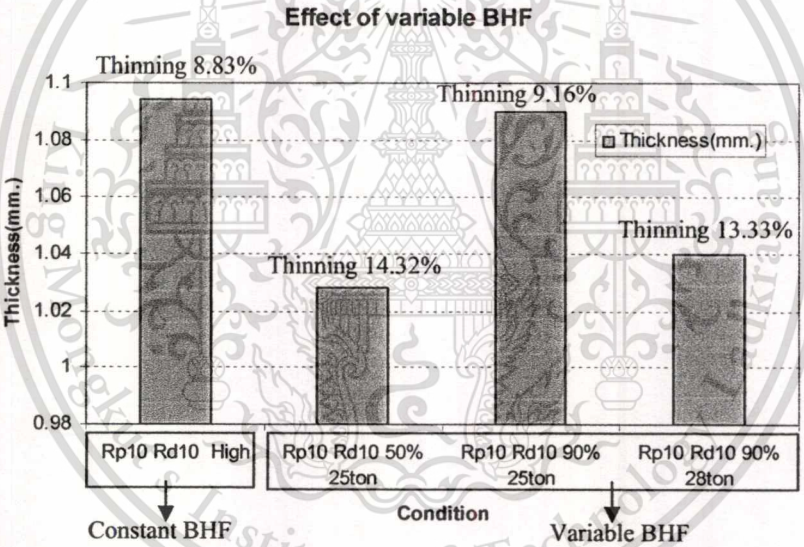

Figure 5.10 Effect of variable blankholder force on thickness

5.2 Effects of Process Parameters on Butt-shape

The Butt-shape part has an added part geometry deviation so called "twisting" caused by the unsymmetrical wall making a 5 degrees angle to the channel axis. The Butt-shape chosen to investigate springback behaviors that are springback angle, curvature of sidewall curl and twisting angle ,with various process parameters. Springback measurements obtained from the springback experiments with various process parameters are shown in Table 5.2. The results of process parameters can be arranged as follows.

Table 5.2 Result of springback experiment on Butt-shape

Result of Springback Experiment								
BHF	Tool gap	Radius of punch	Radius of die	Avg. Springback angle (deg.)	Avg. Curvature of sidewall curl (mm^{-1})	Avg. Twisting angle (deg.)		Thickness (mm.)
						Left	Right	
Low (10 ton)	1t	R=2t	R=2t	3.399275	3.04762	1.395	0.523	0.948
			R=10t	4.825958	4.651105	0.724	0.364	1.114
		R=10t	R=2t	4.173845	3.30104	1.072	0.332	0.95
			R=10t	5.345707	4.708348	0.624	0.15	1.113
	1.1t	R=2t	R=2t	3.548151	3.083352	0.903	0.124	0.947
			R=10t	5.335747	4.765603	0.697	0.127	1.114
		R=10t	R=2t	4.831524	3.018334	1.046	0.268	0.948
			R=10t	6.249208	4.89764	0.474	0.083	1.119
High (20 ton)	1t	R=2t	R=2t	1.147908	1.083779	0.337	0.129	0.869
			R=10t	3.591213	3.171041	0.23	0.176	1.09
		R=10t	R=2t	2.304769	0.299344	0.162	0.187	0.867
			R=10t	3.089168	3.324404	0.555	0.11	1.099
	1.1t	R=2t	R=2t	0.8544	1.207442	0.354	0.113	0.894
			R=10t	3.610201	3.335827	0.705	0.077	1.106
		R=10t	R=2t	2.392861	0.34725	0.364	0.044	0.871
			R=10t	3.83786	3.692573	0.601	0.262	1.106
50%-25	1.1t	R=10t	R=10t	1.705916	0.63953	0.108	0.055	1.053
90%-25	1.1t	R=10t	R=10t	1.416858	0.743039	0.185	0.105	1.094
90%-28	1.1t	R=10t	R=10t	1.1278	0.914965	0.261	0.154	1.039
none HBF	1.1t	R=10t	R=10t	11.91514	7.858563	1.311	0.824	1.16

5.2.1 Punch radius

Figure 5.11 compares springback angle between two levels of punch radii. It clearly shows that the springback angle was decreased from the case of Rp_{10} (punch radius equals to 10 times of thickness) when the Rp_2 (punch radius equals to 2 times of thickness) was applied to form Butt-shape. The effect of each punch radius on the springback angle is obtained from an average of all the eight cases. In comparison, the difference of springback only represents effect of change of the punch radius while the die radius, tool gap and blankholder force remain the same relatively. The small punch radius can reduce springback angle by an average of 27% in all cases.

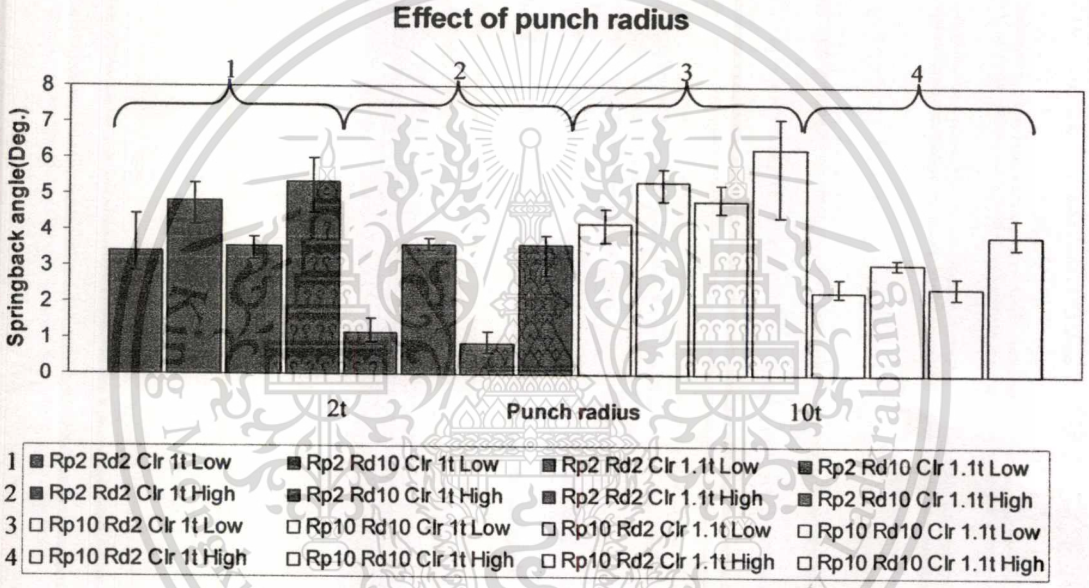

Figure 5.11 Effect of punch radius on springback angle

Figure 5.12 compares curvature of sidewall curl between two levels of punch radii. It clearly shows that the curvature of sidewall was decreased from the case of Rp_{10} (punch radius equals to 10 times of thickness) when the Rp_2 (punch radius equals to 2 times of thickness) was applied to form Butt-shape. In comparison, the difference of springback only represents effect of change of the punch radius while the die radius, tool gap and blankholder force remain the same relatively. The small punch radius can slightly reduce curvature of sidewall curl average which is an average of 3% in all cases.

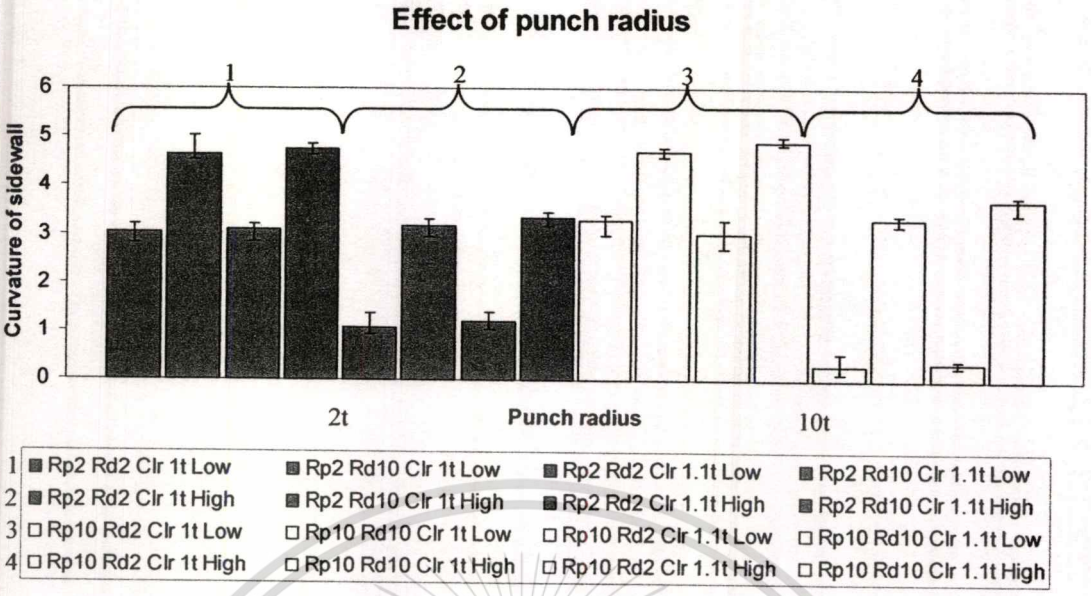

Figure 5.12 Effect of punch radius on curvature of sidewall curl

The twisting angle, the geometry deviations are worse on the slanted wall (channel side 5 degrees) than those of the parallel wall (channel side 0 degree). Twisting most occurs in the slanted wall. Figure 5.13 compares curvature of sidewall curl between two levels of punch radii. It shows that the twisting angle was increase from the case of Rp_{10} (punch radius equals to 10 times of thickness) when the Rp_2 (punch radius equals to 2 times of thickness) was applied to form Butt-shape. The bigger punch radius can slightly reduce twisting angle average which is an average of 5% in all cases.

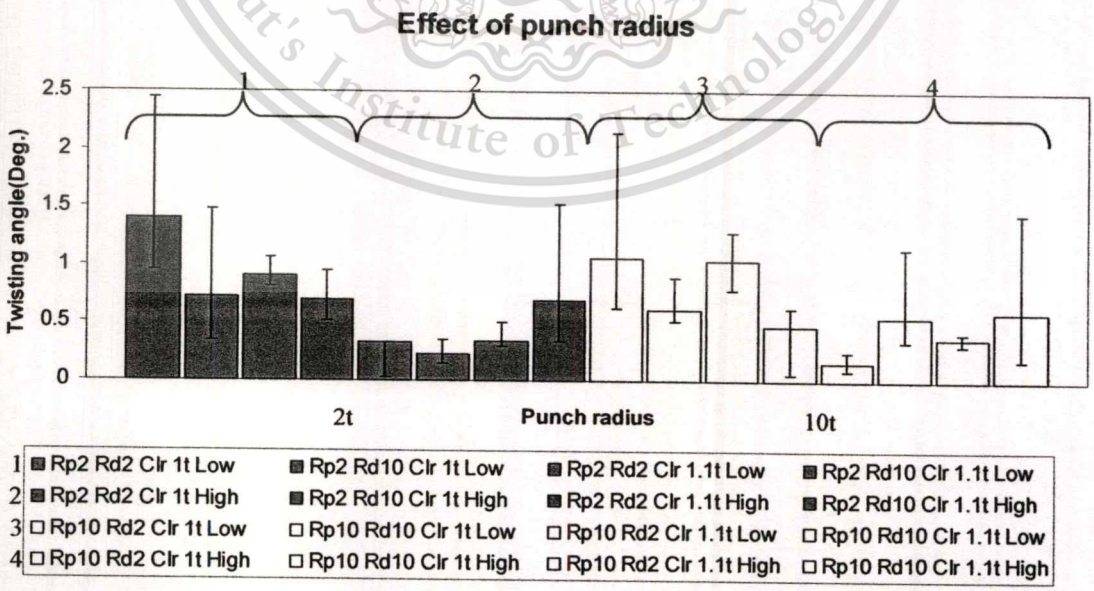

Figure 5.13 Effect of punch radius on twisting angle

5.2.2 Die radius

Figure 5.14 compares springback angle between two levels of die radii. It clearly shows that the springback angle was decreased from the case of Rd_{10} (die radius equals to 10 times of thickness) when the Rd_2 (die radius equals to 2 times of thickness) was applied to form Butt-shape. The effect of each die radius on the springback angle is obtained from an average of all the eight cases. In comparison, the difference of springback only represents effect of change of the die radius while the punch radius, tool gap and blankholder force remain the same relatively. The small die radius can reduce springback angle by an average of 60% in all cases.

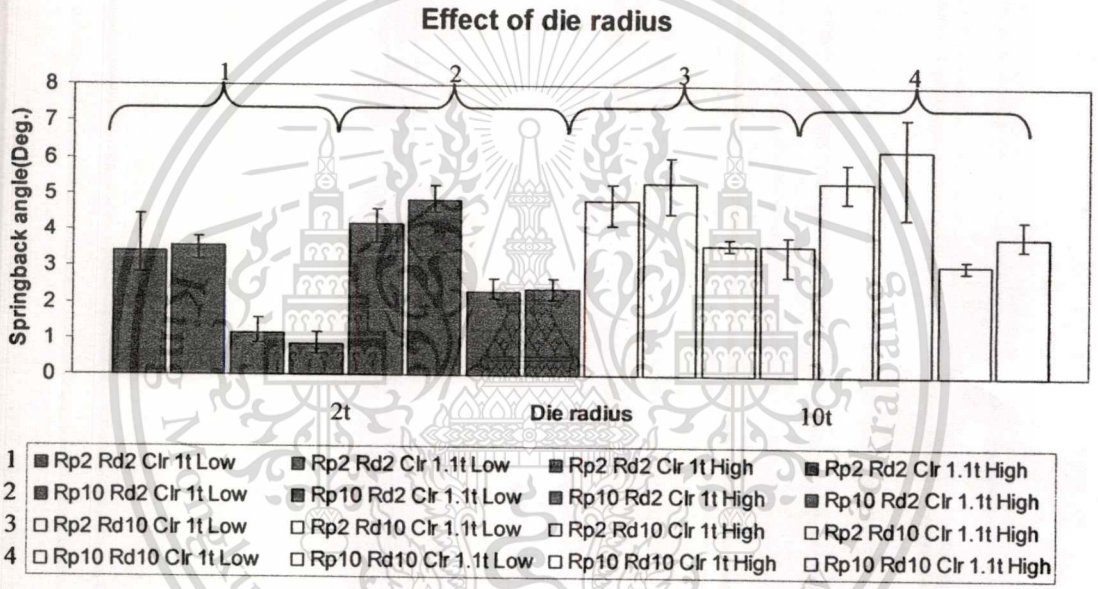

Figure 5.14 Effect of die radius on springback angle

Figure 5.15 compares curvature of sidewall curl between two levels of die radii. It clearly shows that the curvature of sidewall was decreased from the case of Rd_{10} (die radius equals to 10 times of thickness) when the Rd_2 (die radius equals to 2 times of thickness) was applied to form Butt-shape. In comparison, the difference of curvature only represents effect of change of the die radius while the punch radius, tool gap and blankholder force remain the same relatively. The small die radius can reduce curvature of sidewall curl average which is an average of 64% in all cases.

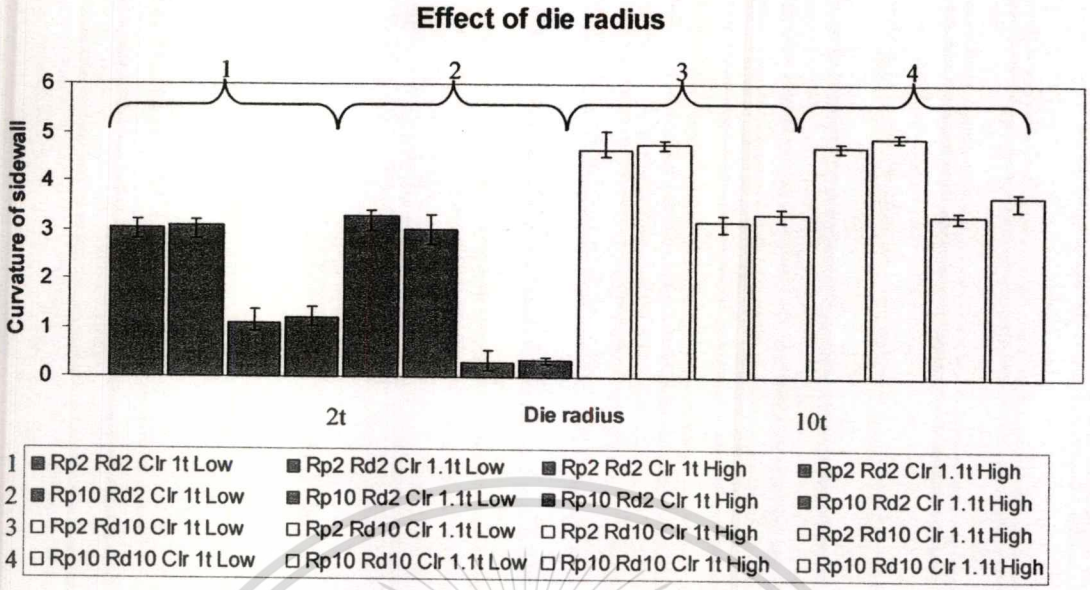

Figure 5.15 Effect of die radius on curvature of sidewall curl

In comparison, the difference of twisting angle only represents effect of change of the die radius while the punch radius, tool gap and blankholder force remain the same relatively. Figure 5.16 compares twisting angle between two levels of die radii. It shows that the twisting angle was increase from the case of Rd_{10} (die radius equals to 10 times of thickness) when the Rp_2 (punch radius equals to 2 times of thickness) was applied to form Butt-shape. The bigger die radius can reduce twisting angle average which is an average of 12% in all cases.

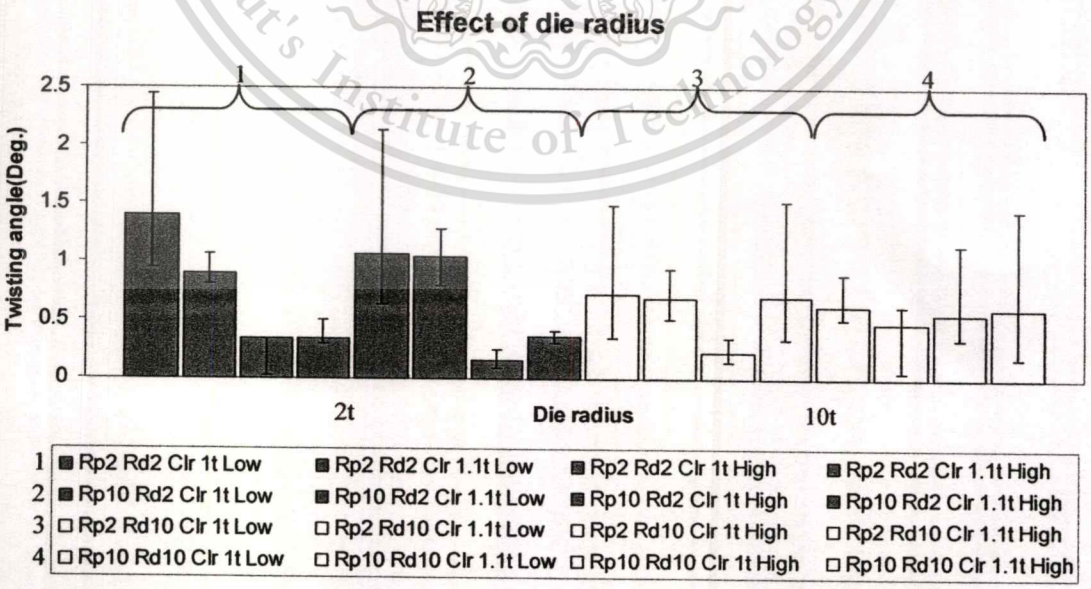

Figure 5.16 Effect of die radius on twisting angle

5.2.3 Tool gap

Figure 5.17 compares springback angle between two levels of tool gap. It seems that tool gap does not affect the springback angle at all. Nevertheless, the largest springback angle reduced is found when replacing small tool gap with the bigger tool gap while using high BHF. There seems to be an interaction between tool gap and BHF. In comparison, the difference of springback only represents effect of change of the tool gap while the punch radius, die radius and blankholder force remain the same relatively. The small tool gap can reduce springback angle by an average of 13% in all cases.

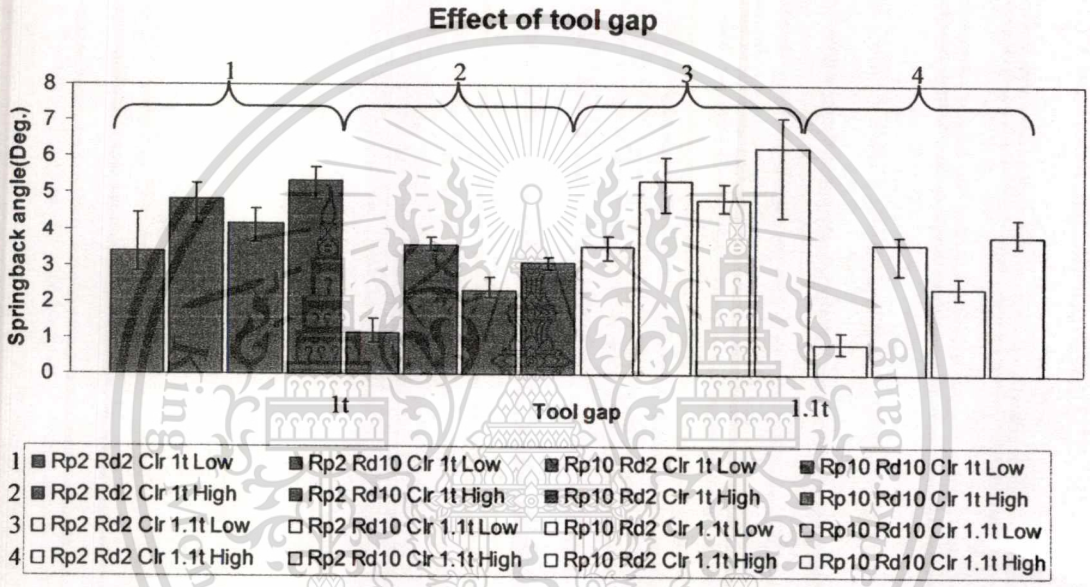

Figure 5.17 Effect of tool gap on springback angle

Figure 5.18 compares curvature of sidewall curl between two levels of tool gap. In comparison, the difference of curvature of sidewall only represents effect of change of the tool gap while the punch radius, die radius and blankholder force remain the same relatively. The small tool gap can reduce curvature of sidewall curl by an average of 3% in all cases. It seems that tool gap does not affect the curvature of sidewall curl at all.

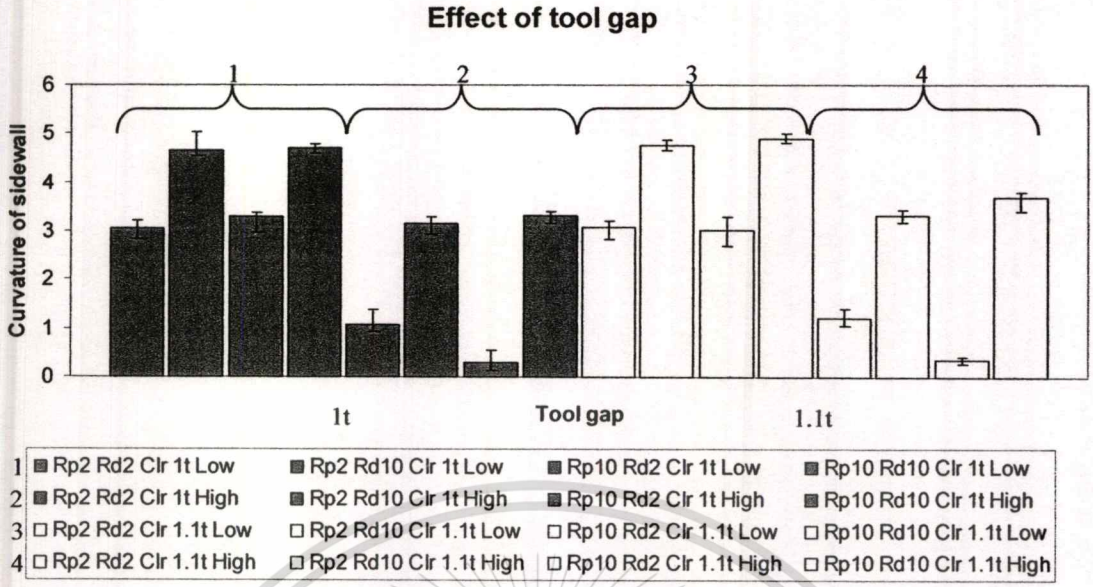

Figure 5.18 Effect of tool gap on curvature of sidewall curl

Figure 5.19 compares twisting angle between two levels of tool gap. It seems that tool gap does not affect the twisting angle at all. Nevertheless, the largest twisting angle reduced is found when replacing small tool gap with the bigger tool gap while using high BHF. There seems to be an interaction between tool gap and BHF. In comparison, the difference of springback only represents effect of change of the tool gap while the punch radius, die radius and blankholder force remain the same relatively. The small tool gap can reduce twisting angle by an average of 1% in all cases. It seems that tool gap does not affect the twisting angle at all.

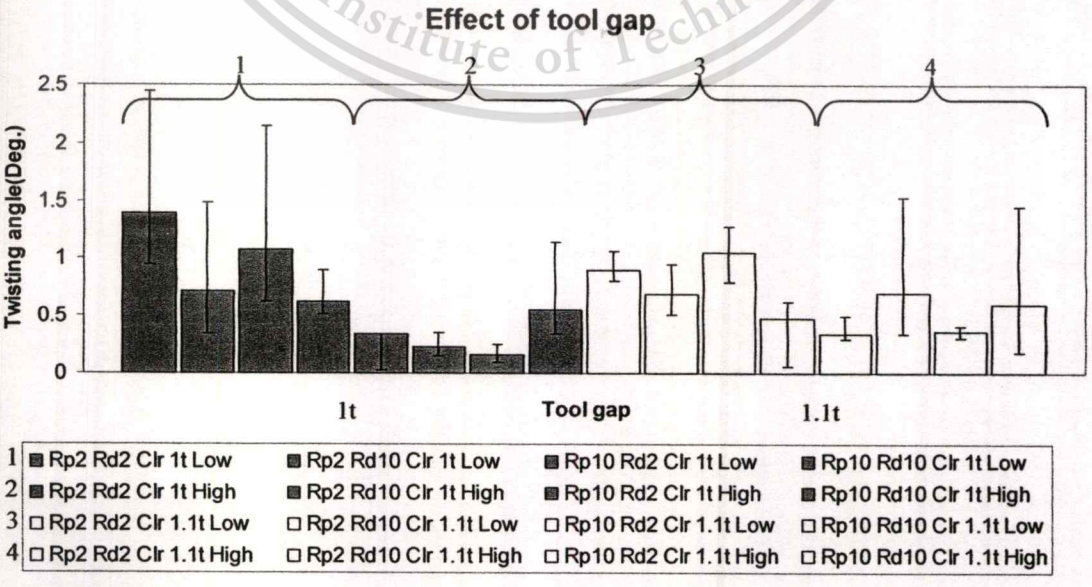

Figure 5.19 Effect of tool gap on twisting angle

5.2.4 Constant blankholder force

Figure 5.20 compares springback angle between two levels of blankholder force. It clearly shows that the springback angle was decreased from the case of BHF_L (Blankholder force 10 ton) when the BHF_H (Blankholder force 20 ton) was applied to form Butt-shape. The effect of each blankholder force on the springback angle is obtained from an average of all the eight cases. In comparison, the difference of springback only represents effect of change of the level of blankholder force while the punch radius, die radius, and tool gap remain the same relatively. The high blankholder force can reduce springback angle by an average of 77% in all cases.

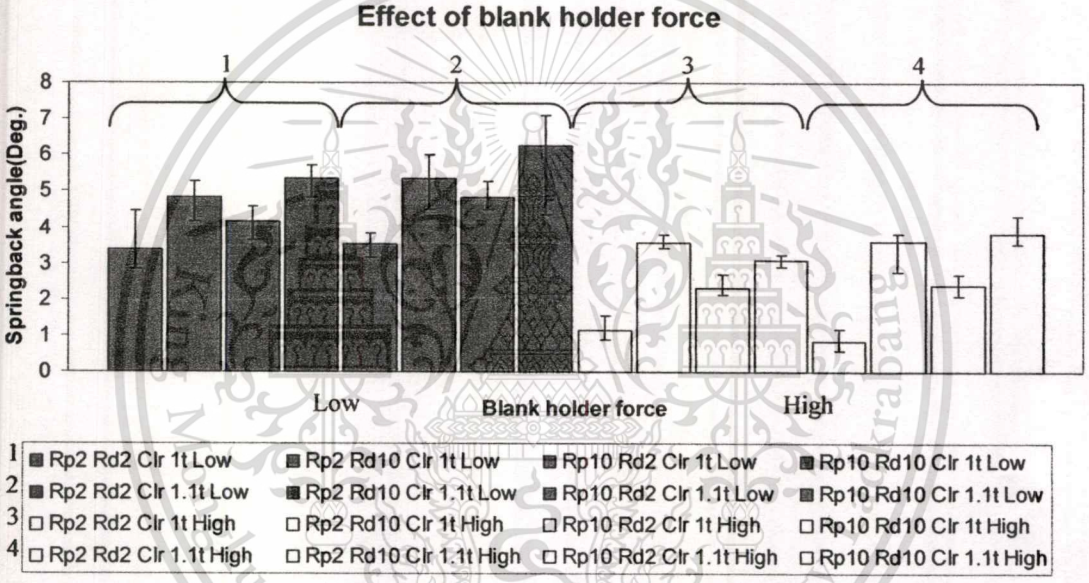

Figure 5.20 Effect of constant blankholder force on springback angle

Figure 5.21 compares curvature of sidewall curl between two levels of blankholder force. It clearly shows that the curvature of sidewall curl decreased from the case of BHF_L (Blankholder force 10 ton) when the BHF_H (Blankholder force 20 ton) was applied to form Butt-shape. The effect of blankholder force on the curvature of sidewall curl is obtained from the average of all differences of eight comparisons. In comparison, the difference of springback only represents effect of change of the level of blankholder force while the punch radius, die radius, and tool gap remain the same relatively. It was found that curvature of sidewall curl decreased as the level of constant BHF profile increased. The high blankholder force can reduce curvature of sidewall curl by an average of 56% in all cases.

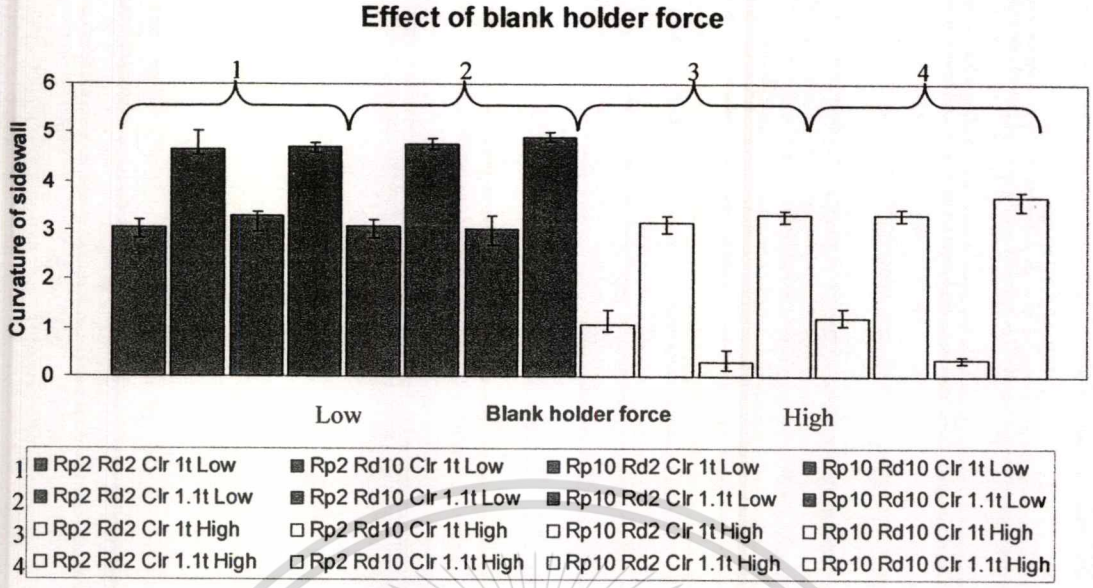

Figure 5.21 Effect of constant blankholder force on curvature of sidewall curl

The twisting angle was considered on the slanted wall (channel side 5 degrees). Twisting most occurs in the slanted wall. In comparison, the difference of springback only represents effect of change of the level of blankholder force while the punch radius, die radius, and tool gap remain the same relatively. Figure 5.22 shows effect of constant BHF on twisting angle relative. It was found twisting angle decreased as the level of constant BHF profile increased. The high blankholder force can reduce twisting angle by an average of 43% in all cases.

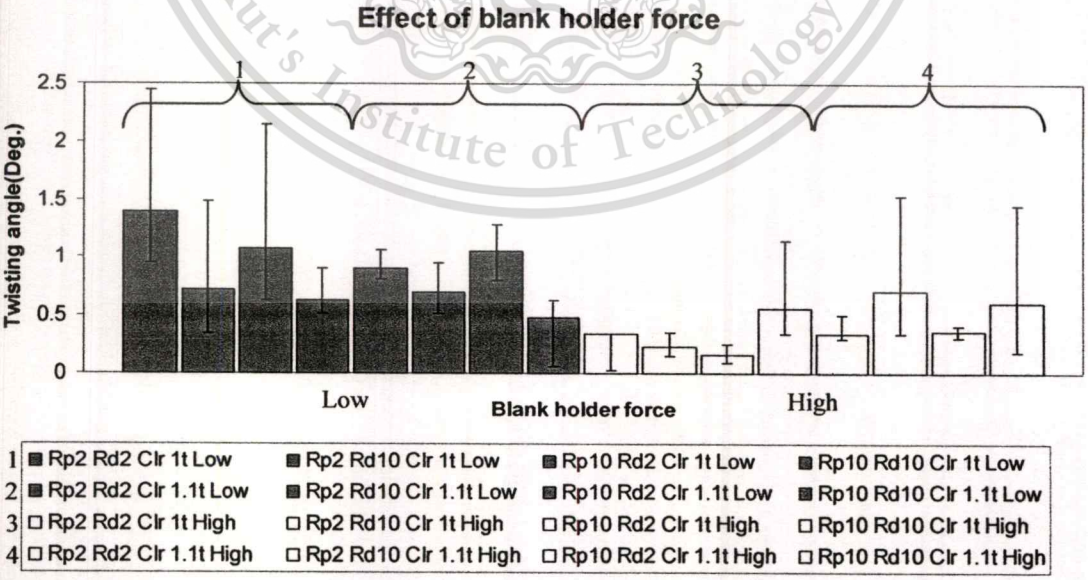

Figure 5.22 Effect of constant blankholder force on twisting angle

5.2.5 Variable blankholder force

It has been found that, high level of constant BHF resulted in reduced springback, curvature of sidewall curl and twisting angle. It was also found that these part deviations could be further reduced when applying appropriate variable BHF profiles. Figure 5.23 , springback angle, curvature of sidewall curl and twisting almost disappeared when applying the variable BHF profile compare with high constant BHF. The Butt-shape was formed with the lowest BHF of 10 tons up until the last 10% forming stroke allowing drawing type of metal flow. Then, a short intense stretching (by rapidly increasing the BHF of 28 tons) was applied during the last 10% forming stroke. Figure 5.24 shows effect of various BHF profiles on the final part thickness.

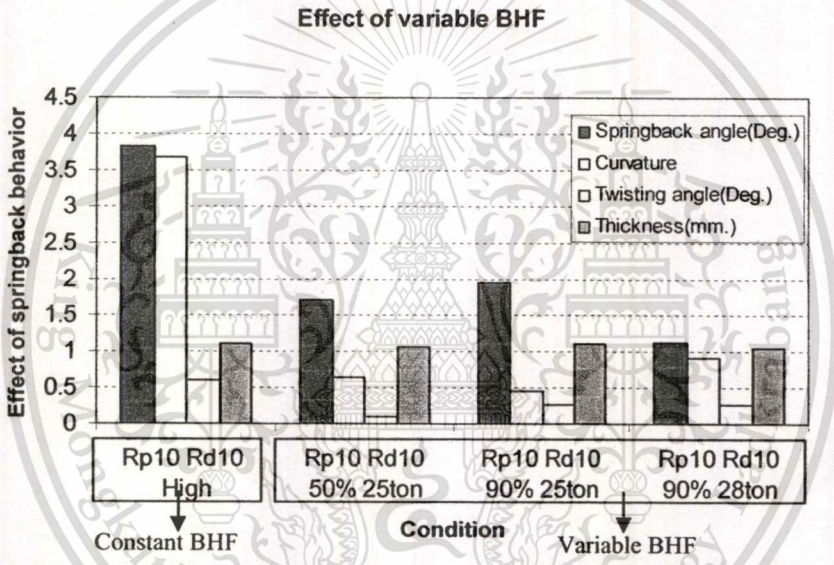

Figure 5.23 Effect of variable blankholder force on springback behavior

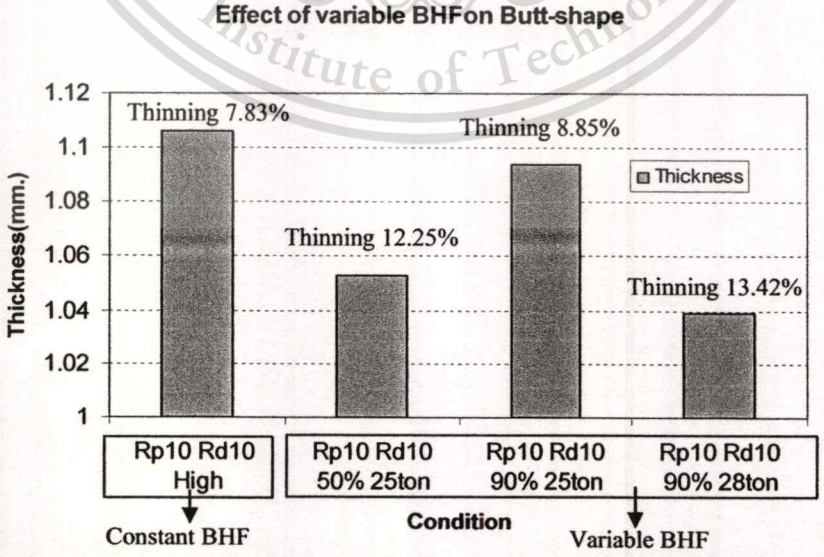

Figure 5.24 Effect of variable blankholder force on thickness

5.3 Main Effect of Process Parameters

The geometry of U-shape and Butt-shape were chosen to examine springback angle, curvature of sidewall curls and twisting angle. The process parameters were conducted to determine their effects on springback behaviors. This section describes normalized effect of all the parameters investigated as to develop die design guideline for springback reduction in a systematical manner.

5.3.1 Main effect of process parameters on U-shape

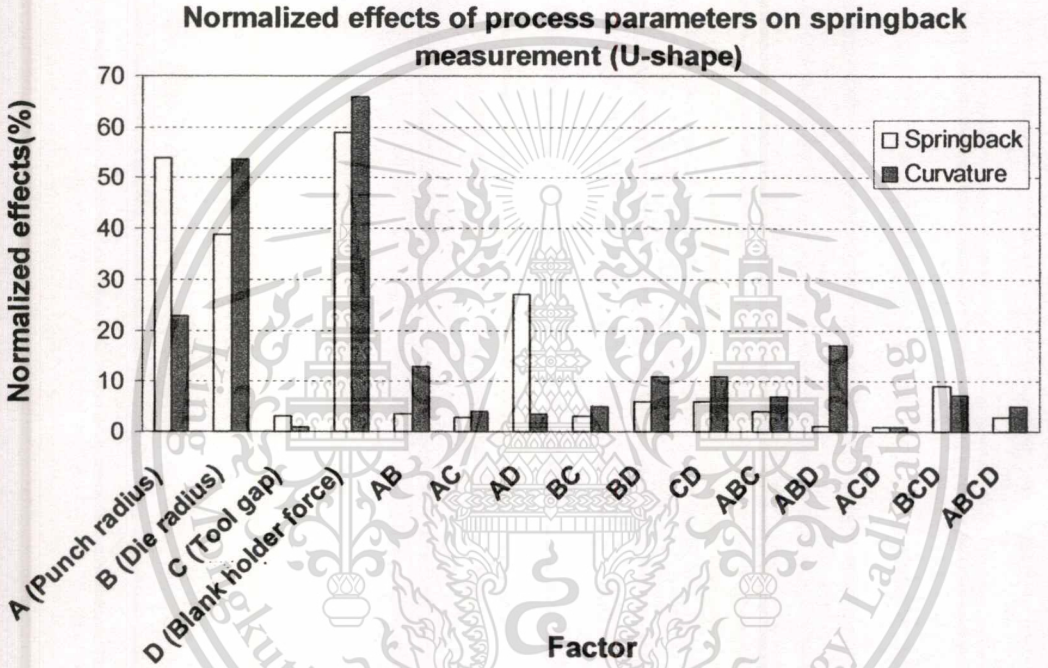

Figure 5.25 Normalized effects of process parameters on springback measurement (U-shape)

The effect of process parameters on springback in this study is defined by the change of springback caused by different settings of process parameters. For instance, the effect of punch radius (factor A) on springback is defined by the difference of springback measurements from parts that are form by two different punch radiuses. The effects are normalized by converting the effect to a percentage based on minimum and maximum springback effect (i.e., vary from 0 to 100%). Once the effects of all factors are determined, they are normalized with the maximum effect. In this case, see Figure 5.25 the blankholder force (factor D) has the maximum effect on both the springback angle and curvature of sidewall curl as in.

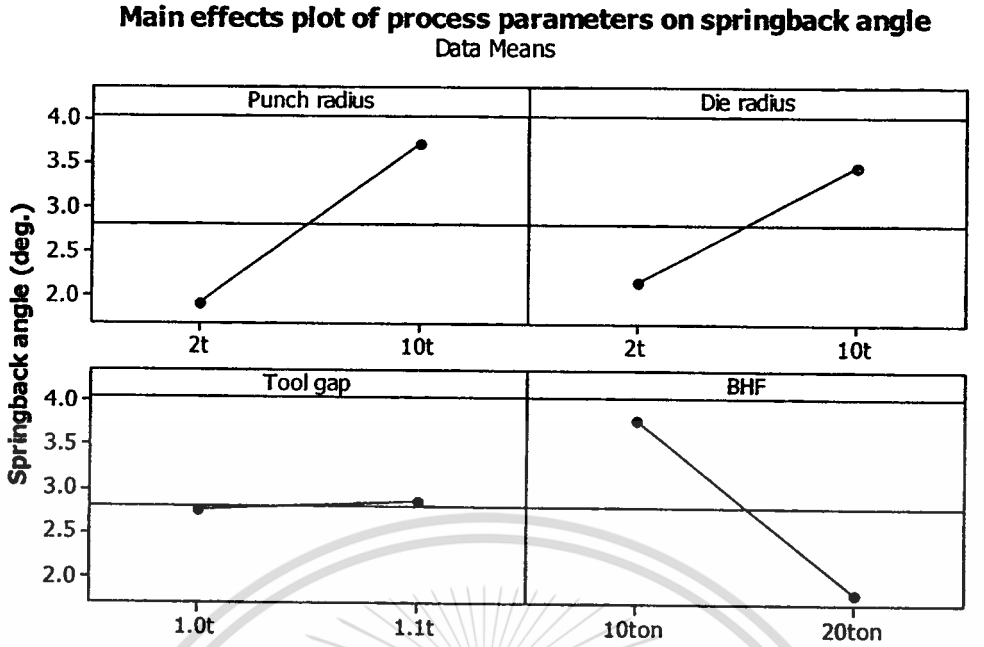

Figure 5.26 Main effects plot of process parameters on springback angle (U-shape)

The main effects of parameters on the springback angle are shown in Figure 5.26. The blankholder force is the most influential parameters to decrease springback. Then, the second, third and least influential parameters are, punch radius, die radius and tool gap. The main effects of all parameters on the curvature of a sidewall curl are shown in Figure 5.27. The blankholder force is the most influential parameters to decrease curvature of sidewall curl. Then, the second, third and least influential parameters are, die radius, punch radius and tool gap.

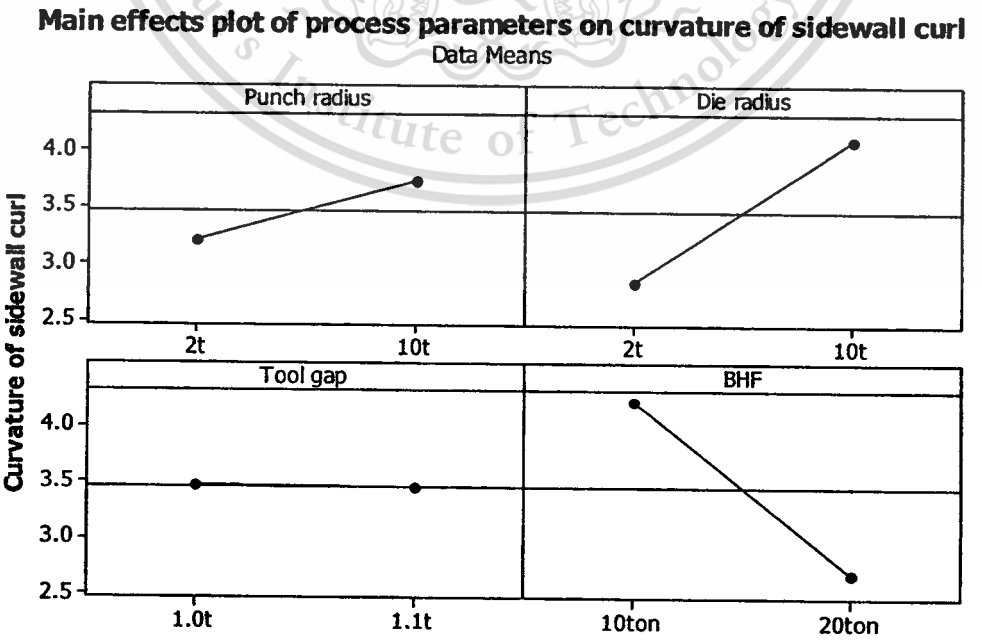

Figure 5.27 Main effects plot of process parameters on curvature of sidewall curl (U-shape)

The die design guideline can be summarized as shown in Table 5.3 for springback reduction.

Table 5.3 Oder of effectiveness of process parameters in reducing the part deviations (U-shape).

Process parameters / Springback behaviors	Punch radius	Die radius	Blankholder force	Tool gap
Springback angle	2	3	1	4
Curvature of sidewall curl	3	2	1	4

5.3.2 Main effect of process parameters on Butt-shape

The Butt-shape, this part has added part geometry deviation, which is twisting angle by the unsymmetrical wall making a 5 degree angle to the channel axis. The effects are normalized by converting the effect to a percentage based on minimum and maximum springback effect (i.e., vary from 0 to 100%). Once the effects of all factors are determined, they are normalized with the maximum effect. In this case, see Figure 5.28 the blankholder force (factor D) has the maximum effect on the springback angle curvature of sidewall curl and twisting angle.

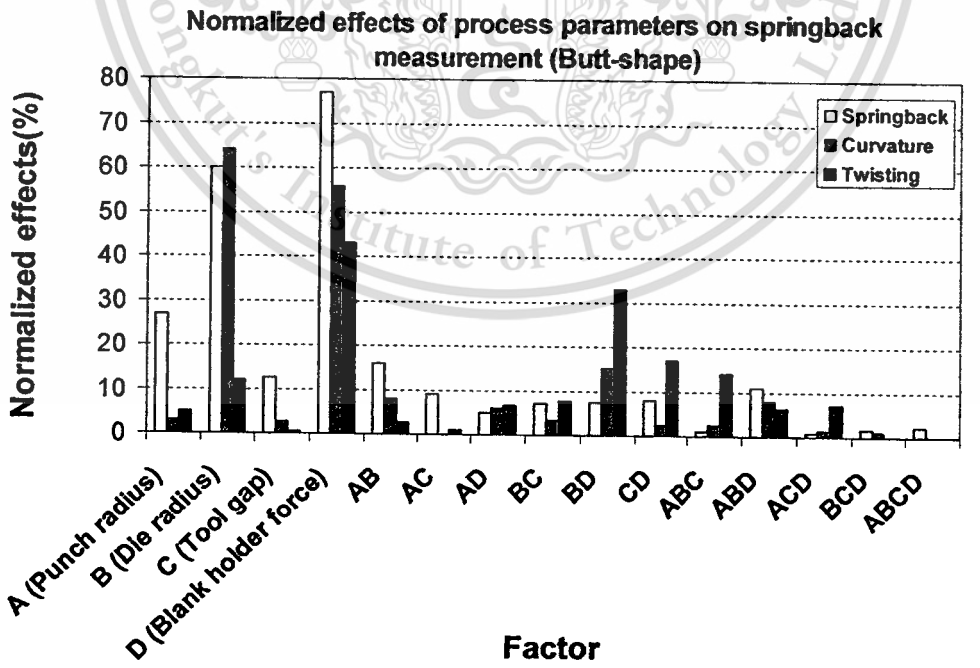

Figure 5.28 Normalized effects of process parameters on springback measurement (Butt-shape)

The main effects of parameters on the springback angle are shown in Figure 5.29. The blankholder force is the most influential parameters to decrease springback. Then, the second, third and least influential parameters are, punch radius, die radius and tool gap. The main effects of all parameters on the curvature of a sidewall curl are shown in Figure 5.30. The blankholder force is the most influential parameters to decrease curvature of sidewall curl. Then, the second, third and least influential parameters are, die radius, punch radius and tool gap. The punch radius and the tool gap can slightly reduce curvature of sidewall curl.

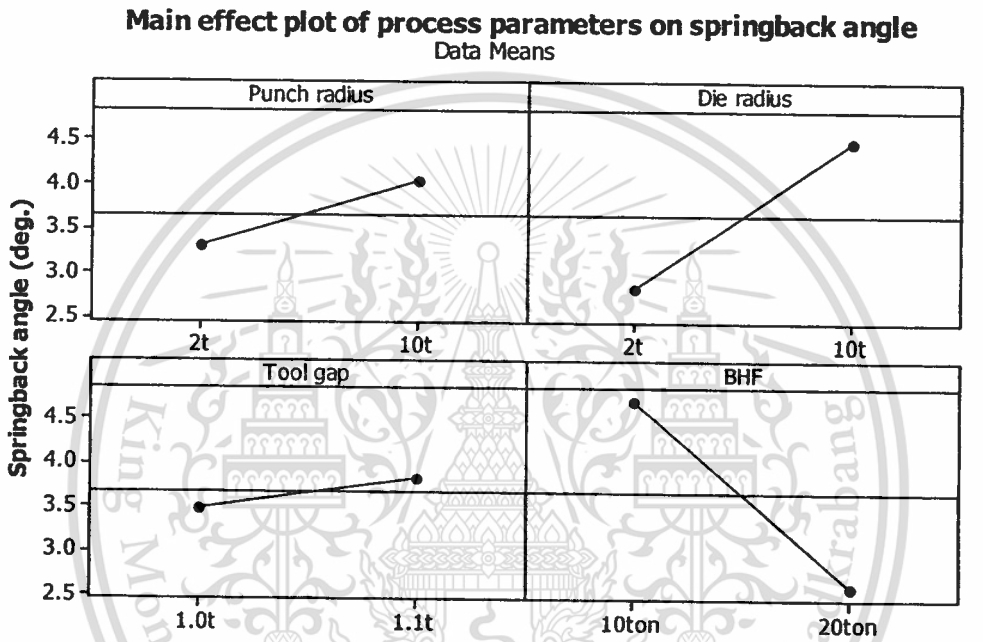

Figure 5.29 Main effect plot of process parameters on springback angle (Butt-shape)

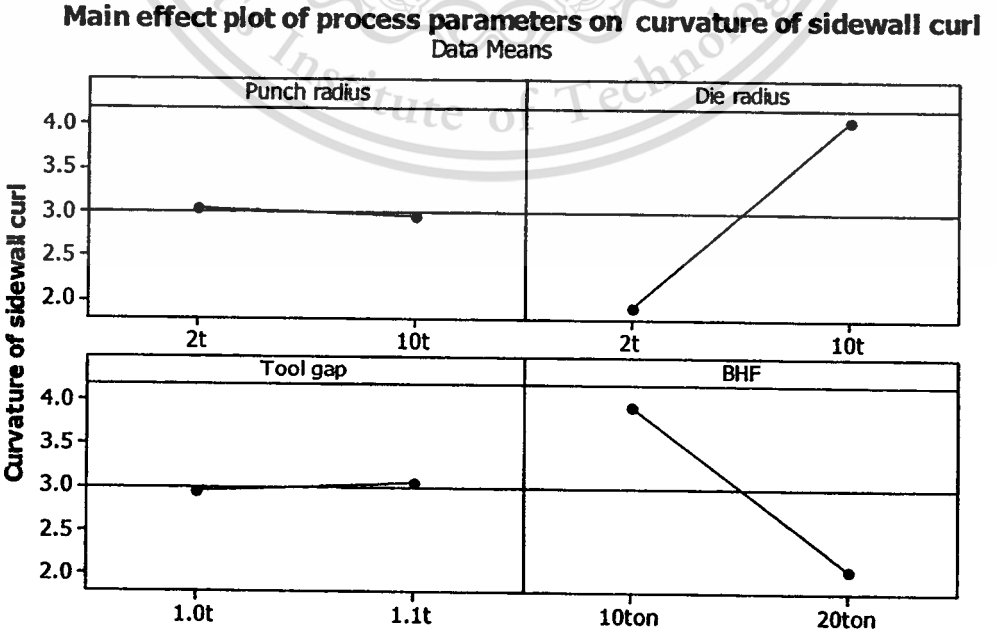

Figure 5.30 Main effect plot of process parameters on curvature of sidewall curl (Butt-shape)

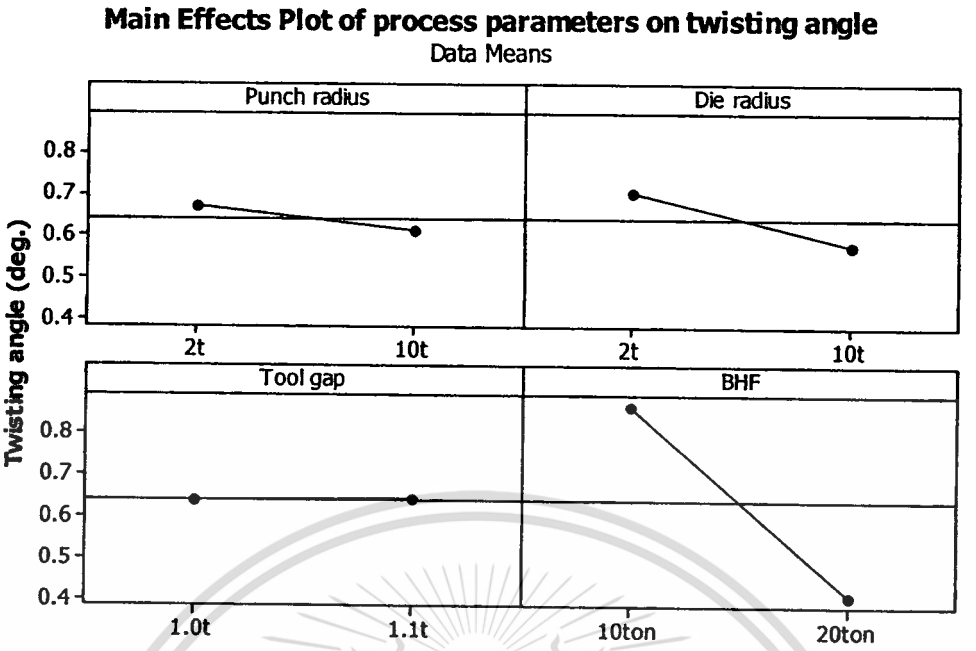

Figure 5.31 Main effect plot of process parameters on twisting angle (Butt-shape)

The main effects of parameters on the springback angle are shown in Figure 5.31. The blankholder force is the most influential parameters to decrease springback. Then, the second, third and least influential parameters are, punch radius, die radius and tool gap. The die design guideline can be summarized as shown in Table 5.4 for springback reduction systematically.

Table 5.4 Oder of effectiveness of process parameters in reducing the part deviations (Butt-shape).

Process parameters / Springback behaviors	Punch radius	Die radius	Blankholder force	Tool gap
Springback angle	2	3	1	4
Curvature of sidewall curl	3	2	1	3
Twisting angle	3	2	1	4

U-shape part and Butt-shape part were used in conducting the process parameter investigation. In order to obtain a springback behavior and die design guideline for springback reduction systematically. The process parameters investigated consist of punch radius, die radius, tool gap and blankholder force, which had two levels in each parameter.

Process parameters can affect the springback on U-shape and hence can significantly influence springback reduction. The most influential process parameter observed in this experiment was the blankholder force. The application of high level of blankholder force showed a much lower springback angle and curvature of sidewall curl. The second most influential, the punch radius can reduce springback angle better than it can to the curvature of sidewall curl. Due to the fact that springback angle occurs around the punch radius, a smaller punch radius will result in greater bending stress thus reducing springback angle. The die radius can reduce curvature of sidewall curl better than it does to springback angle due to the similar reason to in the case of punch radius, curvature of sidewall curls depends on the die radius. The smaller die radius can reduce curvature of sidewall. The least influence parameter, tooling gap slightly reduce springback angle and curvature of a sidewall curl. The results of the above findings indicate that the blankholder force is the most influential process parameter. Therefore, the variable blankholder force profiles were used further to investigate the effect of BHF profile. Both springback angle and curvature of sidewall curl almost disappeared when applying the 90% stroke variable BHF profile. The part thinning obtained is also better than formed by the maximum constant BHF profile.

In the Butt-shape experiments, the effects of process parameters observed in the experiments are quite similar to results of U-shape experiments. However, this part has an added part geometry deviation so called "twisting" caused by the unsymmetrical wall making a 5 degree angle to the channel axis. Twisting most occurs in the slanted wall. The processes parameters can be arranged in an order of their effectiveness to reduce "twisting" as follows blankholder force, die radius, punch radius and tool gap, respectively. Moreover, the variable blankholder force is also found to reduce springbacks including twisting and preserve quality (i.e. thickness distribution) of part.

CHAPTER 6

CONCLUSIONS AND SUGGESTIONS

6.1 Conclusions for Numerical Investigation Finding

The numerical parameters used in finite element analysis of U and Butt-shape forming and springback were studied to understand their effects on the springback prediction. In order to improve accuracy of springback simulation, the numerical parameters consist of element size, adaptive angle tolerance, integration point and time step size. These parameters were used to investigate on U-shape model. Then, the proper numerical parameters were used to investigate an effect of blankholder force profile (i.e. constant BHF and variable BHF) on U-shape and Butt-shape simulation. The numerical parameters investigation can be summarize as follows.

- The bending and unbending occurring around die or punch radius is the cause of springback. The element size over die radius was used to study numerical parameters affecting springback prediction. The element size of 4 degrees of turning angle over die radius seems to be proper parameters when compared with the result obtained from springback experiment.
- The proper element size was conducted to investigate the adaptive angle tolerance. The small adaptive angle tolerance of 1 degree was much more sensitive to observe a significant area of part geometry.
- The proper element size and adaptive angle tolerances were applied to conduct further simulation to examine the effect of a number of integration points. The springback prediction seemed rather constant as the number of integration points increased. While the number of integration point increased, the computational time of springback prediction was increased. Therefore, the number of integration point of 9 was selected to be a proper parameter, when consider computational time.
- The set of proper parameters previously was applied to investigate effect of time step size. The minimum time step of 3 e^{-7} sec. reduced mass increase to be less than 100% and the computational time was reduced by 50%, but the result showed a similar springback prediction to the one without any mass scaling.

The proper numerical parameters setting was used to study of the process parameters, i.e. blankholder force profile, on U and Butt-shape model in order to study blankholder force profile (i.e. constant BHF and variable BHF) affecting springback reduction. The tendency of a springback angle and a curvature of a sidewall curl decreases when as the level of constant BHF profile increased form 10 to 20 ton on both U-shape and Butt-shape. However, the thickness of part on U-shape and Butt-shape were decrease 4.8 to 8.7% and 4.8 to 9.13% respectively due to stretching of material. In order to improve part of quality and reduce springback, so that the variable BHF profiles is applied. It was found that, can reduce deviations of specimen, i.e. (springback angle, curvature of a sidewall curl and twisting angle) and still keep part quality, i.e. thickness when applying the 90% stroke BHF profile. Therefore, the variable blankholder force profile can be very useful if it is applied appropriately.

6.2 Conclusion for Experimental Investigation Finding

The process parameters investigated consists of punch radius, die radius, tool gap and blankholder force, which had two levels of each parameter. The blankholder force can be separated into two groups (i.e. constant blankholder force and variable blankholder force). Then, U-shape and Butt-shape were formed to study springback behaviors, which were springback angle, curvature of a sidewall curl and twist angle. The resultant effect of process parameters on springback then were used to develop die design guideline systematically for springback reduction.

Springback angle reduction

- The most influential process parameter for springback angle reduction was blankholder force. The application of constant blankholder force from 10 to 20 tons resulted in the springback angle decrease by 59%. However, more springback angle decrease of 61.32% was achieved from the application of variable BHF profile (i.e. constant during 0-90% stroke and raised up to 28 tons at the end stroke).
- The second most influential parameter for springback reduction was punch radius. It was found that springback angle was decreased by 54% when applied the smaller punch radius.

- In cases where blankholder force or punch radius cannot be changed to adjust die design, the die radius is next to be reduced to lower springback angle. It was found that when applied the small die radius, springback angle can be reduced by 39%.
- The tool gap was the least influential parameters on angle.

Table 6.1 summarizes all the process parameters in the order that they should be modified to gain the most springback angle reduction.

Table 6.1 Springback angle reduction die design guideline.

Order of effectiveness	Influence parameters	Springback reduction (%)
1	Blankholder force	59
2	Punch radius	54
3	Die radius	39
4	Tool gap	3

Curvature of sidewall curl reduction

- In case of curvature of a sidewall curl reduction, the blankholder force was the most influential process parameter similar to springback angle reduction. It was able to reduce curvature of a sidewall curl by 66% when applied the constant blankholder force from 10 to 20 tons. It was found that curvature of sidewall decreased even more when applying the variable BHF profile (i.e. 90% forming stroke the BHF is raised up to 25 tons rapidly compared with high constant BHF of 20 ton blankholder force). The curvature of a sidewall curl was decreased by 89.46%.
- The curvature of sidewall curl depends on die radius due to bending and unbending that occur over the die radius. The smaller die radius was applied to reduce curvature of a sidewall curl. It was found that curvature of a sidewall curl decreased by 54% when applying the small die radius, which was the second most influential parameter for curvature of sidewall reduction.
- The tool gap again was the least influential parameter.

Table 6.2 summarizes all the process parameters in the order that they should be modified to gain the most curvature of sidewall curl reduction.

Table 6.2 Curvature of sidewall curl reduction die design guideline.

Order of effectiveness	Influence parameters	Curvature reduction (%)
1	Blankholder force	66
2	Die radius	54
3	Punch radius	23
4	Tool gap	1

Twisting angle reduction

- The twisting angle was caused by the unsymmetrical geometry which is the Butt-shape investigated to study of twisting angle behavior. The most influential parameter on twisting angle reduction was also blankholder force. While applying the constant blankholder force of 10 to 20 tons, the twisting angle was decreased by 43%. Moreover, it was found that twist angle decreased even more when applying the variable BHF profile (i.e. 50% forming stroke the BHF is raised up to 25 tons rapidly compared to high constant BHF of 20 ton blankholder force). The twisting angle was decreased up to 82.02%.
- When switching the die radius from 10t to 2t, the twisting angle was decreased on an average of 12%, which represented the second most influential parameter for twisting angle reduction.
- The punch radius and tool gap were found to be the third and fourth most influential parameters. They only reduced the twisting angle 5% and 1%, respectively.

Table 6.3 summarizes all the process parameters in the order that they should be modified to gain the most twisting angle reduction.

Table 6.3 Twisting angle reduction die design guideline.

Order of effectiveness	Influence parameters	Springback reduction (%)
1	Blankholder force	43
2	Die radius	12
3	Punch radius	5
4	Tool gap	1

6.3 Suggestions for Future Work

There are some suggestions for further study parameters affecting springback of advanced high strength steel sheets.

6.3.1 Different material models should be investigation in order to improve springback prediction.

6.3.2 Further investigate the effect of element size using different element formulation.

6.3.3 The contact algorithm should be further examined their real effect in order to study and improve springback simulation for an accurate prediction.

REFERENCES

1. Asnafi N. "pringback and fracture in v-die air bending of thick stainless steel sheets" **Materials & Design**, 21(3):217–236, 2000.
2. ASTM, **Standard Test Method for Plastic Strain Ratio r for Sheet Metal.** American Association State: 487 – 493. 1998.
3. Auto/Steel Partnership. 2000. **High Strength Steel Stamping Design Manual.** Michigan.: Auto/Steel Partnership
4. Carden W.D., Geng L.M., Matlock D.K., and Wagoner R.H. "Measurement of springback." **International Journal of Mechanical Sciences**, 44(1):79–101, 2002.
5. Chirita B. 2003. "Experimental study of the influence of blankholder force on spring-back of sheet metal." **Archives of Civil and Mechanical Engineering.** 3 (2)
6. Chou I.N. and Hung C. "Finite element analysis and optimization on springback reduction." **International Journal of Machine Tools & Manufacture**, 39(3):517–536, 1999.
7. Du C., Wu J., Militisky M., Principe J., Garnett M., and Zhang L. "Springback Control with Variable Binder Force Experiments and FEA Simulation." **AIP Conference Proceedings.** 712:970-976, 2004.
8. Galbraith P.C. 2004. **Springback of the Numisheet '96 S-Rail: Influence of Adaptivity, Coarsening and Stress Mapping on LS-DYNA Predictions.** [Report]. Canada : Metal Forming Analysis Corporation.
9. Hosford W.F. and Caddell R.M. 2007. **Metal Forming Mechanic and Metallurgy.** 3rd ed. Cambridge : Cambridge University Press.
10. Karafillis A.P. and Boyce M.C. 1996. "Tooling and binder design for sheet metal forming processes compensating springback error." **International Journal of Machine Tools & Manufacture**, 36(4): 503-526.
11. Leu D.-K. A "simplified approach for evaluating bendability and springback in plastic bending of anisotropic sheet metals." **Journal of Materials Processing Technology.** 66(1-3):9–17, 1997.
12. Lingbeek R. 2005. **Springback compensation for an analytical elasto-plastic stretch-bending model.** Berlin: Netherlands Institute for metal research.

REFERENCES (CONT.)

13. Lingbeek R., Huetink J., Ohnimus S., Petzoldt M. and Weiher J. 2005. "The development of a finite elements based springback compensation tool for sheet metal products." **Journal of Materials Processing Technology.**

14. Liu G., Lin Z., Xu W. and Bao Y. 2002. "Variable Blankholder Force in U-shaped Part Forming for Eliminating Springback Error." **Journal of Materials Processing Technology.** 120: 259-264.

15. Livatyali H. and Altan T. 2001. "Prediction and elimination of springback in straight flanging using computer aided design methods: Part 1. Experimental investigations." **Journal of Materials Processing Technology.** 117(1-2):262–268.

16. Livatyali H., Wu H.C., and Altan T. 2002. "Prediction and elimination of springback in straight flanging using computer-aided design methods: Part 2: Fem predictions and tool design." **Journal of Materials Processing Technology.** 120(1-3):348–354.

17. Maker N.B. and Zhu X. 2001. **Input Parameters for Springback Simulation using LS-DYNA.** California: Livermore Software Technology Corporation.

18. Marciniak, Z., Duncan, J.L. and Hu, S.J. 2002. **Mechanic of Sheet Metal Forming.** 2nd ed. Oxford : Butterworth Heineman.

19. Pourboghrat F. and Chu E. 1995. "Springback in plane strain stretch/draw sheet forming." **International Journal of Mechanical Sciences.** 37(3):327.

20. Wagoner R.H. and Gan W. 2004. "Die design method for sheet springback." **International Journal of Mechanical Sciences.** 46:1097–1113

21. Wagoner R.H. and Li M. 2007. "Simulation of springback: Through-thickness integration." **International Journal of Plasticity.** 23: 345–360.

22. Wang J., Verma S., Alexander R. and Gau J.T. 2008. "Springback Control of Sheet Metal Air Bending Process." **Journal of Manufacturing Processes.**

23. World Auto Steel. 2009. **Advanced High Strength Steel (AHSS) Application Guidelines.** Ohio: World Auto Steel.

24. Xu W.L., Ma C.H., Li C.H. and Feng, W.J. 2004. "Sensitive factors in springback simulation for sheet metal forming." **Journal of Materials Processing Technology.** 151: 217–222.

REFERENCES (CONT.)

25. Yao H., Liu S.D., Du C. and Hu Y. 2002. "Techniques to Improve Springback Prediction Accuracy Using Dynamic Explicit FEA Codes." **Society of Automotive Engineers Technical paper.** No.159.

26. Zhang D., Cui Z., Ruan X. and Li Y. 2007. "An analytical model for predicting springback and side wall curl of sheet after U-bending." **Computational Materials Science.** 38: 707–715.

27. Zhang L.C., Lu G., and Leong S.C. 1997. "V-shaped sheet forming by deformable punches." **Journal of Materials Processing Technology.** 63(1-3):134–139.

APPENDIX A

3rd INTERNATIONAL CONFERENCE ON ASIAN SIMULATION AND MODELING 2009

Appendix A-1: FEA Study on Parameters Affecting Springback of Forming of Advance High Strength Steel sheets (AHSS)

Appendix A-1: FEA Study on Parameters Affecting Springback of Forming of Advance High Strength Steel sheets (AHSS)

International Conference

ASIMMOD 2009

Proceedings

"Simulation for Unsolved Problems"

3rd International Conference on

Asian Simulation and Modeling 2009

January 22-23, 2009 Miracle Grand Convention Hotel

Bangkok, Thailand

Edited by ASIMMOD2009 Technical Committee

Supported by

Kasetsart University

Sripatum University

Royal Project Foundation

Modeling and Simulation Society of Thailand

Preface

This proceedings volume contains a set of full manuscripts accepted for presentations and publications at the third ASIMMOD 2009, an international conference held at Miracle Grand Convention Hotel, Bangkok, Thailand on January 22-23. As the chair of this conference, I would like to thank all participants who have contributed papers, all committee and other relative groups of interest who have directly and indirectly help organizing and setting up this meeting. My deeply sincere respect also goes to our technical committee for reviewing and editing this published workbook. It is my honor to write this preface on their behalves. This continued event would not have been possible without the initial leadership and continuous support from Professor Santas Rojanasunthorn, Royal Project Foundation of Thailand. Having set such a high standard on organizing the previous two meetings by Professors, Voratas Kachitvichyanukul from Asian Institute of Technology, Thailand and Benchaphun Ekasingh from Chiang Mai University, Thailand respectively should also be acknowledged. I also would like to acknowledge the support from our co-organizing partner, Sripatum Univesity led by President Rutchaneeporn Pookayaporn. Sripatum staffs have played a major role on resolving many jigsaw puzzles occurred during the last stage of organizing this conference. Last but not least, I would like to apologize for all mistakes if existed during the conference and we will use this experience of a better future and wish you all the best. Your continuous supports for the future ASIMMOD events will be expected and see you again on 2011.

Vudtechai Kapilakanchana,
President, Kasetsart University
President, Modeling and Simulation Society of Thailand (MSST)
ASIMMOD 2009, Organizing Chair

Proceedings of ASIMMOD 2009, January 22-23, Bangkok, Thailand

FEA Study on Parameters Affecting Springback of Forming of Advance High Strength Steel sheets (AHSS)

Watcharapong Sirigool[1],Nattawoot Depaiwa[1], Suwat Jirathearanat[2], Adachi Tadaharu[3]
Department of Mechanical Engineering, Faculty of Engineering,
King Mongkut's Institute of Technology Ladkrabang[1]
Near Net Shape Metal Manufacturing Research Group, National Metal and Materials Technology Center[2]
Department of Mechanical Sciences and Engineering, Tokyo Institute of Technology[3]

Abstract: Recently, advanced high strength steels (AHSS) are becoming widely used in many applications in place of mild steels, especially in automotive part manufacturing, due to its low weight, high strength and fairly good formability. However, the unavoidable obstacle of AHSS sheet metal forming is springback, which is a result of elastic recovery and residual stress. The aim of this study is to determine proper process parameters enabling reduction of springback defects in AHSS forming process. In this paper, a U-shape and a Butt-shape forming were used to examine springback behaviors, which are springback angle, sidewall curl, and twist, through finite element analyses. Simulation numerical parameters affecting springback prediction, which are element size, number of integration poinnts through thickness, adaptive meshing, and mass scaling increase were investigated to identify suitable simulation numerical settings for accurate springback prediction. Then, the simulation model was applied to study effects of blank holder force on springback behaviors and formability of the U-shape and Butt shape forming in an attempt to find proper blank holder force profiles for springback reduction emphasized die design guidelines.

Key words: Springback, AHSS, Stamping die designs

1. Introduction

Recently, advanced high strength steels (AHSS) such as dual-phase steels are becoming widely used in many applications in place of mild steels, especially in automotive parts manufacturing, owning to its light weight, high strength and good formability. However, the unavoidable obstacle of AHSS sheet metal forming is springback, which is referred to as the geometry changes of a part after tool removal. In metal forming process, springbacks are mainly caused by residual stress distributions after elastic recovery both in plane and through thickness of product. The severity of that residual stress depends on sheet metal mechanical properties (E, YS and n-value), material thickness, die geometry (die & punch radii, tool clearance), as well as forming process parameters (blank holder force and part-die lubricity) used during forming. With severe spring back defects, AHSS part assembly are difficult if not possible at all due to each individual part geometric deviations. Consequently, inevitably die geometry and process parameters need to be adjusted in the expense of time and money. This paper focuses on shape fixation techniques based on proper application of blank holder force profiles determined through well-adjusted FE simulations.

Many studies have been carried out in various aspects of springback in sheet metal forming. Specifically, as for numerical simulation related issues, Xu [1], Li and Wagner [2], Maker [3], Shi et al. [4], Lee and Yang [5] Yao and Lui [10] found that FEM simulations of springback are much more sensitive to numerical tolerances than forming simulations. The numerical parameters include the number of integration point [1-5] [10], size of element [1-5] [10], adaptive angle in tolerance and minimum time step [10]. According to the literature review, the numerical parameters such as the size of element, number of integration through thickness and adaptive meshing tolerance degree can affect the accuracy of FEA simulation. In this paper, finite element analyses were conducted to study effects of simulation numerical parameters on calculation of springbacks and, thus, to define their suitable values for accurate springback simulation. The simulation model was then utilized to determine proper process parameters, i.e. blank holder force profiles, for reducing springback defects in AHSS, SPHC590, forming process.

2. Methodology

In this study, simplified part geometries, which are U-shape and Butt-shape were used for forming and springback simulations. The geometry of U-shape resembling to rail components and pillar-like Butt-shape were chosen to examine part springback angle,

Corresponding Author: Watcharapong Sirigool , Department of Mechanical Engineering, Faculty of Engineering, King Mongkut's Institute of Technology Ladkrabang, Thailand

curvature of sidewall curl, and twisting. The punch and die radii of the U-shape and Butt shape are 12 mm. which is 10 times of its thickness. Fig. 1 shows the geometry of U-shape and Butt-shape.

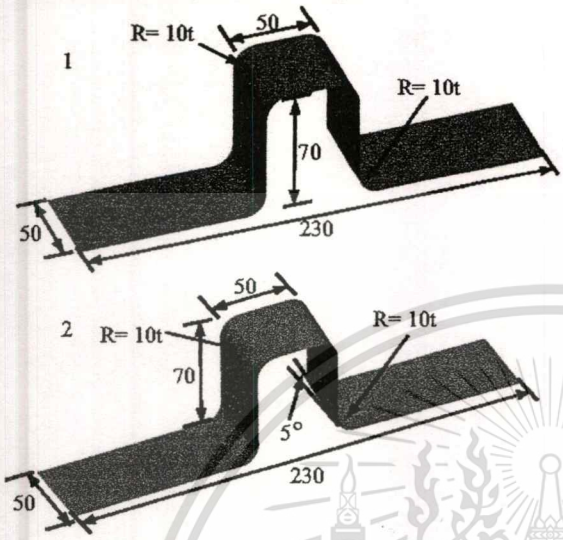

Fig. 1: top) U-shape bottom) Butt-shape

Fig. 2 shows three types of springback, which are springback of wall opening angle (θ_1), curvature of sidewall curl (ρ) and twist angle(θ_2).

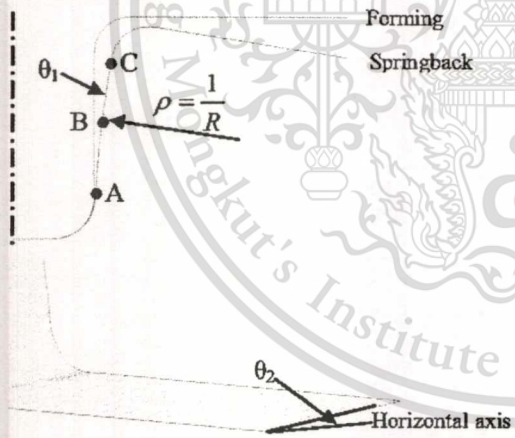

Fig. 2: Mesurement for U-shape and Butt-shape

θ_1 is an angle that a straight line passing through point A, C makes to the referenced vertical axis. ρ is a curvature of the sidewall curl constructed by point A, B and C. θ_2 is a twisting angle that the part flange line makes to the referenced horizontal axis.

3. Simulation

3.1 Numerical Parameter Investigation

Dynamic explicit and static implicit finite element analyses of the part forming and the formed part springback were performed by Dynaform 5.5 code [7]. First, the forming simulation was done using dynamic explicit analysis. Then, the data obtained form the forming simulation such as blank property, stress , plastic strain distributions and, deformed geometry, were saved to apply in the springback simulation using static implicit analysis. In forming and springback simulations, the blank was modeled with fully integrated shell element type having nine integration points along the thickness direction [7]. The material model was applied following the research work of Barlat–Lian [6], with isotropic hardening and m= 6. The dimension of initial blank is 350x50x1.2 mm. The material used in this study was SPHC 590 high strength steel sheets. The sheet metal mechanical behavior was characterized by tensile tests as shown in table1 below. Coulomb friction coefficient of 0.125 was assumed. A constant blank holder force profile of 10 tons was used to form the part in all the simulation cases.

Table1 Mechanical properties

Material	t,mm	E,GPa	YS,MPa	K,GPa	n
SPHC590	1.2	198.821	336.297	937.942	0.195

R_0=1.372, R_{45}=1.167, R_{90}=1.543

An array of U-shape forming and springback simulations was conducted to investigate numerical parameters affecting accuracy of springback prediction. The procedure of numerical parameter investigation followed was to study one parameter at a time, shown in Fig. 3, in such an order that interactions between these parameters are made minimum. First, the effect of element size is investigated, and then a proper element size was chosen to analyze effect of adaptive remeshing. The proper element size and adaptive remeshing are chosen to further analyze effect of number of integration point. Then, effect of mass scaling (time-step size) was studied with a proper set of previously determined parameters. Finally, the proper set of all numerical parameters was determined to conduct simulation analyses determination of proper blank holder force profiles with confidence.

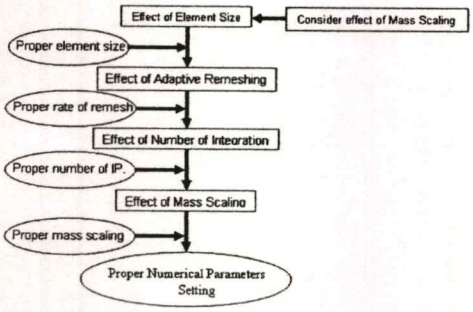

Fig. 3: Flowchart of numerical parameters simulation

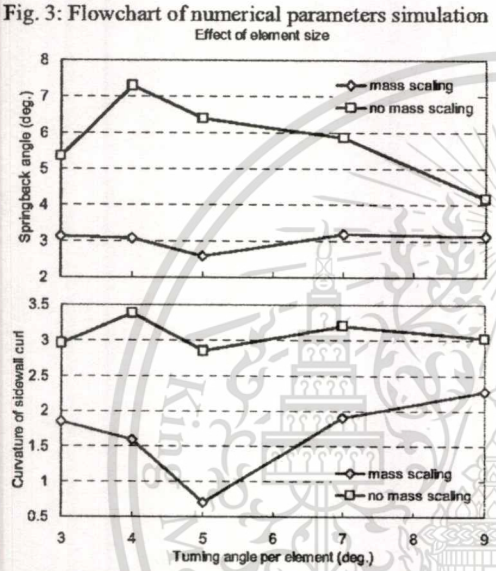

Fig. 4 Effect of element size

Fig. 4 shows effects of element size and use of mass scaling on calculation of springback opening angle and curvature of sidewall curl. The effect of mass scaling was consistent; simulations without mass scaling predicted more springbacks than with mass scaling for all the element sizes considered. Generally, a no mass scaling model should give more accurate results, because it has no additional inertial force incurred by the added mass. The element size per turning degrees of tool radii is known to greatly affect accuracy of springback prediction as it can better represent part geometry when it becomes smaller but at the expense of increased computation time, Fig. 4. From the figure, springbacks seem to increase as the element size becomes smaller except at element size of 3 degrees. With the absence of experimental data, the size of element per 4 degree seems to be a proper choice considering it giving maximum springbacks at reasonable computational time (about one third of the simulation with element size of 3 degrees).

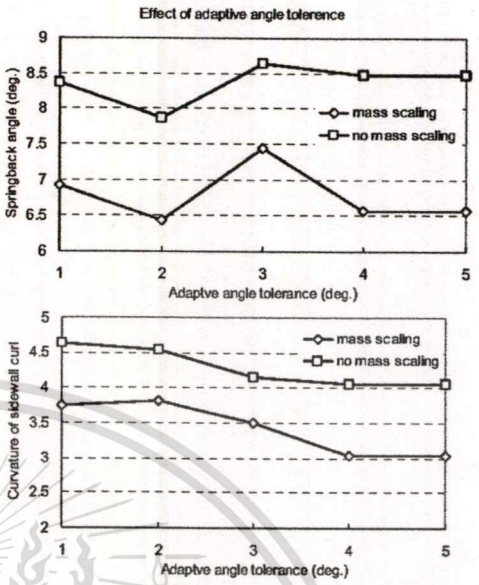

Fig. 5: Effect of adaptive angle tolerance

Fig. 5 shows effect of adaptive angle tolerance, by which the part mesh is refined when the angle between any adjacent elemental normal vectors exceed. In the case without mass scaling simulation, the springbacks were again larger than the case with mass scaling for all the adaptive angle tolerance. The springback predictions are stagnant at first but later become larger as the adaptive angle tolerance is much smaller; elements become smaller at a faster rate. The small adaptive angle tolerance of 1 degree is much more sensitive to part geometry based mesh refinement than 5 degree tolerance. Therefore, 1 degree tolerance is chosen as a proper adaptive angle tolerance.

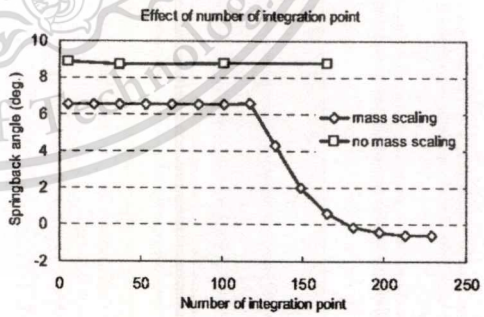

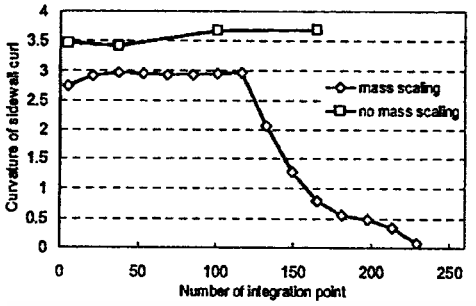

Fig. 6: Effect of number of integration point

Effect of number of integration point through thickness is shown in Fig. 6. With no mass scaling applied, springback angle prediction seemed somewhat constant while the curvature of sidewall curl increased slightly as the number of integration points increased. Interestingly, it can be found from the figure that the proper number of integration point is low for springback angle calculation compared to that of curvature of sidewall curl calculation. Considering computational time spent, in this case, the number of integration point of 9 was chosen to be proper. The simulations employing mass scaling clearly underpredicted the springbacks, especially when the number of integration point was larger than 125.

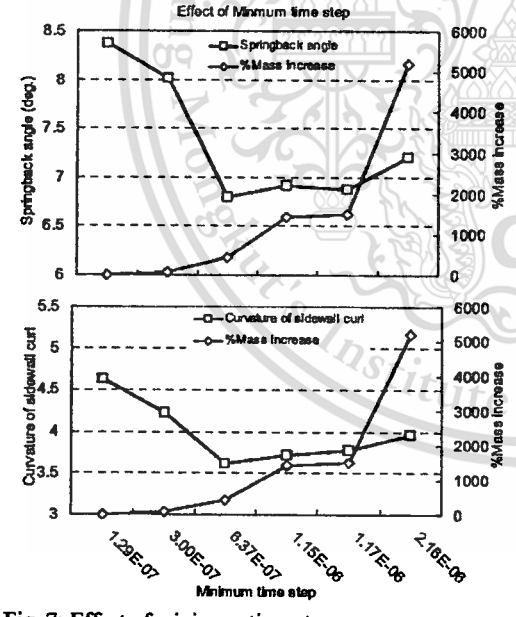

Fig. 7: Effect of minimum time step

Based on the simulation results up to this point, it is evident that simulations with mass scaling technique give erroneous springback prediction. However, it is usually more time-efficient to allow a careful application of mass scaling when adaptive mesh refinement is used to avoid too small of minimum time step leading up to extremely long computational time. Fig. 7 shows relationship of mass scaling increase and minimum time step, and their effect on springback prediction. The necessary minimum time step decreases as the mass scaling decreases requiring more computational time. Springback is predicted larger as minimum time step decreases. In this case, the minimum time step is 1.29E-07 sec when no-mass scaling is used. However, if only a small amount of mass scaling is applied (i.e. 70% mass increase) the necessary minimum time step is increased to 3.0E-07 sec resulting in 50% computational time reduction but with similar springback prediction. Thus, minimum mass increase (i.e. less than 100%) or equivalent to necessary minimum time step of 3.0E-07 sec seems to be a proper numerical setting for the proceeding process simulations.

3.2 Process Parameter Investigation

Effect of various Blank Holder Force (BHF) profiles on springback behavior and formability of the U-shape and Butt shape forming is investigated in an attempt to find proper BHF profiles for part springback reduction. Fig. 8 shows various profiles of BHF used in this study for both part geometries. Many researchers [8] [9] have suggested that proper part stretching during forming can reduce part springback. The underlying idea of these various BHF profiles is to determine when and how much to stretch the part through BHF action as to reduce part springbacks. All the numerical parameter settings determined previously were used here.

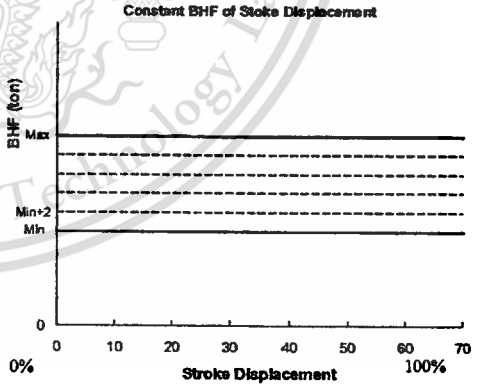

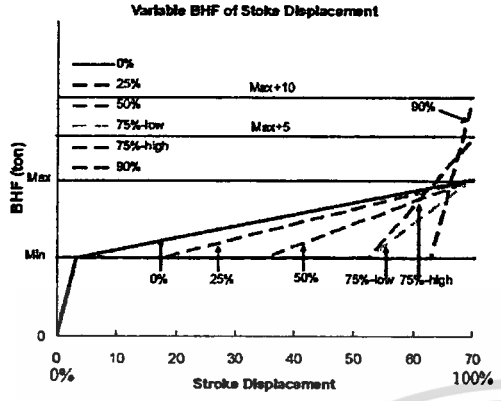

Fig. 8: Constant blank holder force profiles (top) and variable blank holder force profiles (bottom)

All the trial BHF profiles can be grouped in two; 1) BHF is kept constant throughout the forming stroke – "constant BHF profiles", and 2) BHF is kept constant up to certain forming strokes then increased linearly up to the end stroke – "variable BHF profiles". For each part geometry all constant BHF profiles are bounded by the lowest BHF, which is 10 tons as it is the lowest BHF available in our hydraulic press, and the highest BHF, by which the part can be form without necking. It was found that the highest BHF is 20 tons for U-shape and 22 tons for Butt shape. Most of the trial variable BHF profiles run between these lowest and highest values of BHF applied in the cases of constant BHF. However, two variable profiles exceeding the highest BHF value were applied without any part fracture.

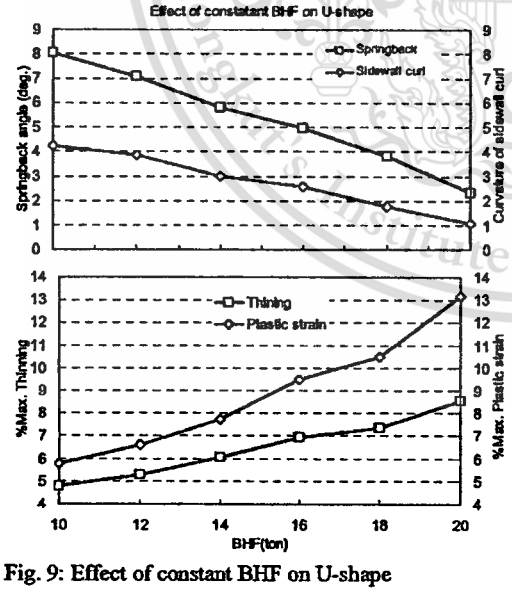

Fig. 9: Effect of constant BHF on U-shape

Fig. 9 shows effect of constant BHF profiles and corresponding part formability. The tendency of springback behavior was reducing. When blankholder forces increase springback and curvature of sidewall curl, the blank holder force was limited to 20 ton because higher values led to broken parts. The springback angles θ_1 and curvature of sidewall curl vary more substantially for smaller values of blankholder force. An increase of blank holder force from 10 ton to 20 ton, the %max thinning and %max plastic strain were increment.

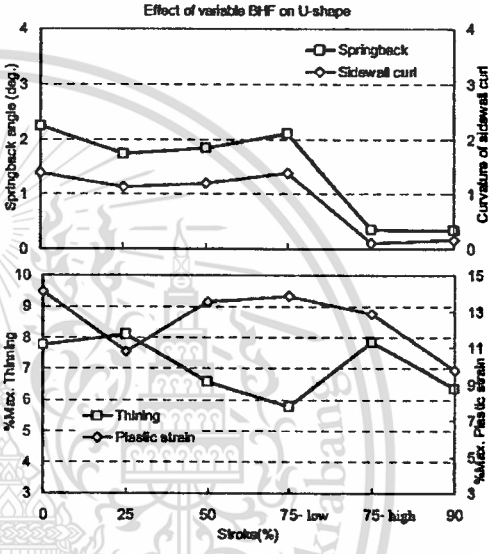

Fig. 10: Effect of variable BHF on U-shape

Fig. 11: Effect of variable BHF profiles and corresponding part formability. The tendency of springback behavior was reducing then the springback behavior was increment at 50% stroke. The variable blankholder forces were the most reductional springback behavior especially in cases 75%-high and 90%. The value of %maximum thinning was reducing, when the stroke% was increment until 75%-low. In case 75%-high, the thinning was increment then the 90% was reduce thinning. The % maximum plastic strain was reducing. When blankholder forces increase %maximum plastic strain.

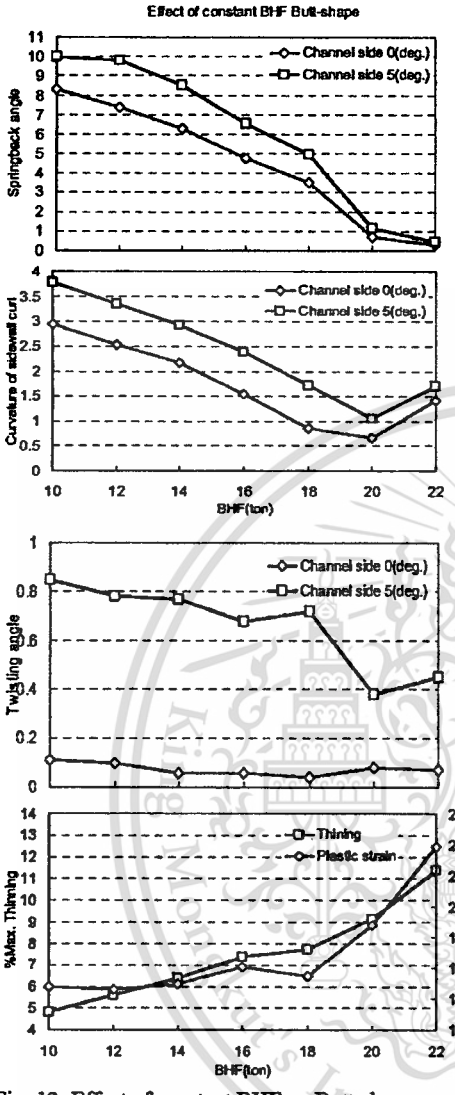

Fig. 12: Effect of constant BHF on Butt-shape

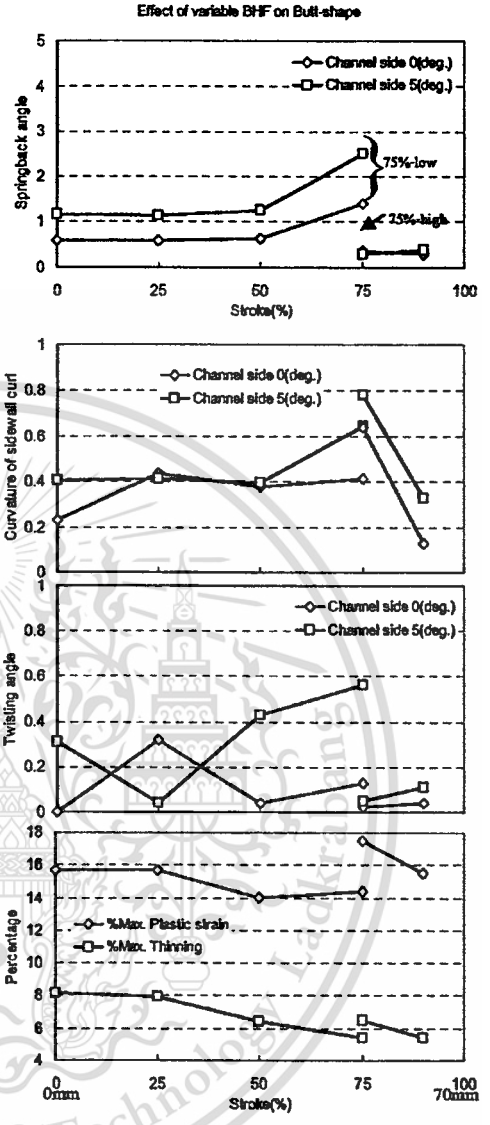

Fig. 13: Effect of variable BHF on Butt-shape

Fig. 11 shows effect of constant BHF profiles and corresponding part formability. The tendency of springback behavior was reducing. When blankholder forces increase springback and curvature of sidewall curl, the blank holder force was limited to 22 ton because higher values led to broken parts. The springback angles θ_1 and curvature of sidewall curl vary more substantially for smaller values of blankholder force. An increase of blank holder force from 10 ton to 22 ton The twists of flange θ_2 on channel side 5° can be reducing twist angle depend on blankholder force. The thinning and plastic strains were increment percentage when the BHF increase force.

Fig. 12 shows effect of variable BHF. The springback angle was similar until case 75%-low, which are both of channel side angle increase. In cases 75%-high and 90% stroke, the springback angles were decrease both of channel side. The curvature of channel side 0° was smaller at 0% of stroke and then increase to constant about 0.4, but the channel side 5° was constant 0.4 and then raise up of curvature at 75%-low. In case

75%-high, the curvature of sidewall curl has high curvature and 90% the curvature of sidewall curl was lower than case 75%-high. The twist angle of flange could reduce twisting at 75%-high. The thinning and plastic were reducing at 0% to 75%-low of stroke. However, the thinning and plastic strain at 75%-high was higher than 75%-low but springback angle smaller than 75%-low. The effect of variable blank holder force can be reduce springback behavior, %maximum thinning and %maximum plastic strain better than constant blankholder force.

4. Conclusion

The numerical parameters are affecting springback simulation accuracy. In this paper investigate numerical parameters influence springback prediction.

- The proper mass scaling and element size are very crucial.
- The number of integration point was important parameter, which is more the number of integration points. The springback behavior simulation was accurate simulation
- The minimum time step should be avoid small minimum time step, the minimum time step shall not exceed 3.0E-07.
- Proper levels of constant blankholder force can reduce springback behavior in U & butt shape, but the variable blank holder force can reduce not only springback behavior more than constant blank holder force but also %maximum thinning and %maximum plastic strain, which can be improve capability of parts

References

[1] W.L. Xu, Sensitive factors in springback simulation for sheet metal forming, J Mater Process Technol 151 (2004) 217–222

[2] Li, K. and Wagoner, R. H., "Simulation of Springback", Simulation of Material Processing: Theory, Methods and Applications, Huetink and Baaijens (eds),1998, 21-31.

[3] Maker, B. N., "implicit Springback Calculation using LS-DYNA", Livermore Software Technology Corporation, 1998.

[4] Shi, M. F., Prince, D. G., and Song, W., "A Sensitivity Study of Simulation Parameters in Sheet Metal Forming and Springback Simulation using LSDYNA". Proc. 5th Intl. LS-Dyna User Conf. Southfield, USA,1998.

[5] S.W. Lee, D.Y. Yang, An assessment of Numerical parameters influencing springback in explicit finite element analysis of sheet metal forming process, J. Mater. Process Technol 80–81 (1998) 60–67.

[6] F. Barlat and J. Lian, Plastic behaviour and stretchability of sheet metals. Part I. A yield function for orthotropic sheets under plane stress conditions, Int. J. Plast. 5 (1989) 51–66.

[7] LS-DYNA Dynaform5.6 User's Manual,Livermore Software Technology Corporation, Livermore, 2003.

[8] Gang Lui, Variable blankholder force in U-shape part forming for eliminate springback error, J Mater Process Technol 120 (2002)259-264

[9] B. CHIRITA, Experimental study of the influence of blankholder force on spring-back of sheet metal, Archieves of Civil and Mechnical Engneering, vol. 3, 2003

[10] H. Yao and S.-D. Liu, Techniques to Improve Springback Prediction Accuracy Using Dynamic Explicit FEA Codes, Society of Automotive Engineers, 2002, 01-0159

BIOGRAPHY

Name: Mr. Watcharapong Sirigool

Date of Birth: June 13, 1985

Place of Birth: Bangkok, Thailand

Education:

2003 – 2007 B. Eng. in Agricultural Machinery Engineering, Department of Agricultural Engineering, Faculty of Engineering, Rajamangala University of Technology Thanyaburi (RMUTT)

2007 – 2010 M. Eng. in Automotive Engineering (International program), International College, King Mongkut's Institute of Technology Ladkrabang (KMITL)

Scholarships:

2007-2009 Full scholarship for study in the master degree from National Science and Technology Development Agency (NSTDA)

Publications:

Sirigool W., Depaiwa N., Jirathearanat S., Adachi T. "FEA Study on Parameters Affecting Springback of Forming of Advance High Strength Steel sheets (AHSS)", **Proceeding of the 3rd International Conference on Asia Simulation and Modeling**, Bangkok, Thailand, January 22-23, 2009. pp 396-402.